

PHYS375 – Nuclear Physics

●	PHYS375 Nuclear Physics	1
●	Relevant Textbooks	2
●	Atoms	3
●	Nucleus	4
●	Nucleons	5
●	Nuclear Force	6
●	Dinucleon States	7
●	Even and Odd Internucleon Forces	8
●	Energy and Length Scales	9
●	Mass Number A	10
●	Nuclides	11
●	Chart of the Nuclides	12
●	Nuclear Size	13
●	Nuclear Electron Scattering	14
●	Nuclear Charge Distribution	17
●	Nuclear Deformation	19
●	Nuclear Masses	20
●	Nuclear Binding Energy	21
●	Binding Energy per Nucleon	22
●	Separation Energy, Pairing Energy	23
●	Nuclear Forces	24
●	Bulk Properties	25
●	Liquid Drop Model	26
●	Semi-Empirical Mass Formula	27
●	Terms of the Weizsäcker Formula	28
●	Valley of Stability	31
●	Decay of Isobars	32
●	Beta Decay	33
●	Alpha Decay	34
●	Coulomb Barrier	36
●	Barrier Penetration	37

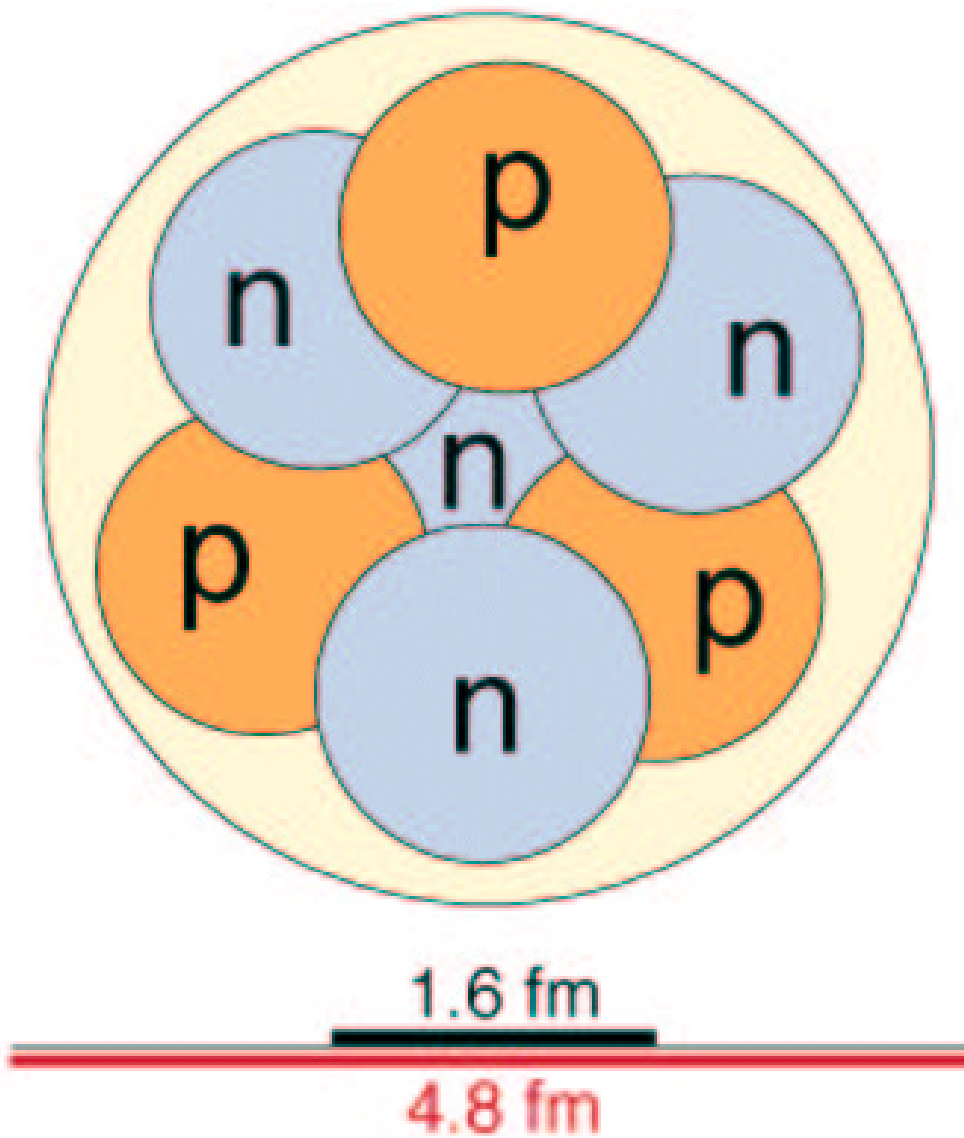
● Geiger-Nutall Rule	39
● Other Decay Modes	40
● Spontaneous Fission	41
● Fission Barrier	43
● The Spherical Shell Model	45
● Concept of a Shell Model	46
● The Mean Field	47
● Single-Particle Shell Model	48
● Potential Wells	50
● Well Comparisons	51
● Square Well Potential	52
● Harmonic Oscillator Potential	54
● Spin-Orbit Potential	56
● Eigenvalues of $\vec{L} \cdot \vec{S}$	57
● Central + Spin-Orbit Potential	58
● Spherical Shell Model Energy Levels	60
● Angular Momentum Barrier	61
● Spins and Parities of Nuclear States	62
● Magnetic Dipole Moments	64
● Calculated single-particle g-factors	66
● Electric Quadrupole Moments	67
● Wavefunction of an Orbital	69
● Nuclear Excitations	70
● Generation of Angular Momentum	72
● Spherical Harmonic Vibrator	73
● Particle-Vibration Coupling	74
● Nuclear Deformation	75
● Microscopic Basis of Deformation	76
● Spherical Harmonic Shapes	77
● Collective Nuclear Rotation	78
● Vibration or Rotation?	79
● Nuclear moment of Inertia	80
● Example for ^{168}Yb	81
● Backbending	82

●	Quadrupole Moment	83
●	Superdeformation	84
●	Deformed Shell Gaps	85
●	Isospin	86
●	Isospin Substates	87
●	Isobaric Analogue States	88
●	Electromagnetic Revision	90
●	Electric Multipole Moments	91
●	Oscillating Moments - Radiation	92
●	Electromagnetic Radiation	93
●	Transition Strengths	96
●	Gamma-Ray Decay	97
●	Selection Rules	98
●	Internal Conversion	103
●	$0^+ \rightarrow 0^+$ Decay	105
●	Nuclear Reactions	106
●	Coulomb Excitation	107
●	Collision Kinematics	108
●	Compound Nucleus Model	110
●	Geometric Cross-Section	112
●	Neutron Capture	113
●	Proton Capture	117
●	Charged Particle Decay	118
●	Fusion-Evaporation Reactions	119
●	Other Reactions	124
●	Transfer Reactions	125
●	Interaction with Matter: α -particles	126
●	Interaction with Matter: β -particles	127
●	Bethe-Bloch Formula	128
●	The Bragg Curve	130
●	Range	131
●	Range - Definitions	132
●	Range of α -Particles	133
●	Gas-filled Detector	134

● Interaction with Matter: photons	137
● Linear Attenuation Coefficients	140
● Scintillation Detectors	142
● Common Inorganic Scintillators	145
● Light Collection	147
● Photomultiplier Tube	148
● Gamma-Ray Spectrum	149
● Semiconductor Detectors	150
● Semiconductor Junction	151
● Silicon and Germanium Detectors	152
● Silicon Detectors	155
● Particle Identification	156
● Germanium Detector	157
● Types of Ge Detector	158
● Compton Suppression	161
● Escape-Suppressed Spectrometer	162
● Multidetector Arrays	163
● Gamma-Ray Coincidences	164
● High-Fold Coincidences	165

Generated: August 11, 2003

1: PHYS375 Nuclear Physics



Generated: August 11, 2003

2: Relevant Textbooks

Lilley : “Nuclear Physics - Principles and Applications”

Williams : “Nuclear and Particle Physics”

Krane : “Introductory Nuclear Physics”

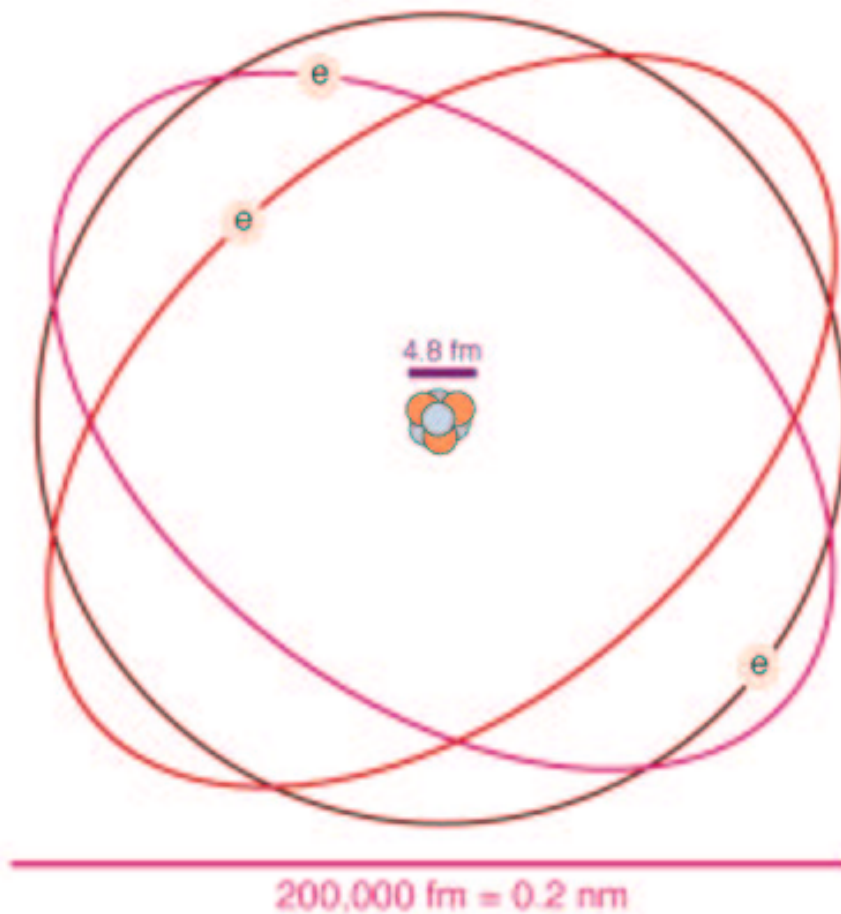
Burcham : “Nuclear Physics”

Enge : “Introduction to Nuclear Physics”

Kaplan : “Nuclear Physics”

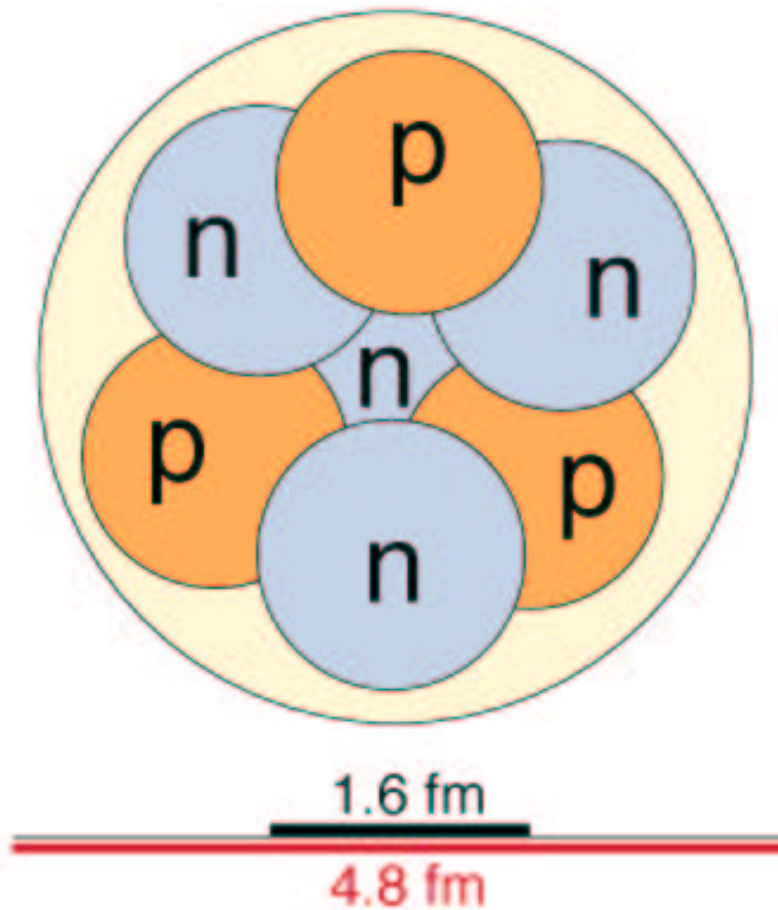
3: Atoms

An **atom** is made up of a positively charged **nucleus** and negatively charged **electrons** held together by the Coulomb force. An atom is $\sim 0.2 \text{ nm}$ ($2 \times 10^{-10} \text{ m}$) across, although the electrons spend most of their time in a region $\sim 0.1 \text{ nm}$ in diameter. The nucleus is much smaller than an atom – a schematic diagram for lithium-7 is shown below:



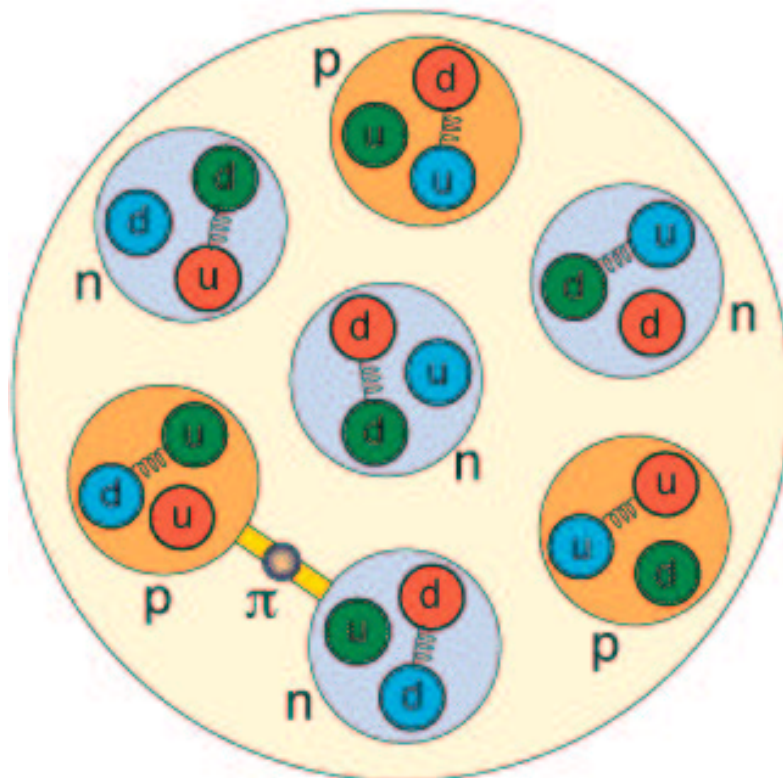
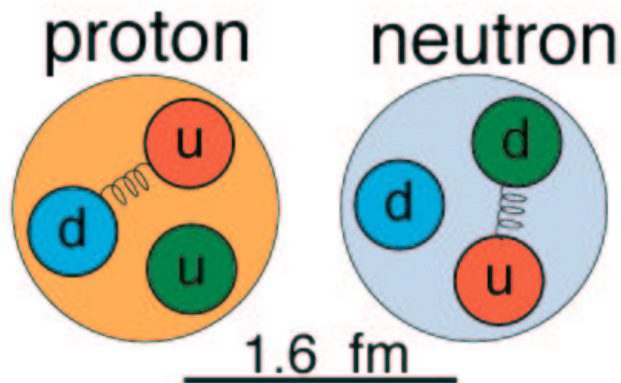
4: Nucleus

A **nucleus** is made up of positively charged **protons** and neutral **neutrons**, known collectively as **nucleons** of diameter $\sim 0.8 \text{ fm}$ ($8 \times 10^{-16} \text{ m}$). An example of a lithium-7 nucleus is shown below, which consists of 3 protons (giving the nucleus charge $+3$ and defining its chemical properties) and 4 neutrons. Another form of lithium only has 3 neutrons (lithium-6).



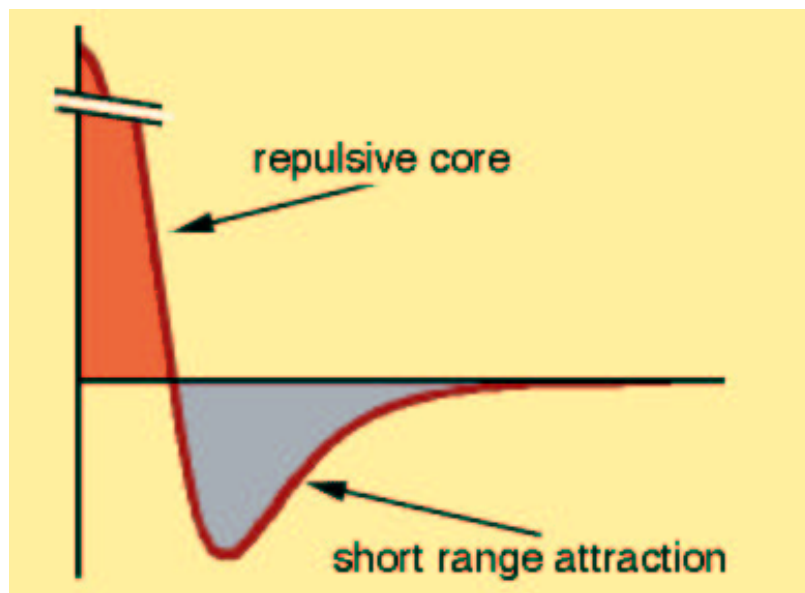
5: Nucleons

Nucleons are themselves made up of **quarks**:



6: Nuclear Force

The force that holds nucleons together is extremely strong – it has to overcome the electric repulsion of the charged protons. It is also of very short range, acting only when two particles are within 1-2 fm of each other. There is an extremely short-range repulsion (repulsive core) that pushes nucleons apart before they can get close enough to touch. There is also a region of attraction that is strongest for separations of 1-2 fm . The size of the nucleus is limited by the fact that the force dies away extremely quickly when nucleons are more than a few fm apart.



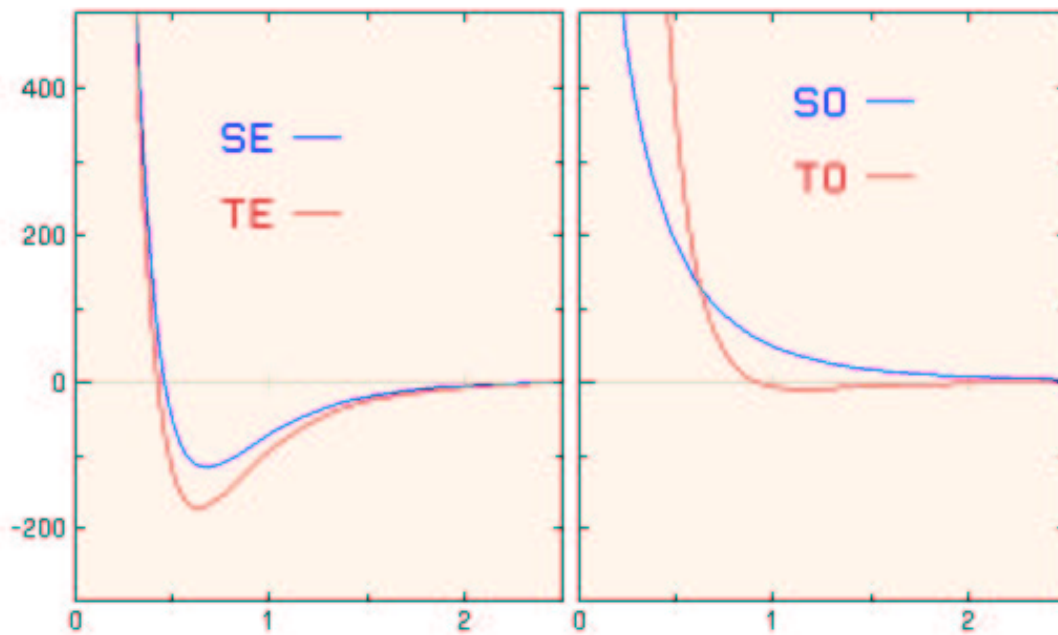
7: Dinucleon States

If the nuclear force were a simple central force (like gravity) that depended on distance, we would expect to find stable $p - p$ (diproton: ${}^2\text{He}$), $n - n$ (dineutron), and $p - n$ (deuteron: ${}^2\text{H}$) configurations. However, the nuclear force depends on many properties, including spin – most of these properties can be understood (at least qualitatively) with simple quark models.

The **even** part of the nucleon-nucleon force applies when the relative wavefunction is symmetric under exchange of the radial wavefunction; the **odd** part of the nucleon-nucleon force applies when it is antisymmetric.

In essence, it follows that the only (barely!) bound dinucleon state is the $p \uparrow - n \uparrow$ configuration – the deuteron (${}^2\text{H}$) in its 1^+ ground state (spin = 1, isospin = 1).

8: Even and Odd Internucleon Forces



9: Energy and Length Scales

The basic energy unit in nuclear physics is the MeV (mega-electron-volt). Many nuclear phenomena occur at this energy scale. 1 eV is the energy gained by unit charge (e.g. an electron) moving through a potential difference of 1V. To convert to SI units, we use the fact that the “unit” charge on the electron is $1.602 \times 10^{-19} \text{ C}$, i.e.:

$$1\text{eV} \equiv 1.602 \times 10^{-19} \text{ J} ; 1\text{MeV} \equiv 1.602 \times 10^{-13} \text{ J}.$$

The nuclear dimensions are of the order of 10^{-15} m , and:

$$10^{-15} \text{ m} \equiv 1 \text{ fm},$$

where *fm* is a fermi or femtometre.

The radius of a nucleus is typically a few *fm*.

The volume of a nucleus is $\sim 10^{-44} \text{ m}^3$.

The mass of a nucleus (^{12}C) is $\sim 2 \times 10^{-26} \text{ kg}$.

The density of nuclear matter is $\sim 2 \times 10^{18} \text{ kg/m}^3$.

Conversion factors for physical constants:

$$\hbar c = 197.3 \text{ MeV fm}$$

$$\hbar = 6.582 \times 10^{-22} \text{ MeV s}$$

$$e^2 = 1.44 \text{ MeV fm}$$

10: Mass Number A

The atomic nucleus is composed of protons and neutrons, known collectively as nucleons. The protons and neutrons may be considered as the same basic nuclear “particle” since the nuclear force is independent of charge, i.e. the $p - p$, $p - n$, and $n - n$ forces are the same.

The mass number A is equal to the total number of nucleons in a nucleus and is the nearest integer to the atomic weight. From chemistry, the atomic weight of the elements was thought to be integer ratios of the atomic weight of hydrogen (Prout’s hypothesis). Several difficulties were found, such as the atomic weight of chlorine (~ 35.5). This was resolved by the concept of isotopes – elements with different numbers of neutrons. For example, chlorine occurs in nature as two isotopes: ${}_{17}^{35}\text{Cl}_{18}$ (75% abundant) and ${}_{17}^{37}\text{Cl}_{20}$ (25% abundant). Taking a weighted average leads to an atomic weight of 35.5. The mass number A of a specific nucleus is simply the sum of Z (number of protons) and N (number of neutrons).

11: Nuclides

Isotope – same Z – defines an element and chemical properties.

Isotone – same N – different elements, same neutron number.

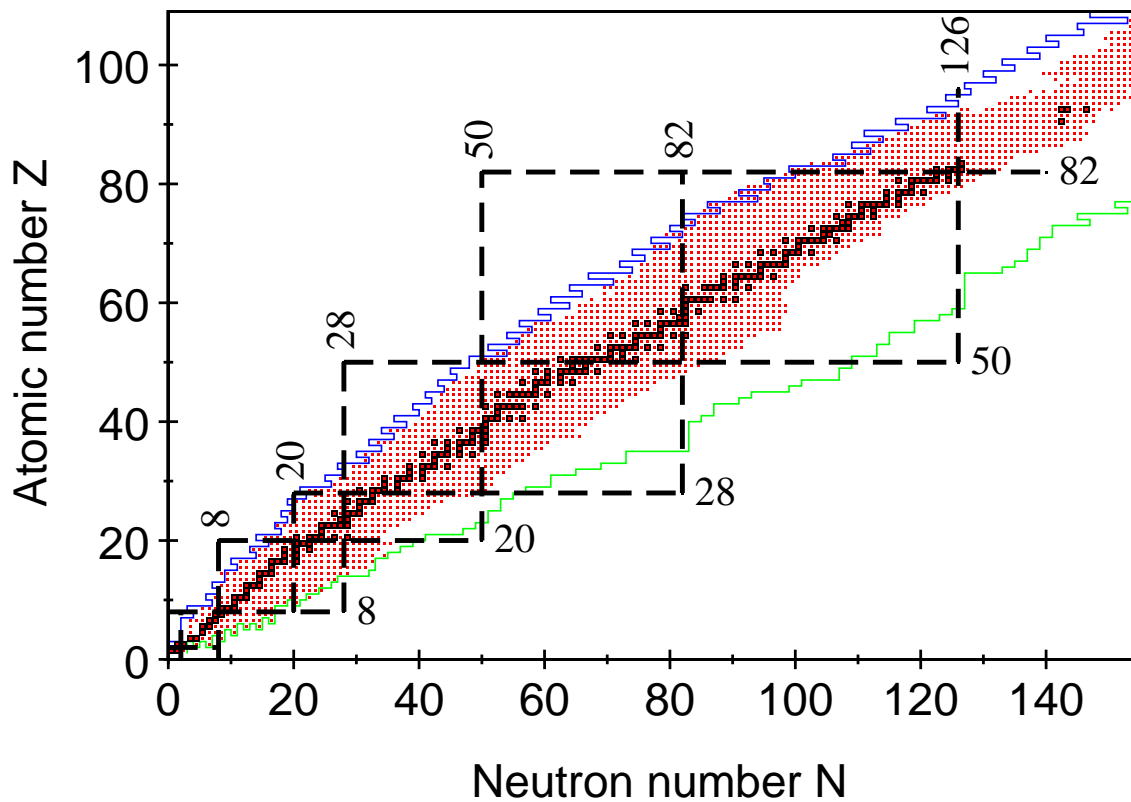
Isobar – same A – but different Z and N .

Nuclide – nucleus with given A , Z , and N – usual notation: A_ZX_N , e.g. ${}^{37}_{17}\text{Cl}_{20}$ (or ${}^{37}\text{Cl}$ – “chlorine-37”).

About 1500 different nuclides are known but only 20% of these are stable. Nuclides are usually shown in a chart of the nuclides (Segre chart). For light mass, the number of protons and neutrons is approximately equal ($Z = N$), but with increasing mass more neutrons are needed for the stable nuclides ($N > Z$) – Coulomb repulsion between the protons. The lightest nuclide is ${}^1_1\text{H}_0$ (hydrogen – single proton); the heaviest stable nuclide is ${}^{209}_{83}\text{Bi}_{126}$ (bismuth) although even heavier nuclides can be artificially produced. The heaviest element is currently $Z = 114$ (unnamed!). There is even an “island of stability” predicted for $Z \geq 114$.

12: Chart of the Nuclides

Here is a plot of the chart of the nuclides:



The numbers correspond to “magic” values where greater stability is found; several isotopes and isotones occur for these values. This suggests a nuclear shell structure similar to atomic shells. The stable nuclides lie along the valley of stability.

13: Nuclear Size

(Williams chapter 3)

How can we measure the size of a nucleus? We cannot “look” at it – the wavelength of visible light ($10^{-7}m$) is much larger than the nuclear dimensions ($10^{-15}m$). We need to vastly decrease the wavelength of the probe and look for diffraction effects. “We cannot measure the size of a pea by throwing a football at it and observing when it bounces back ” (Twin). For a particle beam we consider the de Broglie wavelength, which is related to its energy:

$$E = \hbar\omega = h\nu = hc/\lambda.$$

An electron beam is a useful probe since both the nucleus and the beam are charged and the electromagnetic (Coulomb) interaction is well understood. This probe measures the charge density (radius) of the nucleus. Furthermore, the electron can be considered as a point charge (no size) with no internal structure.

14: Nuclear Electron Scattering

If the nucleus is a point charge, the scattering cross-section is given by the Rutherford formula (low-energy α scattering) modified by a relativistic correction term (high electron velocity v) to give the Mott scattering formula:

$$\frac{d\sigma}{d\Omega} = \frac{Z^2 \alpha^2 \hbar^2 c^2}{4\rho^2 v^2} \operatorname{cosec}^4 \left(\frac{\theta}{2} \right) \left[1 - \frac{v^2}{c^2} \sin^2 \left(\frac{\theta}{2} \right) \right].$$

In this equation, α is the fine structure constant. However, as the nucleus is in fact of finite size, we can observe diffractive effects and the scattering formula must be modified:

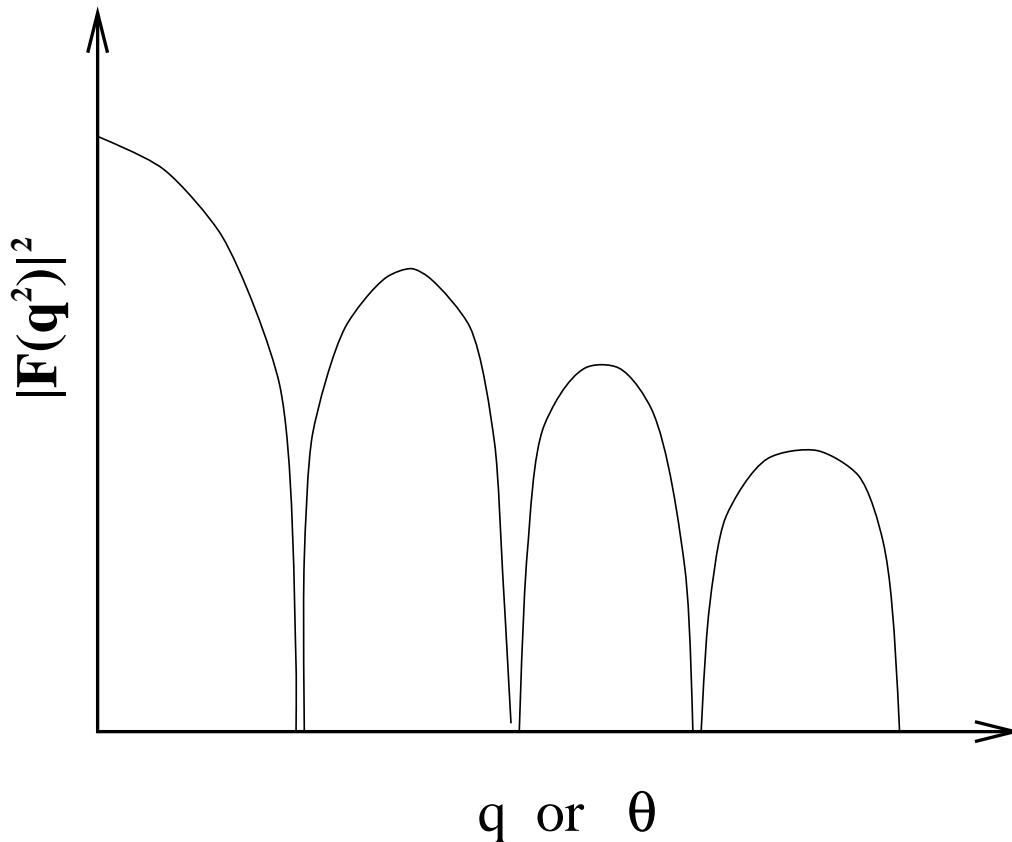
$$\left(\frac{d\sigma}{d\Omega} \right)_{finite\ size} = |F(q^2)|^2 \left(\frac{d\sigma}{d\Omega} \right)_{point\ size},$$

where $F(q^2)$ is the Form Factor given by the following volume integral over the whole nucleus:

$$F(q^2) = \frac{1}{Ze} \int \int \int \rho(r) \exp \left[\frac{i\vec{q} \cdot \vec{r}}{\hbar} \right] dr^3;$$

it is the Fourier transform of the nuclear charge distribution. In these equations, q is the momentum transferred to the nucleus in the scattering process.

If we can measure $F(q^2)$, we can determine the nuclear charge distribution and size of the nucleus. What is $F(q^2)$? – If we assume the nucleus has a sharp edge, the square of the form factor looks like:



How do we obtain the relevant data?

The easy way to vary q (recall: $|q| = 2p \sin(\theta/2)$) is to fix p (i.e. the beam energy: $E = pc$) and measure the cross-section $d\sigma/d\Omega$ at various scattering angles θ . This will give different q 's up to the maximum of $2p$ ($\theta = 180^\circ$).

What do the experimental results look like?

(see Williams)

The condition for diffractive effects is:

$$\frac{\vec{q} \cdot \vec{r}}{\hbar} > 1 \text{ or } q > \frac{\hbar}{r}.$$

In the example from Williams (450 *MeV* electron beam scattering from ^{58}Ni), it can be seen that we need $q \sim 300 \text{MeV}/c$ in order to clearly see the first minimum. This corresponds to a beam energy (or p) equal to 150 *MeV*. At this energy, the de Broglie wavelength of the beam of electrons is:

$$\frac{\lambda}{2\pi} = \frac{\hbar}{p} = \frac{197}{150} = 1.3 \text{ fm},$$

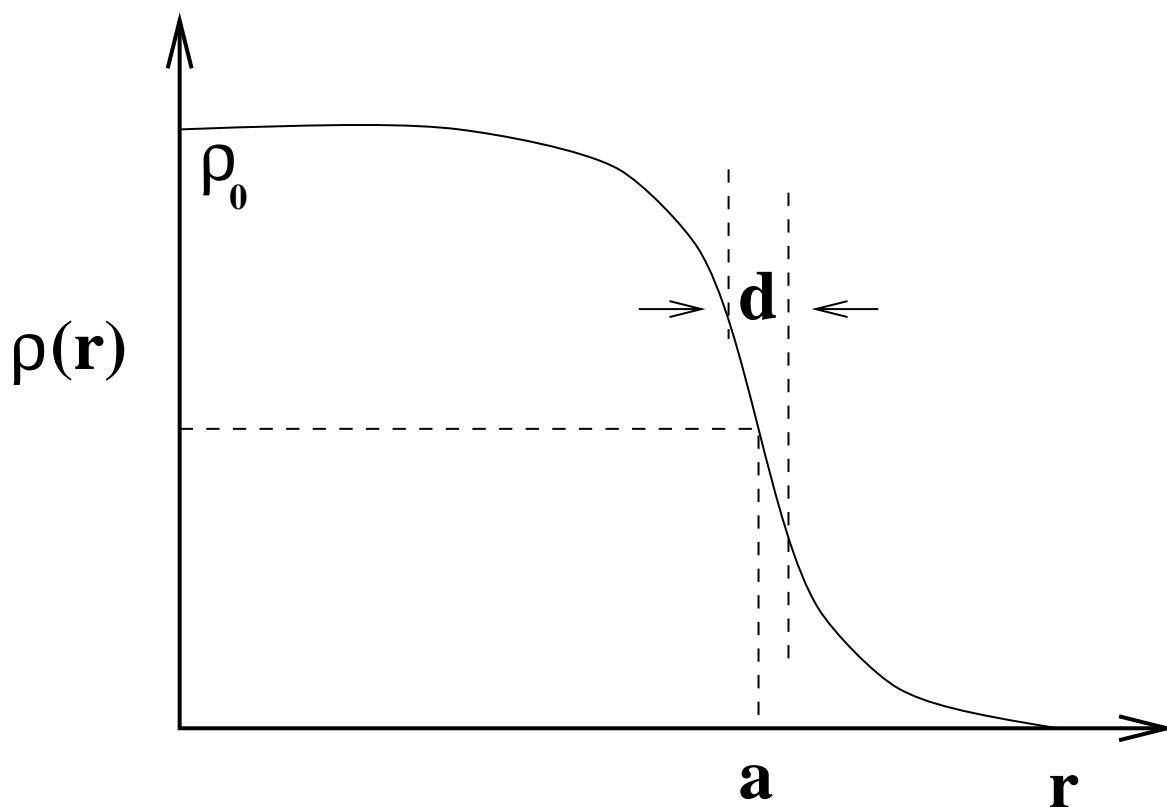
i.e. smaller than the nuclear radius (4.1 *fm*).

In reality, the minima are filled in – this is not due to problems with experimental resolution, but our assumption that the nucleus has a sharp edge. In fact, nuclei have fuzzy edges – the nuclear surface is diffuse. This explains why the minima are filled in.

15: Nuclear Charge Distribution

The charge density of a nucleus may be expressed as (Fermi distribution):

$$\rho(r) = \frac{\rho_0}{1 + \exp [(r - a)/d]}.$$



Another parameter is the surface thickness t – the distance between the 10% and 90% density points:

$$t = 4.4d.$$

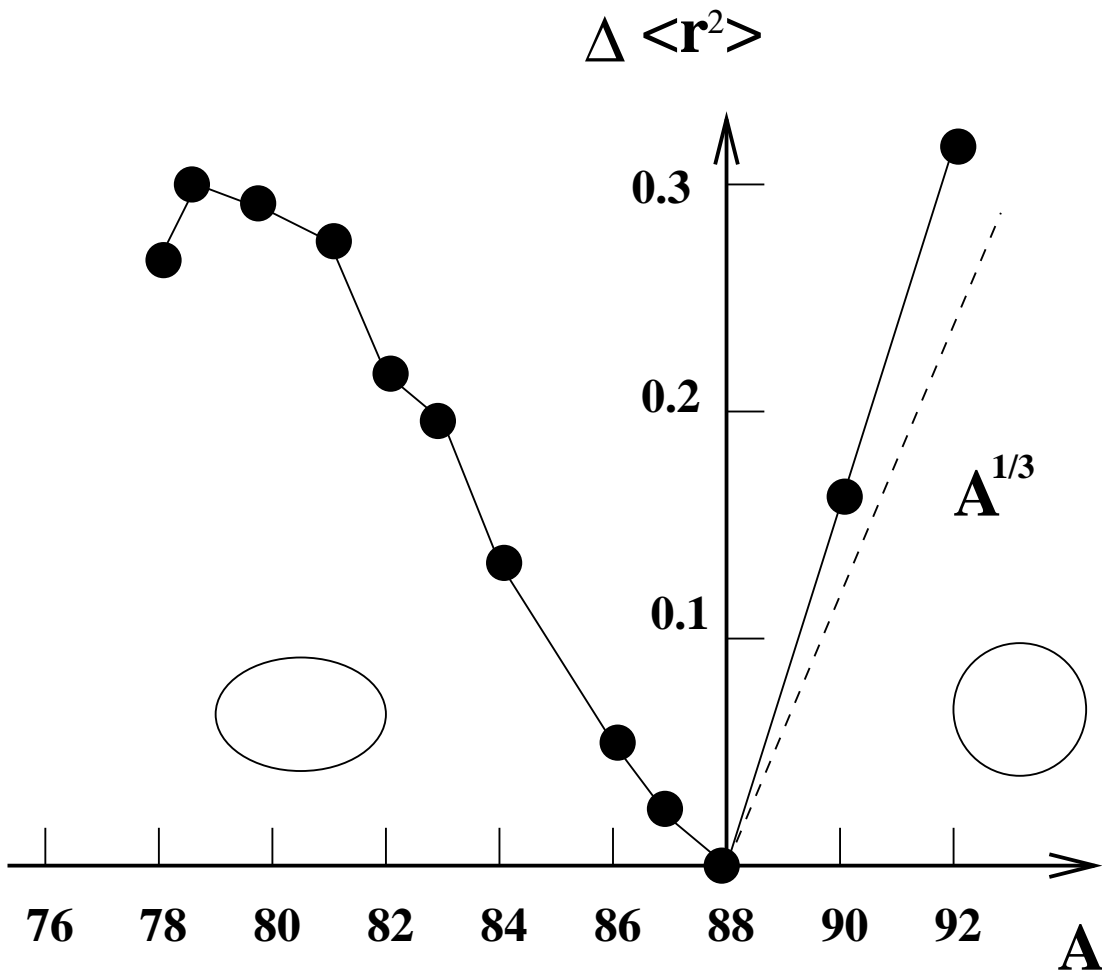
Data for many nuclei show that:

- $a \propto A^{1/3} \Rightarrow a \approx 1.2A^{1/3} \text{ fm}$,
- $d \approx 0.55 \text{ fm}$; $t \approx 2.4 \text{ fm}$, independent of A ,
- charge density is higher in the interior of light nuclei.

The last point arises since the ratio of neutrons to protons (N/Z) is different for light and heavy nuclides. However, correcting for this the nuclear charge density appears independent of A . Nuclei are incompressible and hence the Volume is proportional to the Number of Nucleons. It then follows that the Radius is proportional to $A^{1/3}$.

So far we have assumed that nuclei are spherical. This is not true! Only nuclei near filled (or empty) proton or neutron shells are spherical. The nuclei in between tend to be prolately deformed (like a rugby ball). Oblate nuclei (like a smartie) are rare.

16: Nuclear Deformation



This schematic figure shows the difference in the mean square radii of strontium isotopes relative to $A = 88$. Above this number, the heavier isotopes approximately follow the $A^{1/3}$ dependence. However, below this number the values again increase indicative of nonspherical shapes.

17: Nuclear Masses

The atomic mass unit (amu) is defined as $\frac{1}{12}$ the mass of the ^{12}C atom:

$$1 \text{ amu} = 931.478 \text{ MeV}/c^2 = 1.66042 \times 10^{-27} \text{ kg},$$

chosen as opposed to ^1H so that $A \approx$ mass of the nuclide. In these units:

- Mass of the proton: $m_p = 1.0073 \text{ amu}$,
- Mass of the neutron: $m_n = 1.0087 \text{ amu}$.

In terms of MeV ($E = mc^2$):

- Mass of the proton: $m_p c^2 = 938.28 \text{ MeV}$,
- Mass of the neutron: $m_n c^2 = 939.57 \text{ MeV}$,
- Mass of the electron: $m_e c^2 = 0.511 \text{ MeV}$.

The mass defect Δ is defined as the difference between the exact atomic mass of an isotope $M(Z, A)$ and its mass number A :

$$\Delta = M(Z, A) - A; \quad \Delta \equiv 0 \text{ for } ^{12}\text{C}.$$

18: Nuclear Binding Energy

The binding energy $B(Z, A)$ is given by:

$$B(Z, A) = [M(Z, A) - ZM_H - (A - Z)m_n] c^2,$$

where M_H is the mass of the hydrogen atom and m_n is the mass of the neutron. The binding energy is a negative contribution to the nuclear mass ($E = mc^2$), implying that the mass of a nuclide is less than the sum of its constituent parts (free protons and neutrons) – energy must be input to break up a nucleus.

Example — ^{12}C :

$$B(Z, A) = -0.099 \text{ amu} = -92.2 \text{ MeV}.$$

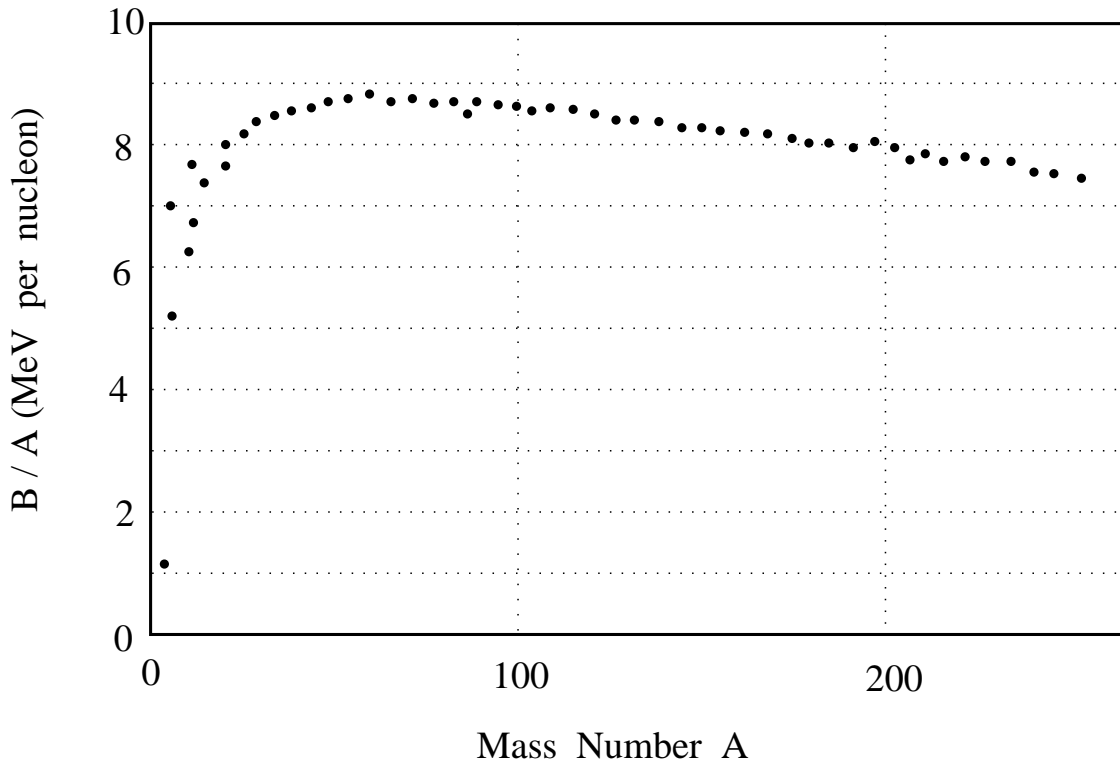
A useful quantity is the binding energy per nucleon:

$$\frac{B(Z, A)}{A} = -7.68 \text{ MeV/nucleon for } ^{12}\text{C}.$$

The mass defect and total binding energies are different — Δ is measured with respect to A (integral *amu*), while $B(Z, A)$ assumes the nucleus is made up of protons and neutrons (i.e. m_n is the difference).

19: Binding Energy per Nucleon

Here is a schematic diagram (© A.T. Semple) of the nuclear binding energy per nucleon:



It can be seen that, except for the very light nuclides, the binding energy per nucleon is approximately constant. The most stable nuclide (greatest binding energy) is iron-56 (${}^{56}_{26}\text{Fe}_{30}$).

20: Separation Energy, Pairing Energy

The separation energy (energy required to remove a single particle) is defined as:

$$\begin{aligned} S_n &= B(Z, A) - B(Z, A - 1) \\ &= M(Z, A - 1) - M(Z, A) + m_n, \end{aligned}$$

for neutrons, while for protons it is:

$$\begin{aligned} S_p &= B(Z, A) - B(Z - 1, A - 1) \\ &= M(Z - 1, A - 1) - M(Z, A) + M_H. \end{aligned}$$

The separation energy is also termed the binding energy for that particle in the nucleus (Z, A) . In general, this is not the same as B/A , the average binding energy per nucleon.

The pairing energy (energy required to remove a pair of like nucleons) is defined as:

$$P_n(Z, A) = S_n(Z, A) - S_n(Z, A - 1),$$

for neutrons, while for protons it is:

$$P_p(Z, A) = S_p(Z, A) - S_p(Z - 1, A - 1).$$

21: Nuclear Forces

Some properties of the nuclear force:

- Short range, $10^{-15}m$ ($1fm$) or less.
- Independent of electric charge, i.e. $n - n$, $p - p$, $n - p$ forces the same – concept of nucleons.
- Depends on relative orientations of the spins of interacting nucleons, i.e. for a $n - p$ pair, $\uparrow\uparrow$ is stable (deuteron), $\uparrow\downarrow$ is not.
- Depends on the orientations of the spins relative to the line joining the two nucleons. The deuteron is a linear combinations of $l = 0$ and $l = 2$ wavefunctions.
- Repulsive core (Pauli exclusion principle) – leads to constant average separation between two nucleons, and the nuclear Volume is proportional to the Number of Nucleons. It then follows that the Radius is proportional to $A^{1/3}$.

22: Bulk Properties

The nuclear binding energy per nucleon (B/A) is approximately constant for $A \geq 12$, implying a saturation of the nuclear force ($B/A \approx -8 \text{ MeV}$). This is similar to intermolecular forces (van der Waals) between molecules, e.g. H_2O . The forces have a short range and each molecule experiences interactions only with its nearest neighbours.

Scattering experiments (n or e^-) indicate that the nuclear density is approximately uniform and is independent of A . The nuclear radius is thus proportional to $A^{1/3}$:

$$R = r_0 A^{1/3} \quad (fm, = 10^{-15}m),$$

where $r_0 \approx 1.4 fm$ (matter) or $r_0 \approx 1.2 fm$ (charge). The average nuclear density is $1.49 \times 10^{18} \text{ kg/m}^3$, (matter density $\sim 0.15 \text{ nucleons/fm}^3$, charge density $\sim 10^{-20} \text{ C/fm}^3$) about 10^{15} times greater than normal bulk matter!

Nuclear matter also has a very low compressibility – an analogy can thus be drawn with a macroscopic drop of incompressible fluid: Liquid Drop Model.

23: Liquid Drop Model

The Liquid Drop Model (LDM) approximates the nucleus as a constant-density sphere of radius R . Phenomena such as particle evaporation and fission can be thought of in terms of their liquid drop analogies, i.e. molecular evaporation from the surface and the division of the drop into two smaller droplets.

However, the LDM is a classical macroscopic model which takes no account of quantal behaviour. For example, in a liquid, the mean distance between two particles is given by the minimum of the interparticle potential $\Rightarrow 0.7 fm$ in nuclei. In a nucleus, however, nucleons are $\sim 2.4 fm$ apart because of the Pauli exclusion principle, and the system represents a quantum liquid. The larger separation means that nucleon scattering processes are rare compared to the scattering events of molecules in a liquid.

The LDM predicts that nuclear properties vary in a smooth way with mass number.

24: Semi-Empirical Mass Formula

A semiclassical approach (Weizsäcker) was to try to fit the following expression for nuclear binding energy to experimental data:

$$B(Z, A) = a_v A - a_s A^{2/3} - a_c \frac{Z^2}{A^{1/3}} - a_a \frac{(A - 2Z)^2}{A} + \delta$$

Typical values (MeV) of the parameters are:

Volume term $a_v = 15.56,$

Surface term $a_s = 17.23,$

Coulomb term $a_c = 0.70,$

Isospin term $a_a = 23.28,$

$$\text{Pairing term } \delta = \begin{cases} +12A^{-1/2} & \text{even-even nuclei,} \\ 0 & \text{odd-even, even-odd,} \\ -12A^{-1/2} & \text{odd-odd.} \end{cases}$$

This formula accounts very well for the general trend of observed nuclear masses.

25: Terms of the Weizsäcker Formula

The various terms of the semi-empirical mass formula are derived from two models, namely the Liquid Drop Model and the nuclear Shell Model taking into account quantal effects. The coefficients are found by fitting to experimental data.

From the Liquid Drop Model we obtain:

$$B(Z, A) = a_v A - a_s A^{2/3} - a_c \frac{Z^2}{A^{1/3}}$$

- Volume Term a_v

This is the major term in the binding energy formula and is based on the fact that $B(Z, A)/A$ is approximately constant for $A > 60$, i.e.

$$B(Z, A) \propto A;$$

there is a saturation of the nuclear force. The binding energy per nucleon is primarily influenced by nearest neighbours (as in a liquid) and is related to short-range forces. Therefore, $B(Z, A) \propto A$ rather than $B(Z, A) \propto A^2$.

- Surface Term a_s

Nucleons at the surface of the nucleus are surrounded by fewer neighbours than those nucleons in the centre of the nucleus. Thus the volume term overestimates the binding energy due to the surface tension (as in a liquid). Therefore, we have to subtract a term proportional to the surface area (R^2), i.e. $A^{2/3}$.

- Coulomb Term a_c

From the chart of the nuclides, $N > Z$ for large A . This is due to the Coulomb repulsion of the protons which make the nucleus less bound. Therefore we have to subtract a term proportional to the Coulomb energy. Note that the Coulomb force is long range and affects all the protons in the nucleus.

The potential energy of a charged sphere (radius R) with a uniform charge distribution is given by:

$$E_c = \frac{3}{5} \frac{Z^2 e^2}{4\pi\epsilon_0 R}.$$

Since $R = r_0 A^{1/3}$, it follows that $E_c \propto Z^2 / A^{1/3}$.

We have everything we can hope to achieve from the LDM. We need to now consider the Shell Model – the nucleus is composed of independent particles and quantal effects are important.

- Isospin (asymmetry) Term a_a

For low A , $N \sim Z$. We assume that the binding is identical for neutrons and protons, and the binding for $N = Z$ is a minimum. However, replacing protons by neutrons for fixed A costs energy (Williams page 57!) and hence the binding is reduced for nuclei with $N > Z$. The form of this term is:

$$E_i \propto \frac{(A - 2Z)^2}{A} \text{ or } \frac{(N - Z)^2}{A}.$$

- Pairing Term δ

Even-even (Z even, N even) nuclei are more bound than odd A (Z even, N odd, or Z odd, N even), which are in turn more bound than odd-odd nuclei. In fact only four odd-odd nuclides are stable. This implies that protons or neutrons like to be “paired”, i.e. a pairing correlation energy increases the binding energy. These correlations are similar to the electrons (Cooper pairs) in a superconductor.

26: Valley of Stability

Given a fixed A , what is the Z of the most stable isobar?

We can combine the binding energy formula:

$$B(Z, A) = [M(Z, A) - ZM_H - (A - Z)m_n]c^2,$$

with the semi-empirical mass formula to investigate the stability of isobars. A mass parabola formula is found:

$$M(Z, A) = C + DZ + EZ^2, \text{ with}$$

$$C = Am_n - a_v A + a_s A^{2/3} + a_a A + \delta A^{-3/4},$$

$$D = M_H - m_n - 4a_a,$$

$$E = a_c A^{-1/2} + 4a_a A^{-1}.$$

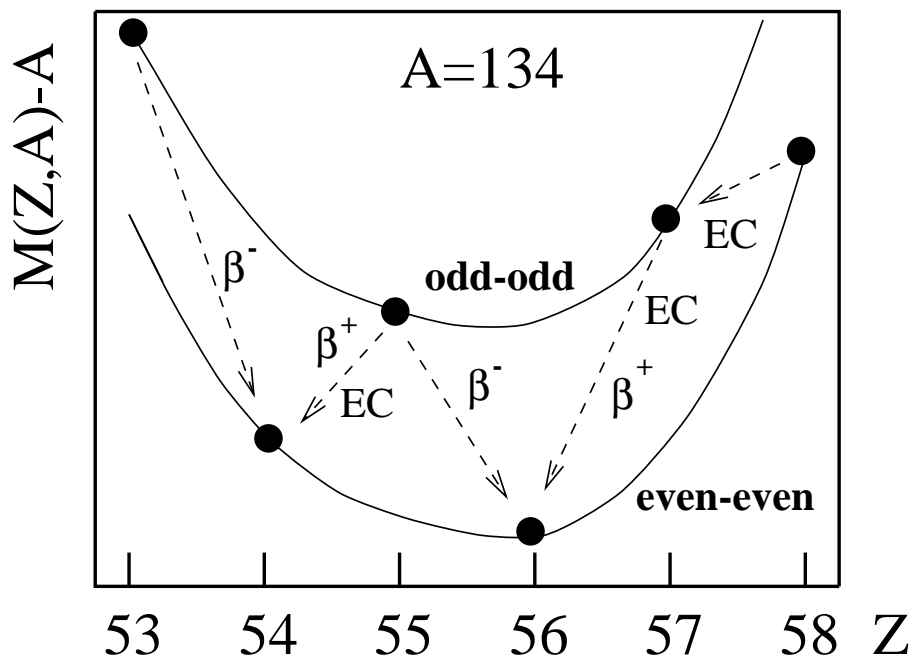
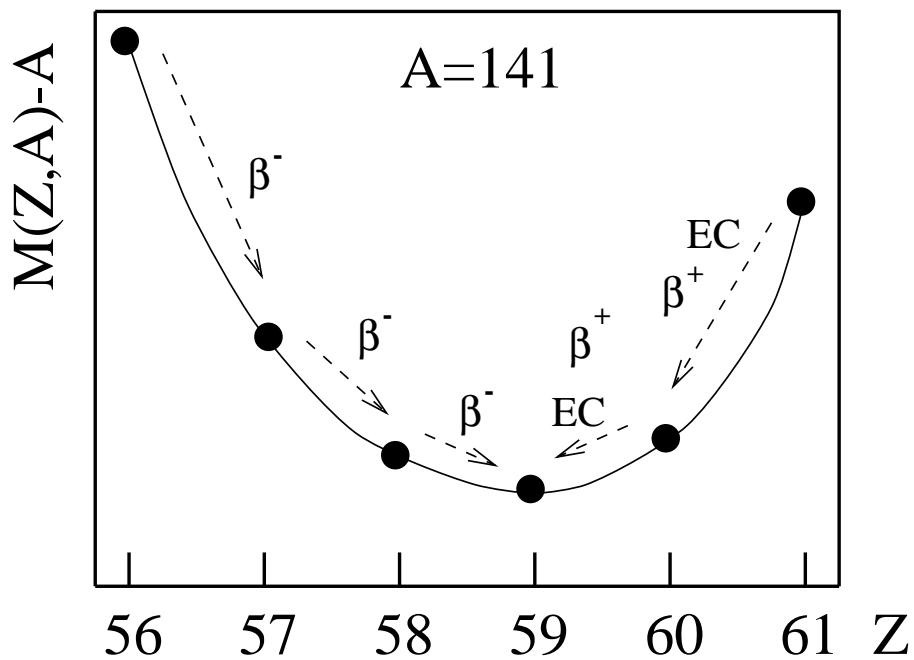
This is a parabola with a minimum:

$$Z_{min} = -\frac{D}{2E} = \frac{M_H - m_n - 4a_a}{2[a_c A^{-1/2} + 4a_a A^{-1}]}.$$

Note we only need to know the a_a and a_c terms.

e.g. for $A = 141$, $Z_{min} = 59.1$, i.e. the most stable isobar with $A = 141$ has $Z = 59$ (praeeseodymium).

27: Decay of Isobars



28: Beta Decay

• β^- decay: $(Z, A) \rightarrow (Z + 1, A) + e^- + \bar{\nu}_e$

Occurs for $Z < Z_{min}$. The energy condition is:

$$\begin{aligned} Q_{\beta^-} &= [M(Z, A) - M^+(Z + 1, A) - m_e]c^2 > 0, \\ &\approx [M(Z, A) - M(Z + 1, A)]c^2 > 0, \end{aligned}$$

• β^+ decay: $(Z, A) \rightarrow (Z - 1, A) + e^+ + \nu_e$

Occurs for $Z > Z_{min}$. The energy condition is:

$$\begin{aligned} Q_{\beta^+} &= [M(Z, A) - M^-(Z - 1, A) - m_e]c^2 > 0, \\ &\approx [M(Z, A) - M(Z - 1, A) - 2m_e]c^2 > 0, \end{aligned}$$

Note there is an energy threshold of $2m_e c^2$ (1.022 MeV) in the mass difference for β^+ decay to occur.

• Electron capture: $(Z, A) + e^- \rightarrow (Z - 1, A) + \nu_e$

Occurs for $Z > Z_{min}$. The energy condition is:

$$\begin{aligned} Q_{EC} &= [M(Z, A) - M^*(Z - 1, A)]c^2 > 0, \\ &\approx [M(Z, A) - M(Z - 1, A)]c^2 > 0, \end{aligned}$$

The approximation signs indicate we have neglected electron ionisation energies (β^- and β^+ decay) or electron binding energies (EC) – but these are negligible ($\sim eV$).

29: Alpha Decay

Why do nuclei decay by alpha emission?

The α -particle (${}^4_2\text{He}$) is tightly bound compared with the nucleons, but less so than heavier nuclei.

Alpha decay is energetically possible if the mass of the decay product (daughter) plus the α -particle is less than the mass of the original nuclide, i.e.:

$$Q_\alpha = M(Z, A) - M(Z - 2, A - 4) - M_\alpha > 0.$$

This relation can be calculated using the mass formula. The minimum A for α decay can be found from the binding energy formula and with $Q_\alpha = 0$.

The binding energy of the α -particle is:

$$B(\alpha) = B(2, 4) = B(Z, A) - B(Z - 2, A - 4),$$

which can be rewritten (Williams page 76!) as:

$$B(\alpha) = 4 \frac{dB}{dA} = 4 \left[A \frac{d(B/A)}{dA} + \frac{B}{A} \right].$$

Above $A = 120$:

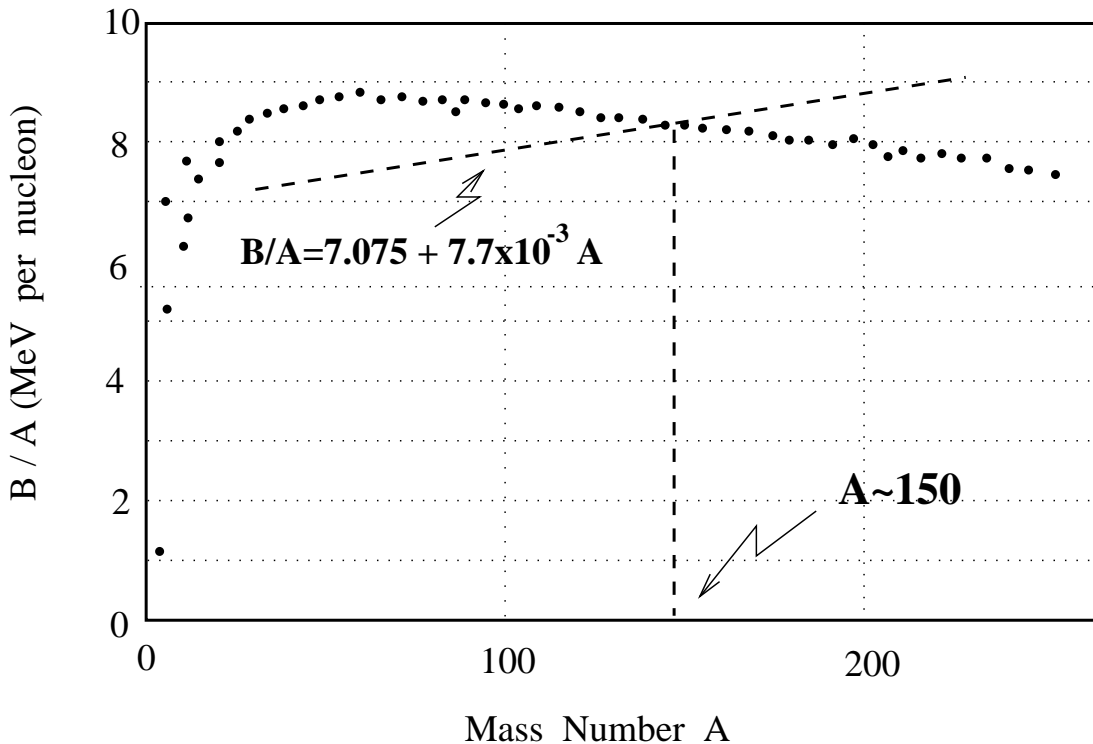
$$\frac{d(B/A)}{dA} \approx -7.7 \times 10^{-3} \text{ MeV},$$

and the binding energy of the α is 28.3 MeV.

Therefore we find that:

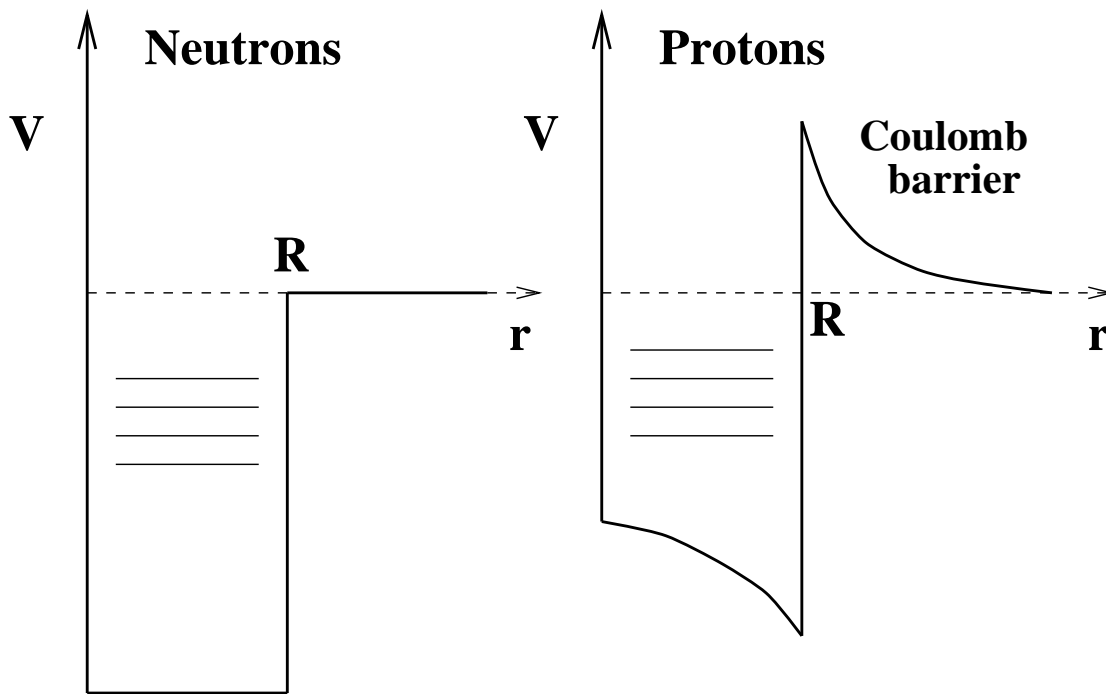
$$B/A \approx 7.075 + 7.7 \times 10^{-3} A,$$

which can be plotted on the binding energy curve:



The lines cross at $A \approx 150$ suggesting that α emission is possible for $A > 150$. Experimentally, α decay is observed down to $A = 140$, although these lighter nuclei are far from stability and Q_α is not zero. In fact, α decay can occur for even lighter nuclei (e.g. $^{108}_{52}\text{Te}_{56}$) that are very far from stability – note: stable Te isotopes have $A = 120 - 130$!

30: Coulomb Barrier



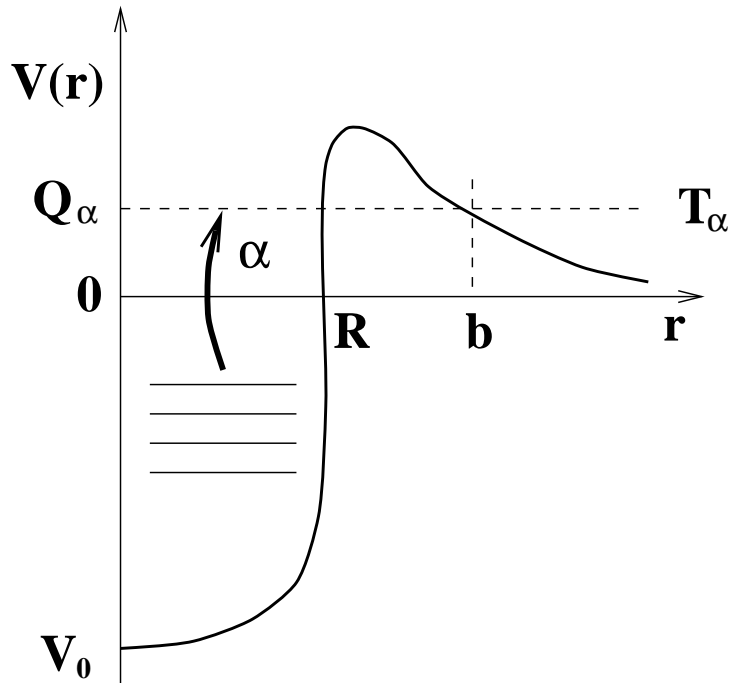
A simple square well potential is shown for neutrons (left) and protons (right). In the case of charged particles, the simple square well is modified by a Coulomb term:

$$E_C = \frac{Z_1 Z_2}{4\pi\epsilon_0 r},$$

and leads to a Coulomb Barrier which hinders charged particle emission.

31: Barrier Penetration

Alpha decay can be considered as a quantum mechanical tunnelling problem.



The binding energy gain of $\sim 28 \text{ MeV}$ when an α -particle is formed overcomes the $\sim 6 \text{ MeV}$ required to remove a nucleon. The α -particle has to tunnel through the Coulomb barrier from R to b to escape. Its kinetic energy is:

$$T_\alpha = \frac{M_D}{M_\alpha + M_D} Q_\alpha \sim Q_\alpha,$$

which takes into account the recoiling daughter.

If we assume (simplify) that the Coulomb barrier is a square barrier, then from quantum mechanics the transition rate (s^{-1}) for penetration is:

$$\omega = fp,$$

- p is the probability of tunnelling through the barrier (see Williams page 85):

$$p = \exp \left[-2 \int_R^b K dt \right] = \exp[-G],$$

$$G = \frac{2}{\hbar} \int_R^b \sqrt{2M_\alpha(V(r) - T_\alpha)} dr.$$

- f is the frequency of “attacking” the barrier :

$$f = \frac{v_0}{2R}; \sim 10^{21} s^{-1},$$

where v_0 is the velocity of the α particle in the nucleus. If $V(R) > T_\alpha$ and $b \gg R$, then:

$$G = 2\sqrt{\left(\frac{M_\alpha Z e^2 b}{\pi \epsilon_0 \hbar^2}\right)} \left(\frac{\pi}{2} - 2\sqrt{\frac{R}{b}}\right),$$

where Z refers to the daughter. These equations can be used to calculate α -decay half-lives.

32: Geiger-Nutall Rule

Experimental data indicate that in general Q_α must be larger than 4 MeV before α -decay is seen. The data also show that the half-lives of the emitters vary strongly with Q_α , about 20 orders of magnitude for Q_α from 4 to 8 MeV ! This was originally expressed by the Geiger-Nutall Rule:

$$\log_{10} \omega = B \log_{10} R_\alpha - C,$$

where ω is the transition rate ($1/\tau$ or $0.693/t_{1/2}$), R_α is the range of α -particles in air. How does this relate to the barrier penetration model? – Since $R_\alpha \propto T_\alpha^{3/2}$ for the α -particles of interest, the Geiger-Nutall Rule can be reformulated as:

$$\ln \omega \propto \ln T_\alpha,$$

while it can be shown from the model (Williams page 87!):

$$\ln \omega \propto -T_\alpha^{-1/2}.$$

However, for the energy range 4-7 MeV , a quantity linear in $\ln T_\alpha$ is within 3% of being linear in $(-T_\alpha^{-1/2})$.

33: Other Decay Modes

Can other charged particles be emitted in radioactive decay? – Yes!

^{14}C decay from ^{223}Ra was observed in 1984, and now ^{24}Ne and ^{20}Ne have also been observed. These are weak decay branches since the Coulomb barrier is higher and the probability of formation within the nucleus is smaller.

As more protons are added to a nucleus, and $Z = N$ is approached, eventually the last proton is only held in by the Coulomb Barrier (proton dripline). Hence, ground-state proton emission is possible – another example of barrier penetration. This process can compete with the usual β -decay (β^+ and electron capture). Only ~ 10 ground-state proton emitters are known experimentally, including $^{109}_{53}\text{I}_{56}$.

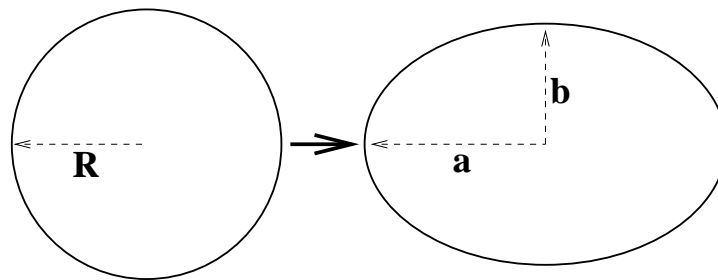
34: Spontaneous Fission

This occurs when the parent nucleus (in its ground state) spontaneously disintegrates into two roughly equal daughter nuclei. We shall simplify the problem by assuming symmetric fission:

$$Q_{SF} = M(Z, A) - 2M(Z/2, A/2) \Rightarrow \frac{Z^2}{A} > 15.4$$

from the semi-empirical mass formula and is satisfied by $A = 80$ (i.e. binding energy per nucleon for $A/2$ is greater than for A). Experimentally fission sets in for $Z^2/A > 35$.

Another approach is to take the binding energy of an initially spherical nucleus as it is stretched, but with constant volume.



$$a = R(1 + \epsilon); \quad b = \frac{R}{\sqrt{1 + \epsilon}}$$

In terms of the eccentricity ε :

the surface area increases by $4\pi R^2 \left[1 + \frac{2}{5}\varepsilon^2 \dots\right]$,

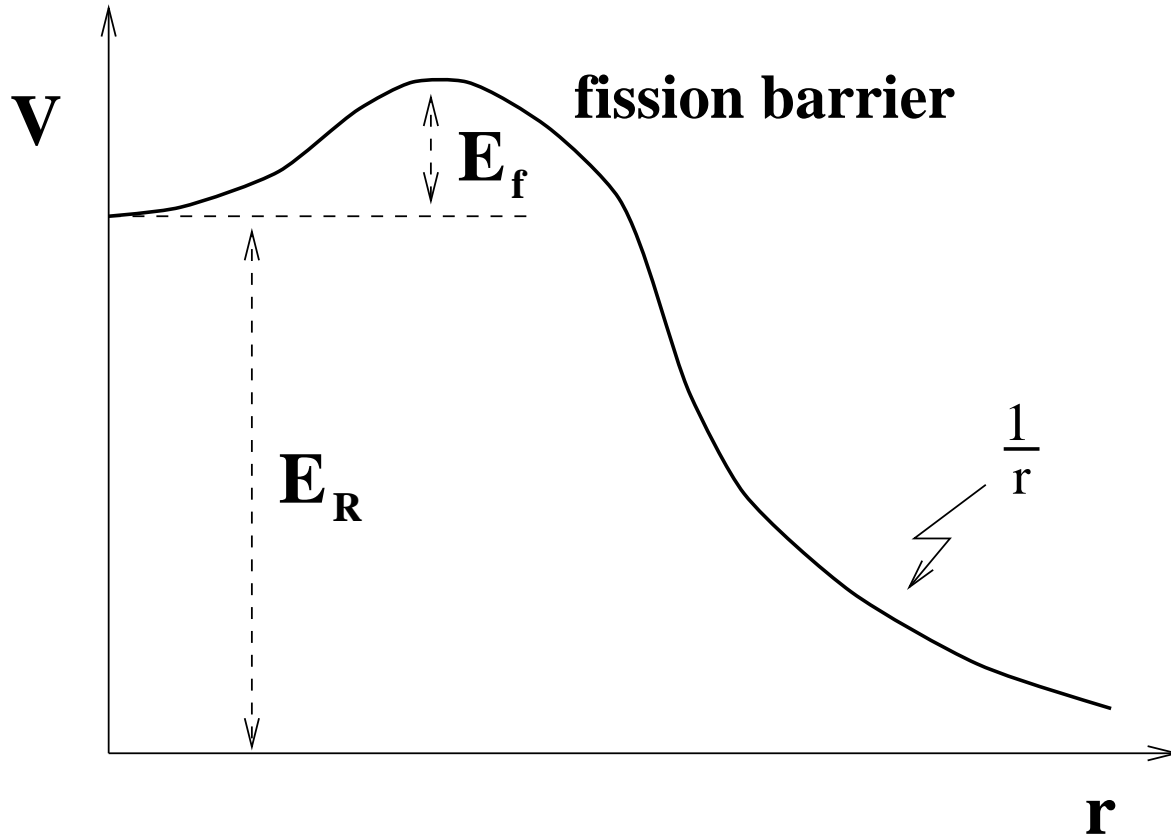
the Coulomb energy reduces by $\left[1 - \frac{1}{5}\varepsilon^2 \dots\right]$,

and the difference in binding energy is given by:

$$\begin{aligned}\Delta BE &= BE(\varepsilon) - BE(\varepsilon = 0), \\ &\approx \left[-\frac{2}{5}a_s A^{2/3} + \frac{1}{5}a_c \frac{Z^2}{A^{1/3}}\right] \varepsilon^2, \\ &= 0.14A^{2/3} \left[\frac{Z^2}{A} - 49\right] \varepsilon^2.\end{aligned}$$

For symmetric fission to take place ($\Delta BE > 0$), it follows that: $Z^2/A > 49$. Experimentally, this parameter is observed in the range 35-43 when fission occurs. We have assumed no potential barrier, but fission is another example of quantum mechanical tunnelling. Heavy nuclei are rich in neutrons and hence the fission products are also neutron rich. In fact, 3 or 4 neutrons are usually emitted during fission. Spontaneous fission is a rare process compared to α decay. For example, the α decay rate of ^{238}U is $\sim 10^{-18} \text{ s}^{-1}$, while the rate for spontaneous fission is $\sim 10^{-24} \text{ s}^{-1}$. The emitted neutrons can induce a self-sustaining chain reaction.

35: Fission Barrier



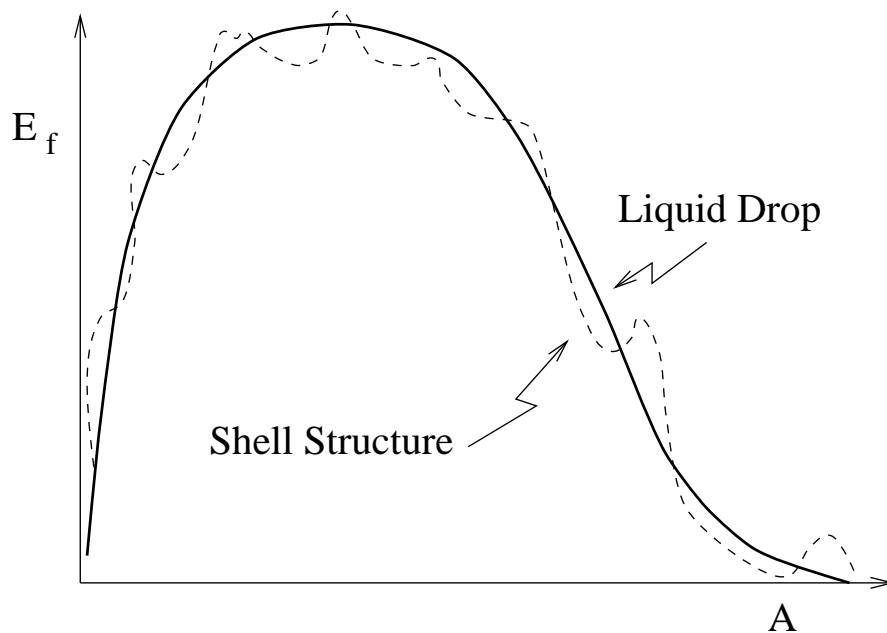
For spontaneous fission, the fission barrier $E_f = 3 - 6 \text{ MeV}$ and the energy released $E_R \sim 220 \text{ MeV}$. The fission barrier is also known as the activation energy, and is large for $A < 200$ (20–50 MeV) but reduces to a few MeV above $A = 230$.

The height of the fission barrier for $A \sim 240$ is given by putting $|\varepsilon| = 0.29$ and noting that $A^{2/3}$ varies slowly with A :

$$E_f \approx 0.455 \left[49 - \frac{Z^2}{A} \right] \text{ MeV},$$

which estimates that the barrier height for ^{238}U is 6.1 MeV . The fission barrier is similar to the Coulomb barrier and fission can take place by quantum mechanical tunnelling.

The lifetime for fission has an exponential dependence upon E_f and hence Z^2/A . This model does well for the general trend of experimental lifetimes, but not the fine details – for example, shell effects are observed:



36: The Spherical Shell Model

Experimental evidence for shell structure:

- Discontinuities in neutron binding energies as a function of A .
- Anomalies in the abundance of elements as a function of N or Z (magic numbers).
- First excited states of even- Z , even- N nuclei are anomalously high ($> 1.5\text{MeV}$) for Z or N magic (2, 8, 20, 28, 50, 82, 126).
- Trends in α - and β -decay energies — highest in magic-number nuclei, i.e. these nuclei are more tightly bound.
- Absorption cross-section measurements.
- Series of nuclei with lowest levels of the same angular momentum and parity (I^π).
- Quadrupole moments, proportional to deformation, are at a minimum for magic nuclei.
- Clusters of nuclear isomers near magic numbers.

37: Concept of a Shell Model

The observation of “magic numbers” indicate some very stable configurations for some kind of “orbits” or “shells” for nucleons similar to atomic electrons:
Magic numbers for Electrons: 2 10 18 36 54 86,
Magic numbers for Nucleons: 2 8 20 28 50 82 126.
The differences are in the Hamiltonian and associated forces.

How can we have orbits?

In an atom this is obvious – small nucleus and orbiting electrons. In a nucleus, there are short-range attractive and repulsive forces between the nucleons with no fixed attractive centre. The mean free path for a 10 *MeV* nucleon in nuclear matter is only ~ 2 *fm* – even one orbit around the nucleus is not possible without collision!

Nucleons are fermions and obey the Pauli Exclusion Principle, and there is a lot of order in the nucleus. Nucleons can only exchange energy in collisions within the nucleus if there is an unoccupied orbit (state or energy level) at lower energy.

38: The Mean Field

Normally these lower-energy orbitals are filled and so orbit-destroying collisions cannot occur. As a consequence, the nucleons move in different orbits (fixed energy states) with certain quantum numbers as though they were moving in a potential well without interacting with other nucleons.

The fundamental assumption of the shell model is that the potential felt by an individual nucleon is a mean field potential created by all the other nucleons, and on average this is a stable potential.

The nucleons, of radius 1 fm which take up $\sim 100\%$ of the nuclear volume of a nucleus of radius $4\text{-}7 \text{ fm}$, orbit as if they are transparent to each other.

For spherical nuclei, the potential must also be spherically symmetric and depend only on the distance r from the centre of the nucleus. The simplest potential is the square well, but is too great an approximation. Better potentials include the Harmonic Oscillator and Woods-Saxon single-particle potentials.

39: Single-Particle Shell Model

Assumption: Ignore detailed interactions between nucleons — each particle moves in a state independent of the other particles. The “mean field” force is the average smoothed-out interaction with all the other particles.

Suppose the actual short range interaction potential between two nucleons, i and j , is $v(r_{ij})$, then the average potential acting on each particle is

$$V_i(r_i) = \left\langle \sum_j v(r_{ij}) \right\rangle.$$

The Hamiltonian,

$$H = \sum_i T_i + \sum_{ij} v(r_{ij}),$$

can be rewritten as

$$H' = \sum_i [T_i + V_i(r_i)] + \lambda \left[\sum_{ij} v(r_{ij}) - \sum_i V_i(r_i) \right].$$

For $\lambda = 1$, $H' = H$. The shell-model assumption is that $\lambda \rightarrow 0$, i.e. the central interaction \gg residual interactions.

Choice of $V(r_i)$: A central potential that depends only on r_i , and is made up of a superposition of short-range internucleon potentials,

$$V(r_i) = \int v|r_i - r'| \rho(r') dr',$$

where $\rho(r')$ is the density distribution of the nucleus. If the internucleon potential is represented as a delta function $\Rightarrow v(r_{ij}) = -V_0\delta(r_{ij}) \Rightarrow$ then

$$V(r_i) = V_0\rho(r),$$

and the bound levels are given by solving the Schrödinger equation:

$$(T + V)\Psi(r) = E\Psi(r).$$

Potentials used include square-well, harmonic oscillator, Yukawa, and Woods-Saxon potentials. However, without the inclusion of a noncentral (spin-orbit) component, these potentials cannot predict the correct magic numbers or shell closures!

40: Potential Wells

Square well: –

$$V(r) = \begin{cases} -V_0 & r \leq R_0, \\ 0 & r > R_0. \end{cases}$$

Gaussian well: –

$$V(r) = -V_0 \exp \left[-(r/a)^2 \right]$$

Exponential well: –

$$V(r) = -V_0 \exp [-2r/a]$$

Yukawa well: –

$$V(r) = -V_0 \frac{\exp [-r/a]}{r}$$

Harmonic oscillator: –

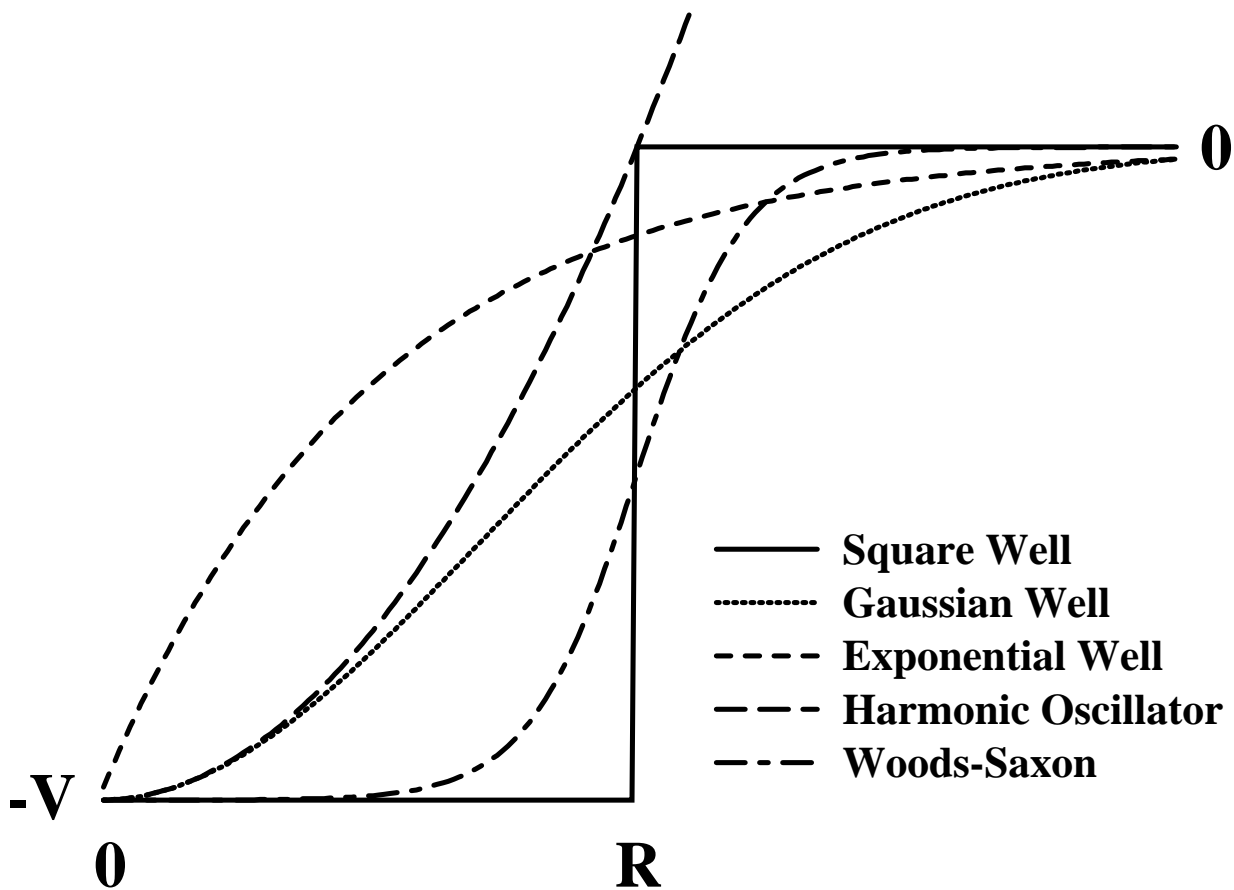
$$V(r) = \begin{cases} -V_0 \left[1 - (r/R_0)^2 \right] & r \leq R_0, \\ 0 & r > R_0. \end{cases}$$

Woods-Saxon: –

$$V(r) = \frac{-V_0}{1 + \exp [(r - R_0)/a]}$$

41: Well Comparisons

Here is a comparison of some of the potential wells that have been used to model the nuclear potential. The Woods-Saxon well represents the most realistic nuclear potential.



42: Square Well Potential

For a nucleon of mass M moving in a spherically symmetric potential $V(r)$ of radius R , with angular momentum $l\hbar$, the radial part of the Schrödinger equation is:

$$\frac{d^2}{dr^2}(rR_{nl}) + \frac{2M}{\hbar^2} \left[E_{nl} - V(r) - \frac{l(l+1)\hbar^2}{2Mr^2} \right] rR_{nl} = 0.$$

The eigenvalues of this problem are:

$$R_{nl} = \frac{A}{(\kappa r)^{1/2}} J_{l+1/2}(\kappa r),$$

where A is a constant, κ is the wave number of the nucleon,

$$\kappa^2 = \frac{2M}{\hbar^2} (E_{nl} + V),$$

$J_{l+1/2}(\kappa r)$ is a spherical Bessel function, and $-V$ is the well depth. If we measure the energy from the bottom of the well,

$$\kappa^2 = \frac{2M}{\hbar^2} E'_{nl}.$$

Boundary condition: the wavefunction must vanish at the potential well boundaries, i.e. $R_{nl}(R) = 0$ – zeroes of the Bessel function. The eigenvalues are labelled by $n = 1, 2, 3, \dots$. The more oscillations for a given l , the larger is n , the larger is κ , and hence the greater is the energy:

$$E'_{nl} = \frac{\kappa^2 \hbar^2}{2M} = \frac{(\kappa R)_0^2 \hbar^2}{2MR^2}.$$

The first few levels are (different to H atom!):

$$1s, 1p, 1d, 2s, 1f, 2p, 1g, 2d\dots$$

e.g. $2p$ represents the second level of orbital angular momentum 1, corresponding to the second zero in $J_{3/2}$. Each level has $2l + 1$ substates:

Level	Occupation	Total
$1s$	2	2
$1p$	6	8
$1d$	10	18
$2s$	2	20
$1f$	14	34
$2p$	6	40
$1g$	18	58

But not the correct magic numbers!

43: Harmonic Oscillator Potential

The Harmonic Oscillator potential may be expressed as:

$$V(r) = -V + \frac{1}{2}M\omega^2r^2,$$

where V is the well depth and ω is the frequency of the simple harmonic motion of the particle (not to be confused with collective rotational frequency!). This potential slowly changes all the way from the origin, tends to infinity for large r , and hence represents an unphysical potential. However, only the exponential tails of the wavefunctions are affected. It does have the advantage of being solvable analytically.

Solutions of the Schrödinger equation now contain Hermite polynomials. The eigenvalues are:

$$\text{1D} \quad E'_n = \left(n + \frac{1}{2}\right) \hbar\omega,$$

$$\text{3D} \quad E'_{n_1n_2n_3} = \left(n_1 + n_2 + n_3 + \frac{3}{2}\right) \hbar\omega,$$

$$\text{or} \quad E'_N = \left(N + \frac{3}{2}\right) \hbar\omega.$$

For each value of N there is a degenerate group of levels with different l , such that $l \leq N$ and even- l corresponds to even- N , odd- l corresponds to odd- N . The parity of the levels is given by:

$$\pi = (-1)^l = (-1)^N.$$

The states are grouped together according to:

N	Levels
0	1s
1	1p
2	1d, 2s
3	1f, 2p
4	1g, 2d, 3s

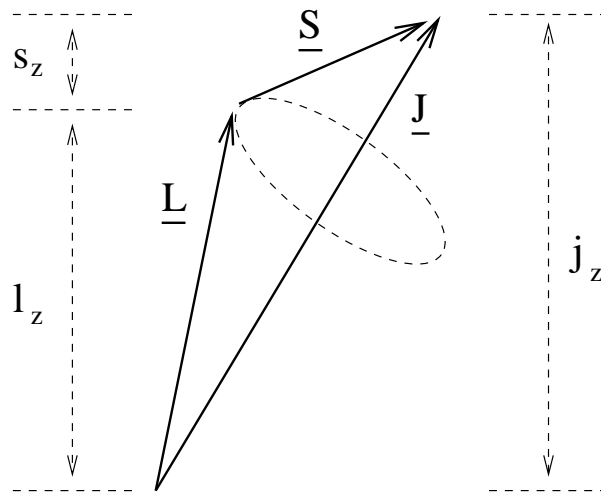
Each set of levels (equally spaced) can be occupied by $(N + 1)(N + 2)$ identical nucleons.

N	Allowed l	$E'_N(\hbar\omega)$	Occupation	Total
0	0	3/2	2	2
1	1	5/2	6	8
2	2, 0	7/2	12	20
3	3, 1	9/2	20	40
4	4, 2, 0	11/2	30	70
5	5, 3, 1	13/2	42	112

Again not the correct magic numbers!

44: Spin-Orbit Potential

In atomic physics, the spin-orbit interaction comes about due to the interaction of an electron's magnetic moment with the magnetic field generated by its motion about the nucleus – this is a very small effect, of the order of 10^{-5} .



A similar interaction was introduced for nuclei to empirically fit the magic numbers:

$$V(r) \Rightarrow V(r) + W(r)\vec{L}\cdot\vec{S},$$

and we now know that a strong nucleon-nucleon spin-orbit interaction exists from $p - p$ scattering experiments. This interaction cancels out in the centre of the nucleus and is strongest at the nuclear surface.

45: Eigenvalues of $\vec{L} \cdot \vec{S}$

The total angular momentum operator \vec{J} and $\vec{L} \cdot \vec{S}$ commute with \vec{J}^2 , J_z , \vec{L}^2 , and \vec{S}^2 , but not L_z or S_z (\vec{L} and \vec{S} precess around \vec{J}). The good quantum numbers are thus:

$$j, j_z, l, \text{ and } s.$$

The eigenvalues of $\vec{L} \cdot \vec{S}$ can be found from:

$$\begin{aligned} \vec{J}^2 &= (\vec{L} + \vec{S})^2 = \vec{L}^2 + 2\vec{L} \cdot \vec{S} + \vec{S}^2, \\ j(j+1)\hbar^2 &= l(l+1)\hbar^2 + 2\vec{L} \cdot \vec{S} + s(s+1)\hbar^2. \\ \text{For } \vec{J} = \vec{l} + 1/2 &\Rightarrow \vec{L} \cdot \vec{S} = \frac{1}{2}l\hbar^2; \\ \text{For } \vec{J} = \vec{l} - 1/2 &\Rightarrow \vec{L} \cdot \vec{S} = -\frac{1}{2}(l+1)\hbar^2, \end{aligned}$$

i.e. the eigenvalues of $\vec{L} \cdot \vec{S}$ are proportional to l .

The magic numbers can only be obtained if the spin-orbit potential $W(r)$ is negative. This is the opposite way to the electron spin-orbit potential in atoms. In nuclei, the $\vec{J} = \vec{l} + 1/2$ orbits are lowered with respect to the $\vec{J} = \vec{l} - 1/2$ orbits.

46: Central + Spin-Orbit Potential

In order to reproduce the correct magic numbers, a noncentral component must be added to the nuclear potential. A relativistic treatment of electrons in atoms yields a spin-dependent force in the form of a spin-orbit coupling:

$$V_{so} = f(r)\mathbf{l}\cdot\mathbf{s}.$$

This potential splits the otherwise degenerate levels with $j = l \pm \frac{1}{2}$. Such a splitting has also been observed experimentally in nuclear physics. Making the spin-orbit attractive accounts for the observation that the $j = l + \frac{1}{2}$ states are always lower in energy than the $j = l - \frac{1}{2}$ states (this is opposite to the spin-orbit interaction in atoms!). The force is given by:

$$f(r) = \lambda \frac{1}{r} \frac{dV}{dr}, \text{ with } \lambda \approx -0.5 fm^2.$$

The levels of the Harmonic Oscillator are split — each j state can hold $2j + 1$ identical particles. The states are labelled by nlj , e.g. $2p_{3/2}$.

The splitting is proportional to l which can give rise to unnatural parity or intruder states. These are states for which the spin-orbit interaction is large enough to reduce the energy of these states such that they “intrude” into the next lowest major oscillator shell.

Nucleons within the centre of the nucleus are screened from the asymmetric distribution that appears at the boundary — they should feel no net force — the central part of the potential should be approximately constant. The addition of an attractive force proportional to l^2 flattens the effective radial shape of the potential.

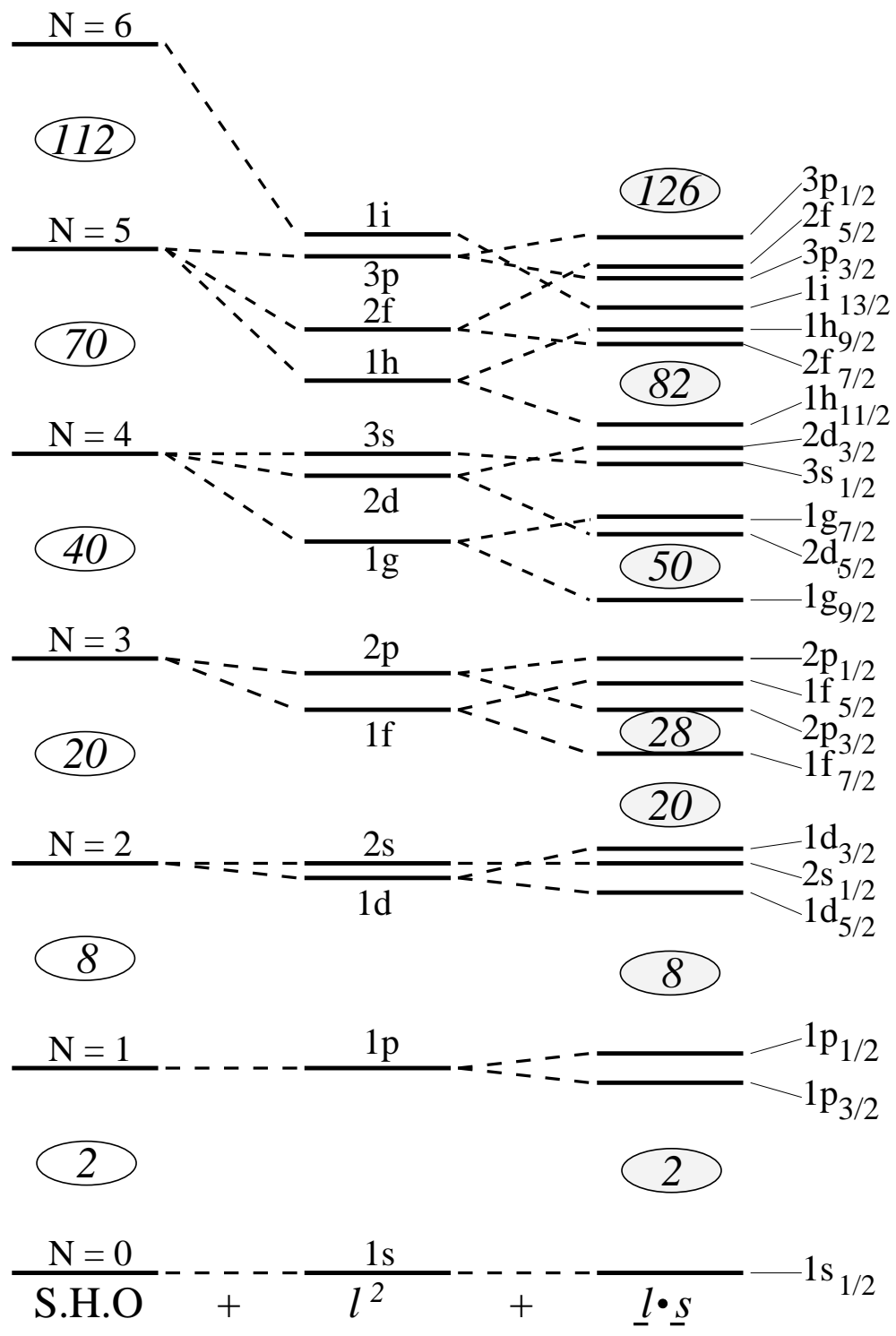
With these modifications, the magic numbers:

$$2, 8, 20, 28, 50, 82, 126$$

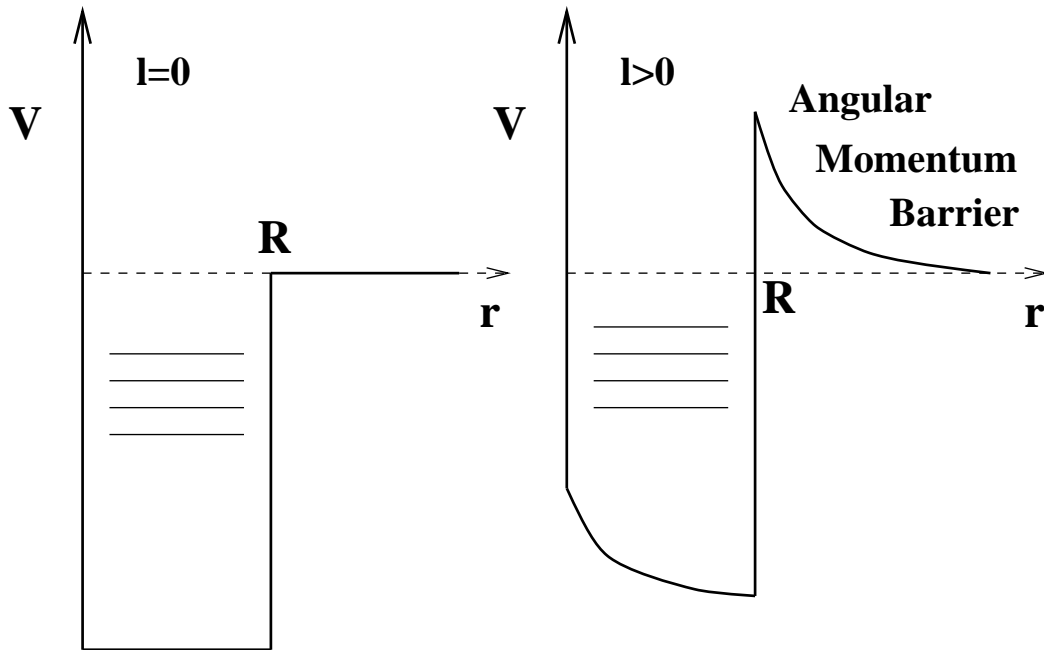
are reproduced. For example, some of the $N = 3$ and $N = 4$ states can be grouped together in a single shell:

$$28... \overbrace{2p_{3/2}, 1f_{5/2}, 2p_{1/2}}^{N=3}, \overbrace{1g_{9/2}}^{N=4} \dots 50.$$

47: Spherical Shell Model Energy Levels



48: Angular Momentum Barrier



A simple square well potential is shown for a neutron with no orbital angular momentum l (left) and with orbital angular momentum (right). The Schrödinger equation for a nucleon in a square well potential contains a term:

$$\frac{l(l+1)\hbar^2}{2Mr^2},$$

which leads to a quantum mechanical Angular Momentum Barrier.

49: Spins and Parities of Nuclear States

- Ground state spins

The shell model scheme can be used to predict the spins of the ground states of nuclei. Any level (n, l, j) which is fully occupied $(2j + 1)$ contributes nothing to the nuclear spin as the angular momentum components sum to zero. The pairing force leads to another simple hypothesis that two neutrons (or protons) occupying the same level (j, l) have their angular momentum coupled to zero – they move in time-reversed orbits. Therefore:

- Even-even nuclei will have a spin and parity 0^+ in the ground state,
- The unpaired nucleon will give the spin and parity of odd nuclei.

${}_{12}^{25}\text{Mg}$ has 13 neutron – last in $1d_{5/2} \Rightarrow 5/2^+$ (\checkmark)

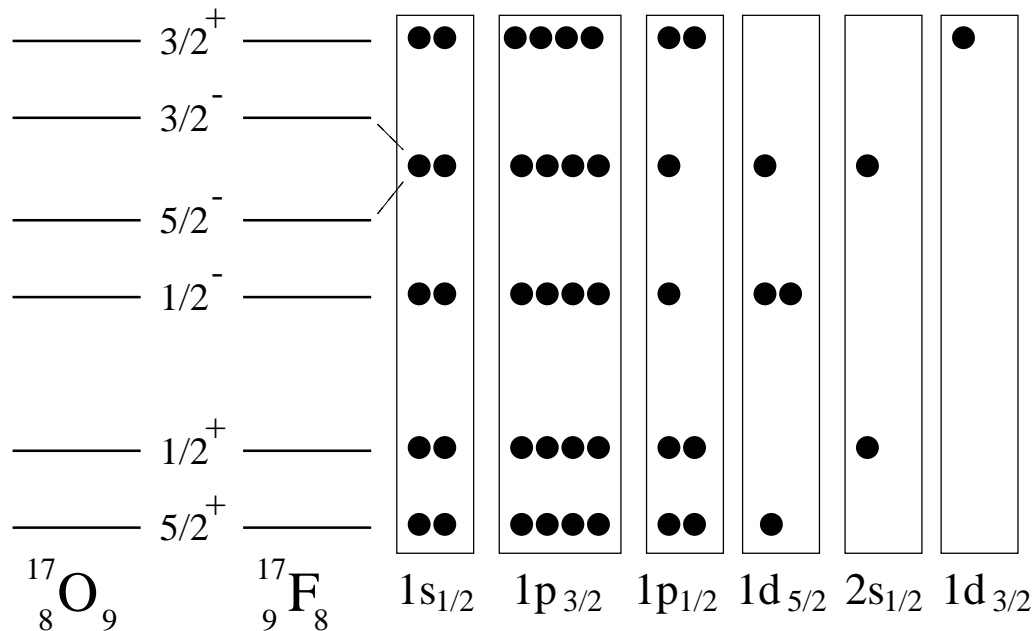
${}_{32}^{73}\text{Ge}$ has 41 neutron – last in $1g_{9/2} \Rightarrow 9/2^+$ (\checkmark)

${}_{56}^{137}\text{Ba}$ has 81 neutron – last in $1h_{11/2} \Rightarrow 11/2^-$ (\times)

The last example should be $3/2^+$ ($2d_{3/2}$) – the scheme works for spherical nuclei.

- Excited state spins

If we give energy to the nucleus, then the odd particle can be promoted to a higher shell-model orbital and create an excited state. Here is an example for the mirror nuclei ^{17}O and ^{17}F .



The ground state corresponds to the odd nucleon in the $1d_{5/2}$ orbital ($5/2^+$). The first excited state corresponds to moving this last nucleon into the higher energy $2s_{1/2}$ level ($1/2^+$). The second excited state ($1/2^-$) corresponds to removing a particle from the lower $1p_{1/2}$ orbital and placing it in the $1d_{5/2}$ orbital. The next configuration has three odd nucleons which can couple to spin $3/2^-$ or $5/2^-$.

50: Magnetic Dipole Moments

Nuclei with a nuclear spin that is greater than $1/2$ will have a magnetic dipole moment μ which provides a measure of the current distribution in the nucleus. It is generated by the orbital motion of the protons and by the intrinsic spins of the nucleons.

Consider a current loop – the magnetic moment is simply the area of the loop times the current:

$$\mu = iA = \frac{ev}{2\pi r} \pi r^2 = \frac{e}{2m} mvr = \frac{e}{2m} l,$$

where l is the orbital angular momentum. From quantum mechanics:

$$\mu = \frac{e}{2m} |\vec{l}| \hbar = |\vec{l}| \mu_N,$$

where μ_N is the Nuclear magneton:

$$\mu_N = 3.15 \times 10^{-8} \text{ eV/T}; (\mu_B = 5.8 \times 10^{-5} \text{ eV/T}).$$

For a nucleon with both spin and orbital motion, we have two contributions – introduce the g-factor:

$$\mu_l = g_l |\vec{l}| \mu_N; \quad \mu_s = g_s |\vec{s}| \mu_N.$$

The orbital and spin g -factors for free protons and neutrons are:

$$g_l = 1 \quad ; \quad g_s^{free} = 5.5856 \quad \text{proton,}$$

$$g_l = 0 \quad ; \quad g_s^{free} = -3.8262 \quad \text{neutron.}$$

These are very different to a $g = 2$, $s = 1/2$ point particle such as an electron and indicate that the nucleon must have an internal structure, i.e. quarks.

The interaction energy of a magnetic moment in a magnetic field is $\vec{\mu} \cdot \vec{B}$, or $\mu_z |\vec{B}|$. We can calculate the expected size of μ_z – Schmidt lines.

• For $j = l + 1/2$:

$$\mu_z = [lg_l + sg_s]\mu_N = \left[\left(j - \frac{1}{2} \right) g_l + \frac{1}{2} g_s \right] \mu_N,$$

• For $j = l - 1/2$:

$$\begin{aligned} \mu_z &= \frac{j}{j+1} [(l+1)g_l - sg_s] \mu_N, \\ &= \frac{j}{j+1} \left[\left(j + \frac{3}{2} \right) g_l - \frac{1}{2} g_s \right] \mu_N. \end{aligned}$$

Most nuclei fall between these limits – bound nucleons have different intrinsic magnetic moments than free nucleons ($g_s \rightarrow 0.6g_s^{free}$).

51: Calculated single-particle g-factors

An estimate of single-particle g-factors can be obtained using the relation:

$$g_K = g_l \pm \frac{1}{2l + 1} [g_s - g_l],$$

where the plus sign is for $l + \frac{1}{2}$ orbitals, and the minus sign is for $l - \frac{1}{2}$ orbitals. Using $g_s = 0.6g_s^{free}$, leads to the following values:

Orbital	g-factor	Orbital	g-factor
$\pi s_{1/2}$	3.351	$\nu s_{1/2}$	-2.296
$\pi p_{1/2}$	0.216	$\nu p_{1/2}$	0.765
$\pi p_{3/2}$	1.784	$\nu p_{3/2}$	-0.765
$\pi d_{3/2}$	0.530	$\nu d_{3/2}$	0.459
$\pi d_{5/2}$	1.470	$\nu d_{5/2}$	-0.459
$\pi f_{5/2}$	0.664	$\nu f_{5/2}$	0.328
$\pi f_{7/2}$	1.336	$\nu f_{7/2}$	-0.328
$\pi g_{7/2}$	0.739	$\nu g_{7/2}$	0.255
$\pi g_{9/2}$	1.261	$\nu g_{9/2}$	-0.255
$\pi h_{9/2}$	0.786	$\nu h_{9/2}$	0.209
$\pi h_{11/2}$	1.214	$\nu h_{11/2}$	-0.209
$\pi i_{11/2}$	0.819	$\nu i_{11/2}$	0.177
$\pi i_{13/2}$	1.181	$\nu i_{13/2}$	-0.177

Note that proton g-factors are always positive, while the neutron g-factors can be positive or negative depending on the $l \pm s$ coupling.

52: Electric Quadrupole Moments

For a nucleus in its ground state, the electric quadrupole moment is related to the energy of the charge distribution as a function of its orientation in an electric field. Classically, $Q_0 \propto (3z^2 - r^2)$ for axial symmetry where z is the orientation of the field. For a sphere,

$$\bar{x}^2 + \bar{y}^2 + \bar{z}^2 = \frac{1}{3}\bar{r}^2 \text{ and } Q_0 = 0.$$

The classical equation:

$$Q_0 = \int_V \rho(r, \theta)(3z^2 - r^2)dV,$$

translates (quantum mechanics) to :

$$\langle Q_0 \rangle = \sum_i^Z \int_V \psi_i^*(3z^2 - r^2)\psi_i dV,$$

for all the protons. For an odd- Z nucleus near a closed shell, Q_0 is entirely due to the last unpaired proton in an equatorial orbit. The simplest model gives:

$$Q_0 = -r^2 = -(r_0 A^{1/3})^2 \text{ electron barns or } e b.$$

Orbits are not exactly in $x - y$ plane, hence:

$$Q_0 = - \left(\frac{2j - 1}{2j + 1} \right) r_0^2 A^{2/3} \text{ and } Q_0 = 0 \text{ for } j = 1/2.$$

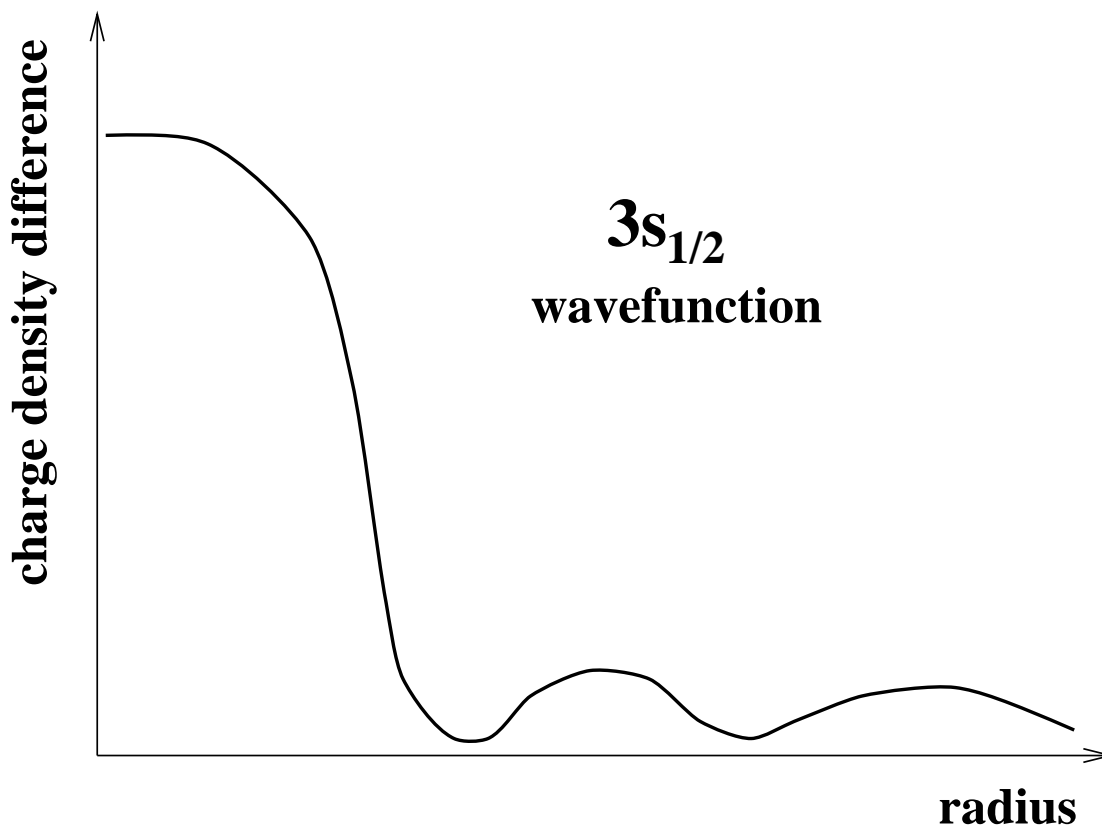
Nuclide	Odd Proton		${}_{16}^{32}\text{S}$	${}_{40}^{91}\text{Zr}$
	${}_{17}^{37}\text{Cl}$	${}_{51}^{121}\text{Sb}$		
Expt. Value	-0.08	-0.36	-0.06	-0.24
Model Values				
r^2	0.15	0.35	0	0
j	$3/2^+$	$7/2^+$	0^+	$5/2^+$
Q_0	-0.06	-0.24	0	0

There is reasonable agreement for odd-proton nuclei, but not for odd-neutron nuclei near closed shells. For odd-neutron nuclei there must be a contribution from the protons. Nuclei with a proton below a closed shell have opposite signs of Q_0 – holes in a closed shell. Very large values of Q_0 have also been measured, e.g. 5.5 e b for ${}^{175}\text{Lu}$, implying nuclear deformation (nonspherical shapes) away from the closed shells.

53: Wavefunction of an Orbital

It is possible to determine the charge density of a nucleon in a specific orbital. This can be achieved from differences in the charge density of neighbouring nuclei measured by electron scattering.

- Example – $^{206}_{82}\text{Pb}$ and $^{205}_{81}\text{Tl}$ differ by a $3s_{1/2}$ proton. The charge density differences look like the $3s_{1/2}$ oscillator wavefunction:



54: Nuclear Excitations

There are two basic types of nuclear excitation:

- Single-particle motion

This represents an “out of phase” motion and leads to shell structure and single-nucleon states. The Shell Model describes those particular nuclear properties in which only the nucleons in the vicinity of the Fermi surface are involved.

- Collective motion

This represents an “in phase” or coherent motion of all the nucleons and leads to deformation, vibrational, and rotational degrees of freedom. The Liquid Drop Model describes the bulk nuclear properties which depend on the nucleon number in a smooth way.

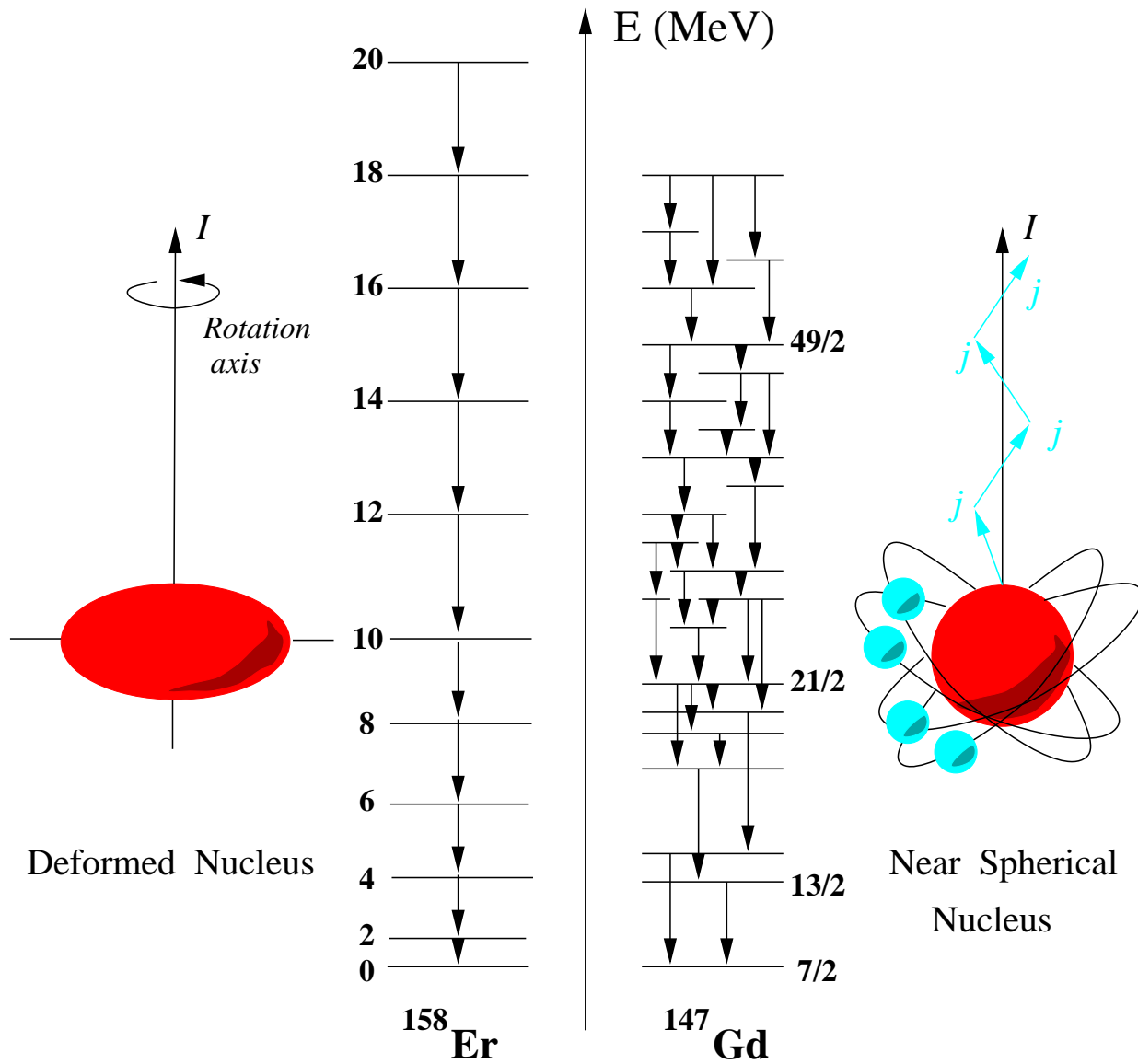
Nuclear structure physics involves the delicate interplay between these two fundamental modes of excitation.

“The interaction of protons and neutrons turns out to be very complicated. It’s like trying to study the behaviour of a herd of animals.” – Prof. John F Sharpey-Schafer, *The Guardian*, Feb 1, 1991.

“The comparison of the nucleons in a nucleus with a herd of animals is certainly not a complete description but a striking one. In the wild, animals often gain shelter by forming a herd. Individual animals may break out of the herd, but these are rapidly attracted back by the safety and guidance of the collective. The collective depends on the contribution of the single members, but when it has been formed it determines the action of the individuals.” – Heiko Timmers, Thesis, Liverpool 1991.

55: Generation of Angular Momentum

Examples of the collective (left) and noncollective (right) generation of the nuclear spin:



56: Spherical Harmonic Vibrator

Spherical nuclei near closed shells show vibrational spectra. The eigenvalues are:

$$E_n = E_0 + n\hbar\omega; \quad n = 0, 1, 2, \dots,$$

i.e. the energy levels are equally spaced. For quadrupole surface vibrations, each phonon carries angular momentum 2 and has positive parity. ^{110}Cd is the best known example of a vibrator.

$$\begin{array}{ll}
 n=3 & \text{————— } 0^+, 2^+, 3^+, 4^+, 6^+ \\
 n=2 & \text{————— } 0^+, 2^+, 4^+ \\
 n=1 & \text{————— } 2^+ \\
 n=0 & \text{————— } 0^+
 \end{array}$$

Note that:

$$\frac{E(4^+)}{E(2^+)} = 2, \quad \frac{E(6^+)}{E(2^+)} = 3.$$

57: Particle-Vibration Coupling

For an odd-A nucleus near a closed shell with small deformation, the odd particle may couple to the surface vibrations of the core:

$$H = [H_{int} + H_{vib}] + H_{coup} = H_0 + H_{coup}.$$

If we assume that the interaction $H_{coup} \rightarrow 0$, the motions are decoupled from each other and the eigenfunctions will take a product form:

$$H_0\phi = E\phi; \quad \phi = \phi_{int}\phi_{vib}.$$

Consider coupling an $h_{9/2}$ proton to the 0^+ and 3^- states in ^{208}Pb , forming states in ^{209}Bi . Seven degenerate states with spins $3/2 \leq I \leq 15/2$ are formed by coupling the spin vectors 3 and $9/2$.



58: Nuclear Deformation

Evidence for static nuclear deformation:

- Large quadrupole moments for nuclei away from closed shells.
- Existence of rotational bands.
- Single-particle spectra which cannot be explained in the framework of the spherical shell model.

In the description of a “drop” of nuclear matter with a sharp surface, the equipotential surface $R(\theta, \phi)$ can be expressed as a sum over spherical harmonics:

$$R(\theta, \phi) = C(\alpha_{\lambda\mu})R_0 \left[1 + \sum_{\lambda\mu} \alpha_{\lambda\mu} Y_{\lambda\mu}(\theta, \phi) \right],$$

where R_0 is the radius of a sphere of the same volume. The factor $C(\alpha_{\lambda\mu})$ is introduced to satisfy the condition of conservation of volume. The expansion is often limited to quadrupole ($\lambda = 2$) and hexadecapole ($\lambda = 4$) degrees of freedom.

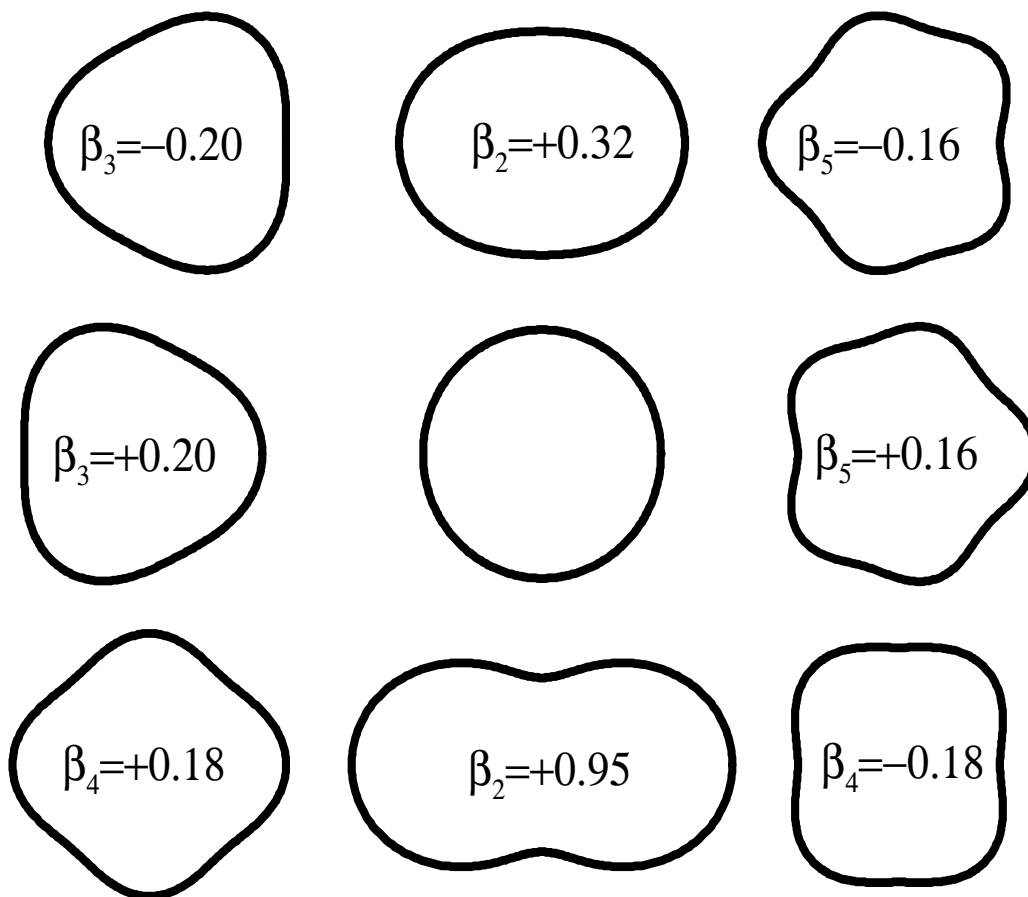
59: Microscopic Basis of Deformation

For closed-shell nuclei, the nucleonic orbits are oriented equally in all directions and the nucleus is spherical. The orbits of individual particles ($j > \frac{1}{2}$) are strongly anisotropic, and the self-consistent field deviates significantly from sphericity. The equilibrium nuclear shape results from a competition between the deforming power of individual nucleons and the effect of pairing forces which favour spherical symmetry.

In the regions of closed shells, the pairing dominates and spherical nuclei result. The addition of a few nucleons drives the equilibrium shape away from sphericity, a coherent effect from all these nucleons. Moving away from closed shells, the nuclei gradually become softer against deformation, which is manifested as a decrease of the frequency for collective vibrations about a spherical equilibrium shape. For sufficiently many particles, the nucleus develops an ellipsoidal shape and collective rotational modes occur.

60: Spherical Harmonic Shapes

The shapes of the lower spherical harmonics are shown below. The overall nuclear shape may be expressed as a sum of these spherical harmonics.



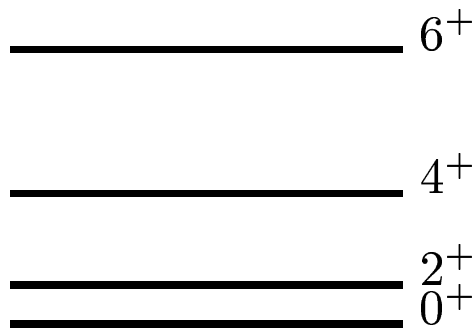
61: Collective Nuclear Rotation

Deformation provides an element of anisotropy allowing the definition of a nuclear orientation and the possibility of observing the effects of rotation in some nuclei — about an axis perpendicular to the symmetry axis. Classically,

$$E_{rot} = \frac{1}{2} \mathcal{I} \omega^2 = \frac{I^2}{2\mathcal{I}}; \quad \omega = \frac{I}{\mathcal{I}},$$

Collective rotation involves the coherent contributions from many nucleons and gives rise to a smooth relation between energy and angular momentum:

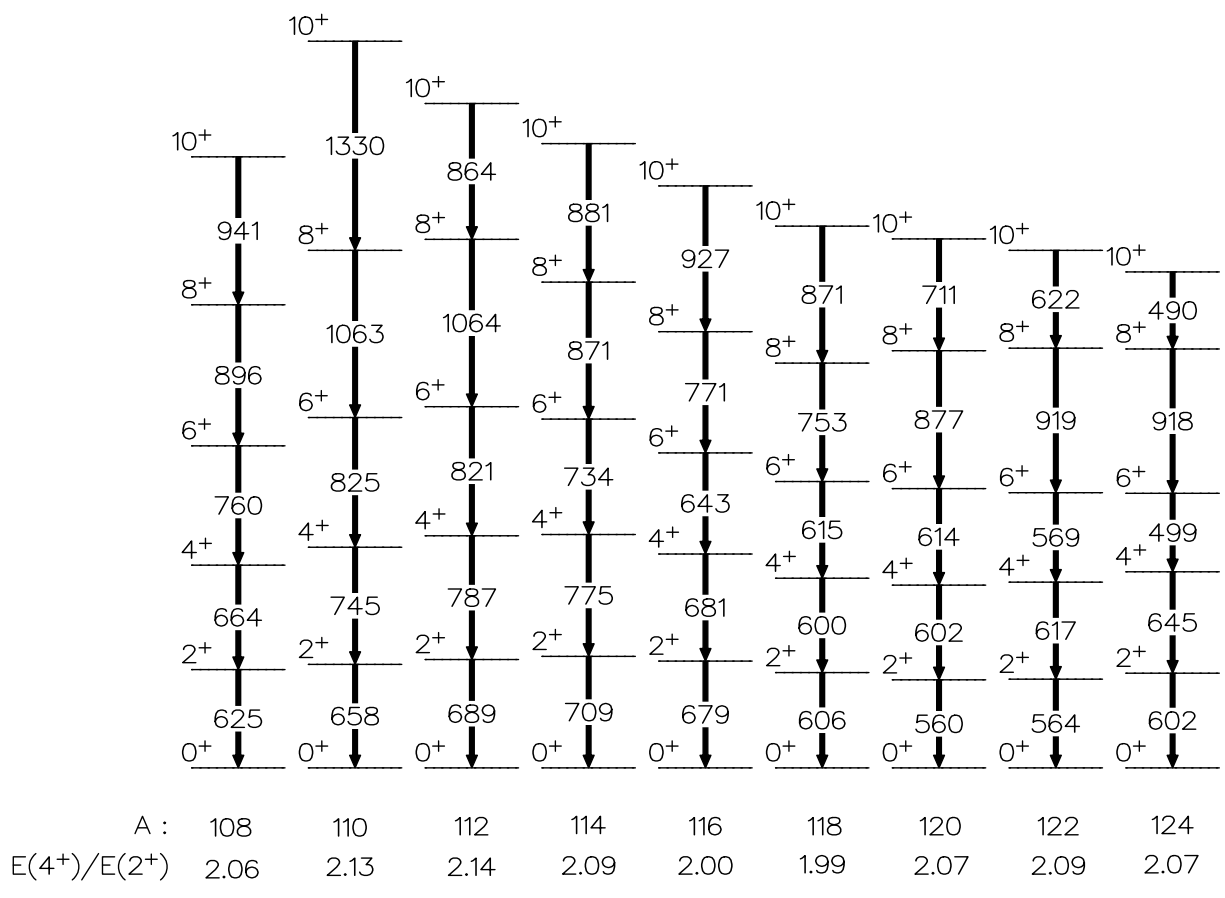
$$E(I) = \frac{\hbar^2}{2\mathcal{I}} I(I + 1).$$



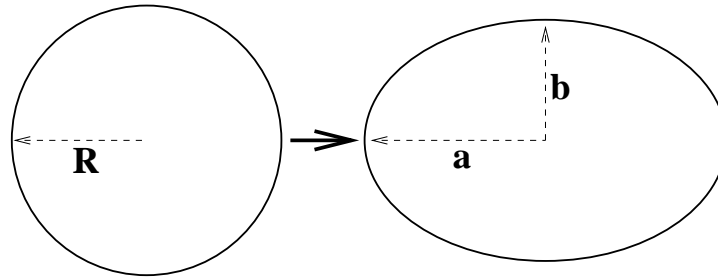
$$\frac{E(4^+)}{E(2^+)} = 3.33, \quad \frac{E(6^+)}{E(2^+)} = 7.0.$$

62: Vibration or Rotation?

The ratio of 4^+ energy levels to 2^+ energy levels gives an indication of whether a nucleus is a vibrator or a rotor. In the vibrational limit, this energy ratio is equal to 2.0 ($E \propto n$), while in the rotational limit it is equal to 3.33 ($E \propto I(I + 1)$). Tellurium ($Z = 52$) systematics are shown below, and appear vibrational ($Z \sim 50$, i.e. closed shell).



63: Nuclear moment of Inertia



$$a = R(1 + \varepsilon); \quad b = \frac{R}{\sqrt{1 + \varepsilon}}$$

For a spherical nucleus, the rigid-body moment of inertia is:

$$\mathcal{I}_{rigid} = \frac{2}{5}MR^2 = \frac{2}{5}A^{5/3}m_N r_0^2,$$

where m_N is the mass of a nucleon ($M = Am_N$) and $R = r_0 A^{1/3}$ ($r_0 = 1.2 \text{ fm}$). For an ellipsoid, the moment of inertia is modified:

$$\mathcal{I}(\varepsilon) = \left[1 + \frac{3}{4}\varepsilon \right] \mathcal{I}(\varepsilon = 0),$$

i.e. the moment of inertia increases for a prolate shape ($\varepsilon > 0$).

64: Example for ^{168}Yb

I^π	E_x (keV)	E_x/E_{2^+}	Model	\mathcal{J} (\hbar^2/MeV)
2^+	87	1.00	1.00	34.5
4^+	287	3.30	3.33	34.8
6^+	585	6.72	7.00	35.9
8^+	970	11.15	12.00	37.1
10^+	1426	16.40	18.33	38.6

$$\begin{aligned}\mathcal{J}_{rigid}(\varepsilon = 0) &= 70 \hbar^2/\text{MeV}, \\ \mathcal{J}_{rigid}(\varepsilon = 0.25) &= 83 \hbar^2/\text{MeV}.\end{aligned}$$

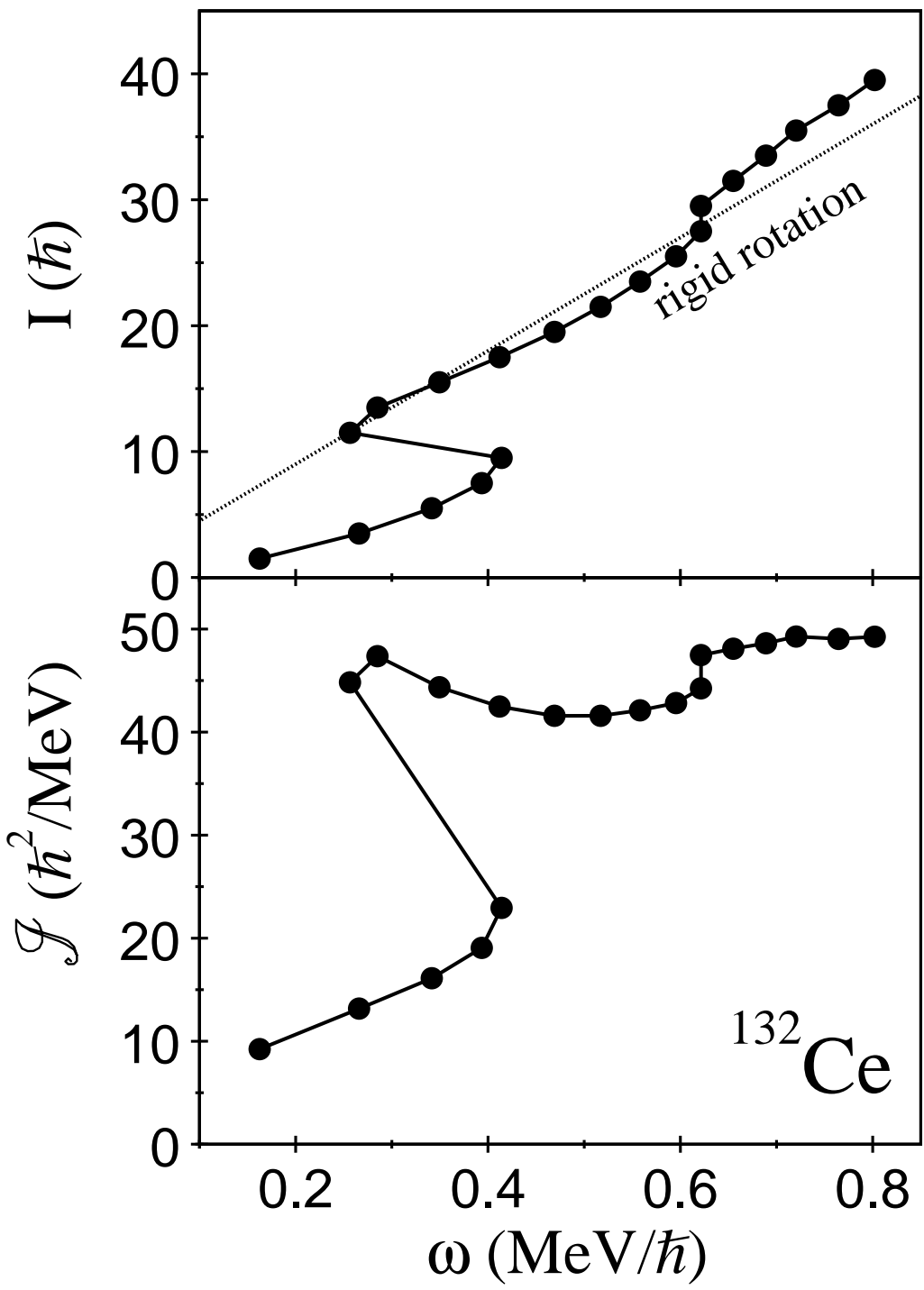
Although the energy level ratios (E_x/E_{2^+}) are in reasonable agreement, the experimental moments of inertia are only 40% of the rigid-body value!

If the nucleus were a fluid:

$$\mathcal{J}_{fluid} \approx \varepsilon^2 \mathcal{J}_{rigid} \sim 7 - 8 \hbar^2/\text{MeV},$$

but this is too small – the nucleus may be considered as a rigid core plus fluid of valence nucleons (compare rotation of a raw egg with a hard-boiled egg!).

65: Backbending



66: Quadrupole Moment

For an ellipsoid of deformation ε , the quadrupole moment is:

$$Q_0 = \frac{2}{5}Z(a^2 - b^2) = \frac{6}{5}Z\varepsilon R^2,$$

i.e. proportional to the deformation. Q_0 is the intrinsic quadrupole moment, measured in the rest frame of the nucleus. The ground-state quadrupole moment of an odd- A nucleus is positive (i.e. prolate). However, if this prolate shape rotates, the average shape appears oblate! – the quadrupole moment has opposite sign, i.e.

$$Q(2^+) \approx -\frac{2}{7}Q_0.$$

e.g. for ${}^{168}_{70}\text{Yb}_{98}$, the measured $Q(2^+) = -2 e b$, from which it can be deduced that $\varepsilon \approx 0.13$ and the nuclear axis ratio is:

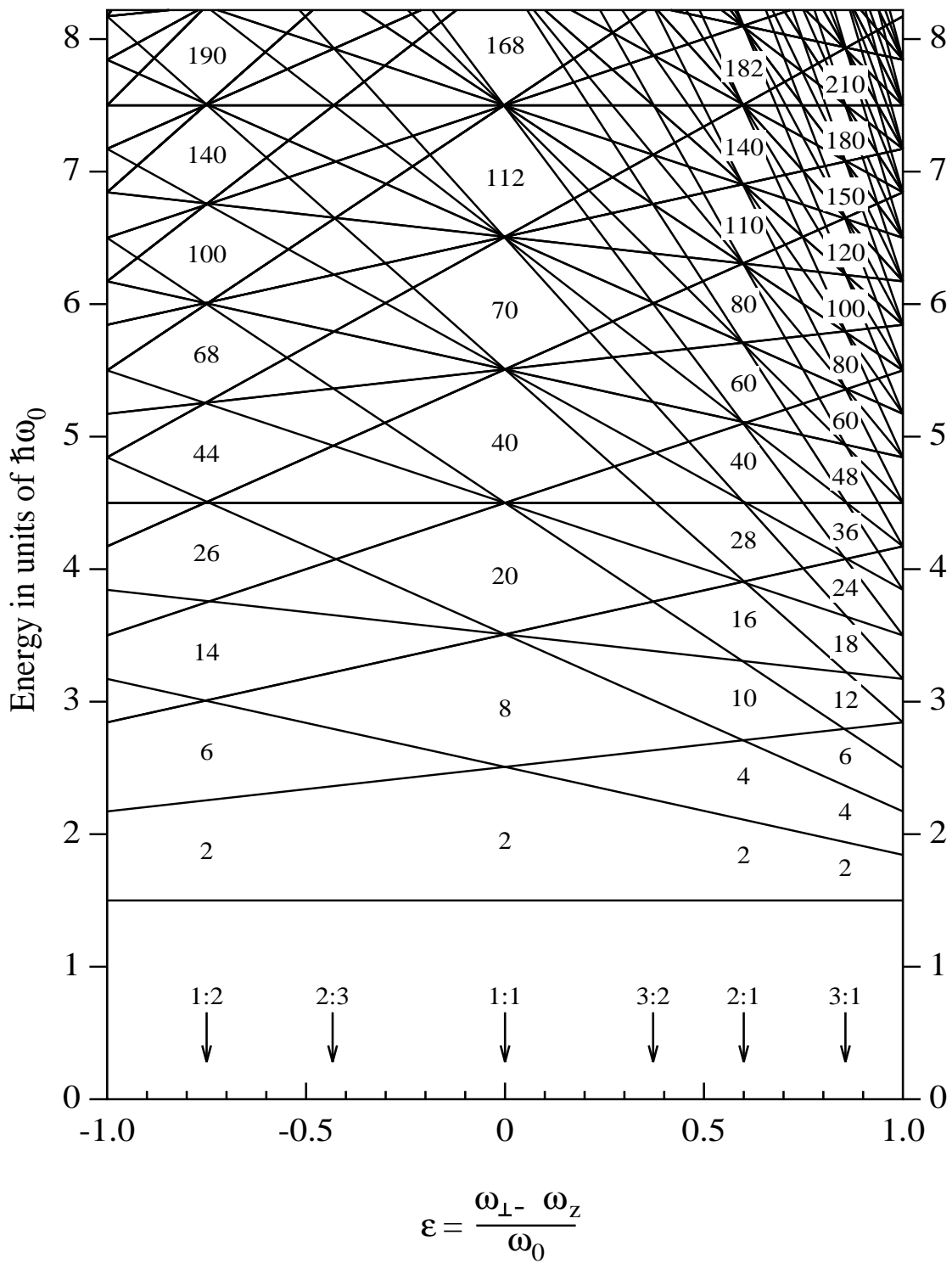
$$\frac{a}{b} = \left[1 + \frac{5}{3}\varepsilon \right] = 1.2.$$

67: Superdeformation

If we consider nuclear energy levels as a function of deformation, the shell model suggests that shell gaps appear for nuclear shapes with simple integer ratios of the axes ($a/b = 3/2, 2/1, \dots$). The shell gaps correspond to magic numbers different from the spherical case. A superdeformed shape corresponds to an axis ratio of 2:1 and a classic example is $^{152}_{66}\text{Dy}_{86}$ at high spin (Liverpool work: P.J. Twin et al.). A very regular sequence of γ -rays is observed with a constant energy separation corresponding to a high moment of inertia ($85 \hbar^2/\text{MeV}$).

Nuclei characteristic of the 3:2 axis ratio are found for $A \sim 130$ around $^{132}_{58}\text{Ce}_{74}$ at high spin (again Liverpool work: P.J. Nolan et al.), while nuclei showing intermediate deformations are found for $A \sim 80$ and $A \sim 190$ – we need to consider other effects (Coulomb energy, surface energy) rather than just shell gaps.

68: Deformed Shell Gaps



69: Isospin

The concept of “isotopic spin” or isospin arises from the charge independence of the nuclear force.

Similar to the intrinsic spin \vec{S} , we can introduce an isospin vector \vec{T} in an “abstract” mathematical space (isospace!) which has similar transformation properties to the intrinsic spin \vec{S} of a nucleon.

Recall that \vec{S} is a vector of length $\sqrt{S(S+1)}\hbar$ ($S = 1/2$) and that the projection S_z on the z quantisation axis can only take values $\pm 1/2$ (in units of \hbar). We can apply the same formalism to isospin (Heisenberg) and define for a single nucleon ($|\vec{T}| = \sqrt{T(T+1)}$, $T = 1/2$):

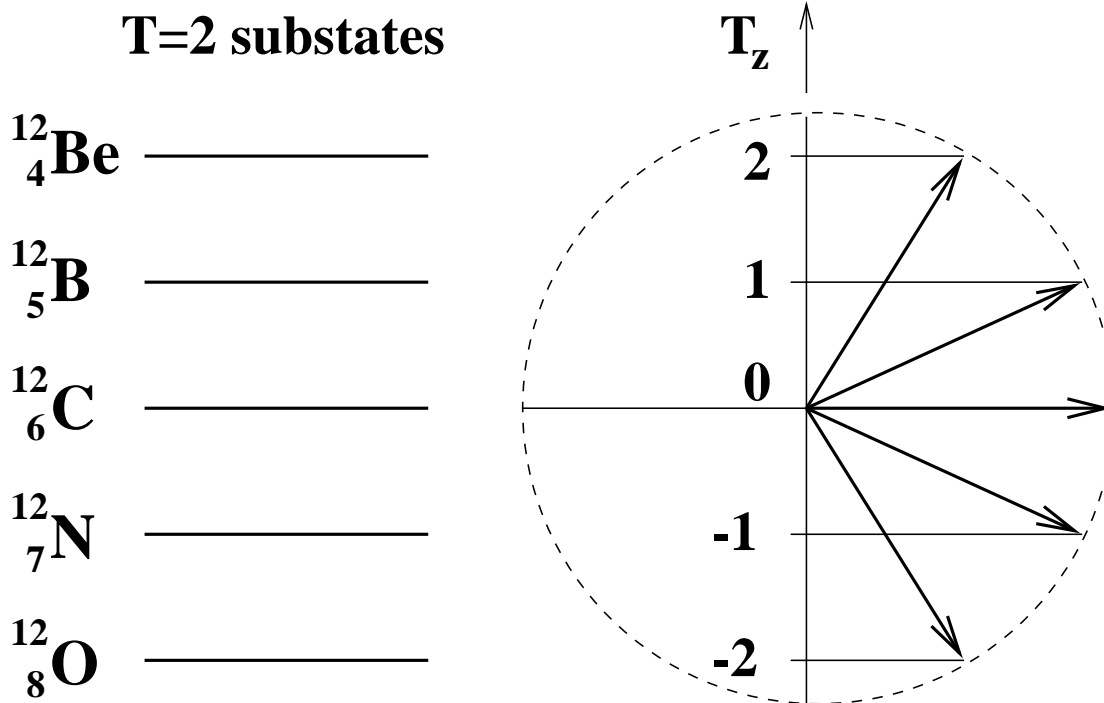
$$T_z = -\frac{1}{2} \Rightarrow \text{proton}, T_z = +\frac{1}{2} \Rightarrow \text{neutron}.$$

\vec{T} is a well defined vector in isospace and is conserved in nuclear processes. For a many nucleon system:

$$\vec{T} = \sum_i \vec{T}_i, \text{ and } T_z = \frac{1}{2}(N - Z).$$

70: Isospin Substates

Again by analogy with spin, an isospin T state has $(2T + 1)$ substates. For example, $T = 2$ corresponds to a vector of length $\sqrt{6}$ with components $-2 \leq T_z \leq +2$. The substates correspond to states in different nuclei, as illustrated below for the $A = 12$ isobars:



71: Isobaric Analogue States

Consider an odd- A nucleus made up of Z protons and N neutrons. A mirror nucleus is made by interchanging the numbers of protons and neutrons. At low mass, we can start with an $N = Z$ nucleus (A, N, Z) and add either one proton ($A + 1, N, Z + 1$) or one neutron ($A + 1, N + 1, Z$). The spectrum of proton states in the first nucleus should be equal to the spectrum of neutron states in the second, reflecting (!) the charge independence of the nuclear force.

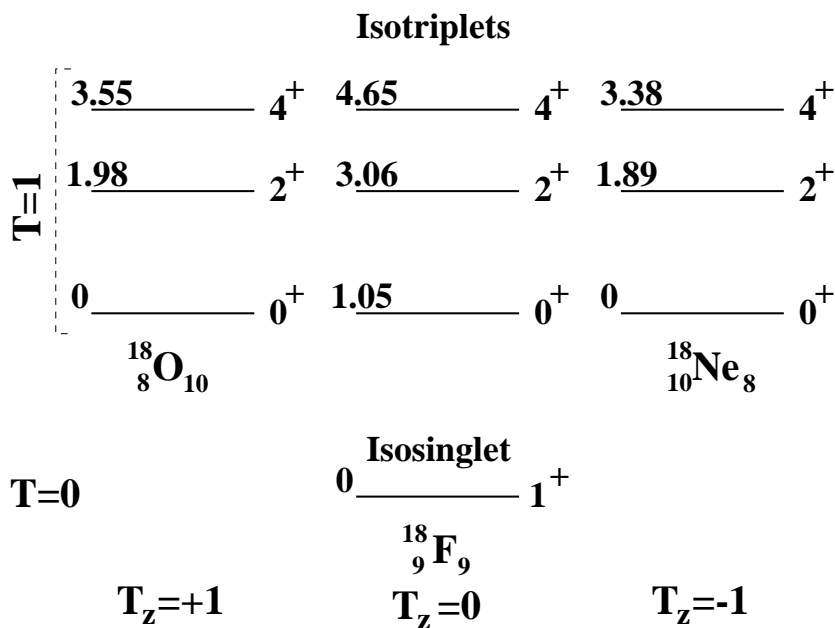
Isodoublets

<u>2.87</u>	$7/2^+$	<u>2.81</u>
<u>2.79</u>	$1/2^+$	<u>2.43</u>
<u>1.75</u>	$7/2^+$	<u>1.71</u>
<u>0.35</u>	$5/2^+$	<u>0.34</u>
0	$3/2^+$	0
${}_{10}^{21}\text{Ne}_{11}$		${}_{11}^{21}\text{Na}_{10}$
$T_z = +1/2$		$T_z = -1/2$

In the example of the mirror nuclei ${}^{21}_{10}\text{Ne}_{11}$ and ${}^{21}_{11}\text{Na}_{10}$, we have set the ground states to be equal by taking into account the neutron-proton mass difference (1.293 MeV). The levels for this $T = 1/2$ system form isodoublets with $T_z = \pm 1/2$. The only differences in the excitation energies should arise from the Coulomb energy (extra proton in ${}^{21}\text{Na}$):

$$\Delta E_{Coulomb} = \frac{6}{5} \frac{Ze^2}{4\pi\epsilon_0 R}$$

Next consider the $A = 18$ isobars. For $T = 0$ there is only an isosinglet state, but for $T = 1$ we can have three substates: $T_z = -1, 0, +1$ – isotriplets.



72: Electromagnetic Revision

The energy of an electromagnetic radiation field can be described mathematically in terms of a multipole moment expansion. This expansion converges rapidly and consequently only the lower orders are of importance. The terms correspond to 2^n -poles and the lowest terms are labelled below:

n	Name
0	Monopole
1	Dipole
2	Quadrupole
3	Octupole
4	Hexadecapole
5	(Latin for 32)pole

The multipole moments are dependent on charge and current densities and so the study of the lower multiple orders allows information to be extracted on these properties.

For example, $M1$ moments are sensitive to nuclear magnetic moments and hence single-particle aspects, while $E2$ moments are sensitive to the nuclear charge distribution and hence collective effects such as deformation.

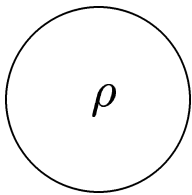
72.1: Electric Multipole Moments

An electric multipole moment can be expressed as:

$$Q_{\lambda\mu} \propto \int r^\lambda \rho(r) Y_{\lambda\mu}^*(\theta, \phi) dV,$$

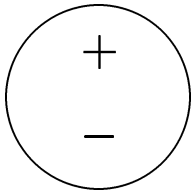
and is tensor of rank λ and parity $(-1)^\lambda$. There are $2(\lambda + 1)$ substates with $-\lambda \leq \mu \leq \lambda$.

- Monopole $\lambda = 0$:



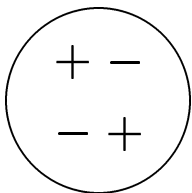
represents the charge distribution.

- Dipole $\lambda = 1$:



represents a separation of charge into a dipole configuration.

- Quadrupole $\lambda = 2$:

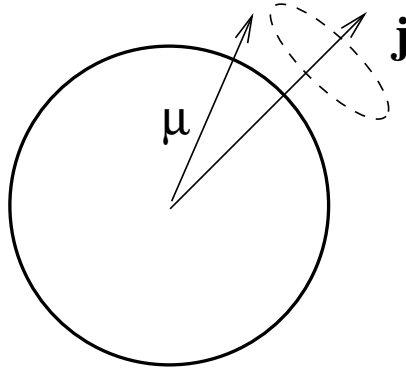


represents a separation of charge into a quadrupole configuration.

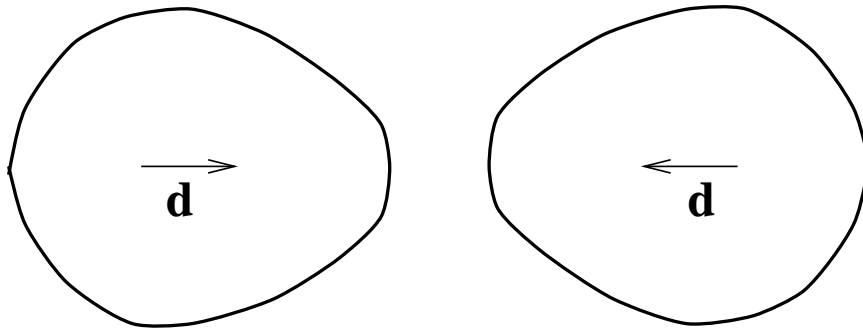
We can generalise to include magnetic multipole moments.

72.2: Oscillating Moments - Radiation

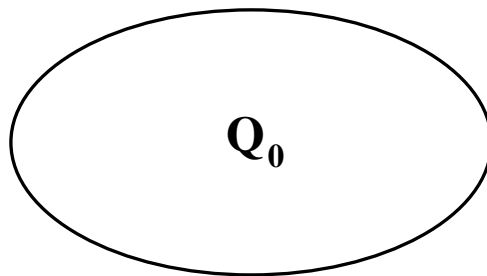
Odd-A nucleus: Magnetic Dipole Radiation (M1)



Octupole Vibration: Electric Dipole Radiation (E1)

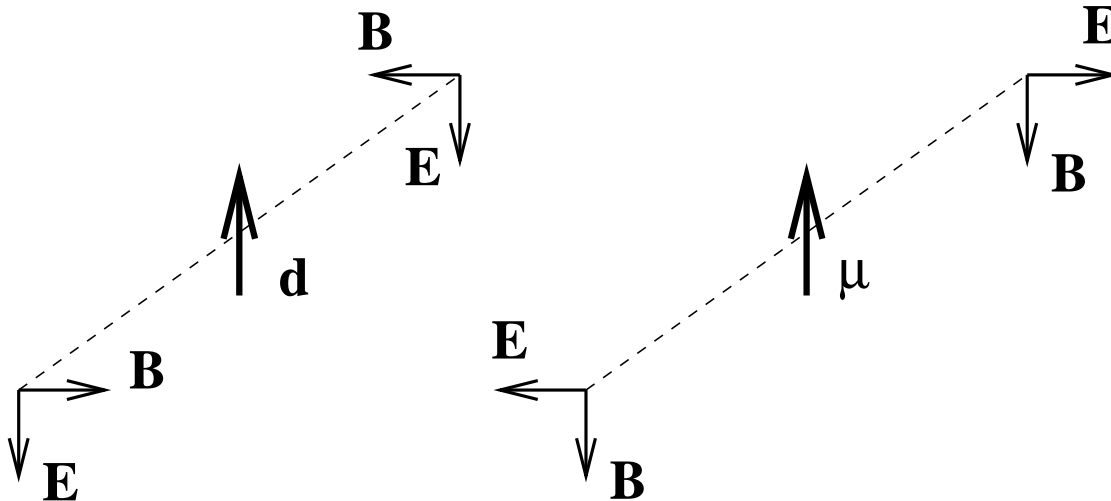


Rotation of quadrupole shape: Electric Quadrupole Radiation (E2)



72.3: Electromagnetic Radiation

Radiation from an oscillating dipole or quadrupole has been dealt with classically. There is a certain parity associated with each field:



Under the parity transformation ($r \rightarrow -r$):

Electric Dipole \vec{d}	Magnetic Dipole $\vec{\mu}$
$E(-r) = E(r)$	$E(-r) = -E(r)$
$B(-r) = -B(r)$	$B(-r) = B(r)$

The parity change for electric (E) and magnetic (M) transitions of order L is:

$$\pi(EL) = (-1)^L; \quad \pi(ML) = (-1)^{L+1}.$$

The angular distribution for radiation of multipole L is described by Legendre Polynomials, $P_{2L}(\cos \theta)$, i.e.

$$L = 1 \quad P_2(\cos \theta) = \frac{1}{2} [3 \cos^2 \theta - 1],$$

$$L = 2 \quad P_4(\cos \theta) = \frac{1}{8} [35 \cos^4 \theta - 30 \cos^2 \theta + 3].$$

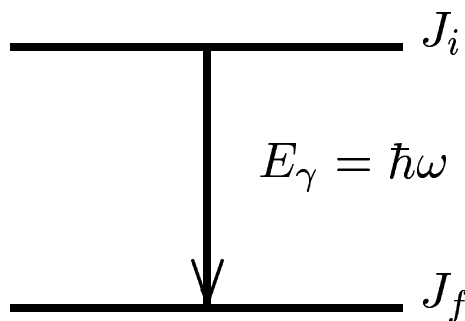
The radiated power of a classical dipole is:

$$P = \frac{1}{12\pi\epsilon_0} \frac{\omega^4}{c^3} d^2,$$

where \vec{d} is the dipole moment and ω is the frequency of oscillation.

In the nucleus, the radiation is quantised – single photon with a definite energy – and is emitted by the nucleus as oscillations of electric and magnetic moments.

- The frequency is replaced by:



- The dipole moment is replaced by the multipole operator:

$$m_{fi}(\sigma L) = \int \psi_f^* m(\sigma L) \psi_i dr.$$

The transition probability (s^{-1}) for radiation of multipole L is:

$$\begin{aligned} \lambda(\sigma L) &= \frac{2(L+1)}{\varepsilon_0 \hbar L [(2L+1)!!]^2} \left[\frac{\omega}{c} \right]^{2L+1} [m_{fi}(\sigma L)]^2, \\ &= \frac{1}{\tau} = \frac{\Gamma}{\hbar}, \end{aligned}$$

where τ is the mean lifetime of the state (s) and Γ is the linewidth of the state (eV). We can estimate $\lambda(\sigma L)$ by considering single particle transitions to calculate Γ_{sp} . For an electric transition:

$$[m_{fi}(\sigma L)]^2 = \frac{e^2}{4\pi} \left[\frac{3r_0^2 A^{1/3}}{L} + 3 \right]^2.$$

Note that all the nuclear structure information is contained within the term:

$$[m_{fi}(\sigma L)]^2.$$

72.4: Transition Strengths

The strength of a transition is defined as:

$$B(\sigma L) = \frac{\Gamma_{expt}}{\Gamma_{sp}},$$

and is measured in single-particle units (*spu*) or Weißkopf units (*Wu*). Theoretical single-particle widths (in *eV*), with E_γ measured in *MeV*, are:

$\Gamma_{sp}(E1)$	=	$6.8 \times 10^{-2} E_\gamma^3 A^{2/3}$
$\Gamma_{sp}(E2)$	=	$4.9 \times 10^{-8} E_\gamma^5 A^{4/3}$
$\Gamma_{sp}(E3)$	=	$2.2 \times 10^{-14} E_\gamma^7 A^2$
$\Gamma_{sp}(E4)$	=	$1.1 \times 10^{-21} E_\gamma^9 A^{8/3}$
$\Gamma_{sp}(M1)$	=	$2.1 \times 10^{-2} E_\gamma^3$
$\Gamma_{sp}(M2)$	=	$1.5 \times 10^{-8} E_\gamma^5 A^{2/3}$
$\Gamma_{sp}(M3)$	=	$7.3 \times 10^{-15} E_\gamma^7 A^{4/3}$
$\Gamma_{sp}(M4)$	=	$2.2 \times 10^{-21} E_\gamma^9 A^2$

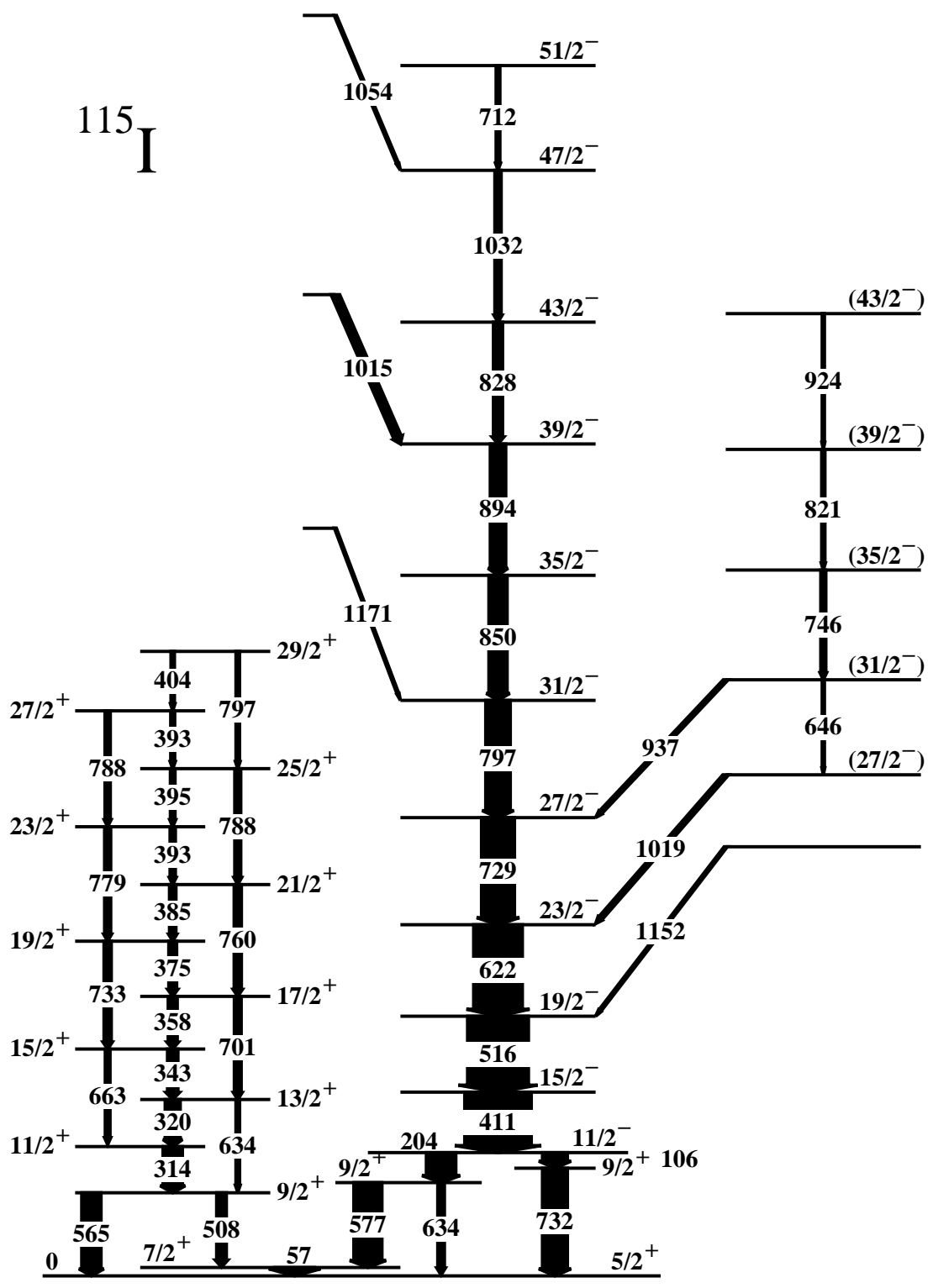
Experimentally, it is found:

$$B(E1) = 10^{-7} - 10^{-2} Wu; \quad B(M1) = 10^{-4} - 1 Wu$$

$$B(E2) = 10^{-1} - 10^3 Wu; \quad B(M2) = 1 - 10^2 Wu$$

Note that for *E2* transitions, the strength can be much larger than the single-particle estimate – collective effects, rotation of nuclei.

72.5: Gamma-Ray Decay



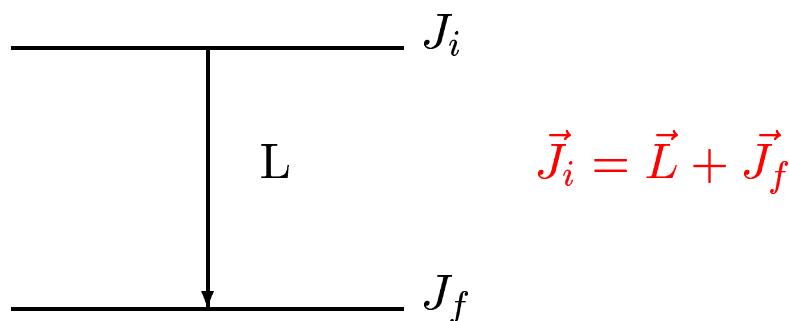
72.6: Selection Rules

A classical electromagnetic field that is produced by oscillating charges and currents transmits angular momentum as well as energy. In quantum mechanics, each photon carries a definite angular momentum L and the multipole operator includes a Spherical Harmonic factor:

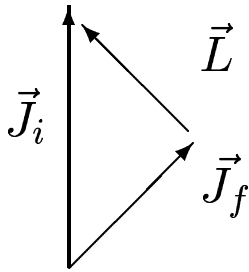
$$Y_{LM}(\theta, \phi).$$

It follows that a multipole transition of order L transfers an angular momentum of $L\hbar$ per photon. Angular momentum (and parity) must be conserved in the process – selection rules for electromagnetic transitions.

- Vector sum:



- Allowed L :



$$|J_i - J_f| \leq L \leq |J_i + J_f|$$

- Example 1

If $J_i = 3/2$ and $J_f = 5/2$, then L is allowed in the range $1 \leq L \leq 4$. But nuclear states also have definite parity (transform $r \rightarrow -r$):

$$\text{Even Parity} : \psi(r) = \psi(-r),$$

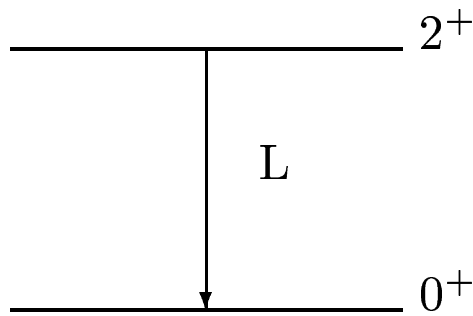
$$\text{Odd Parity} : \psi(r) = -\psi(-r).$$

Hence if the initial and final states have the same parity, then the electromagnetic transition must have even (positive) parity; if they have opposite parity, then the electromagnetic transition must have odd (negative) parity. The parity of the electromagnetic field is:

$$\pi(ML) = (-1)^{L+1} \quad M1 \text{ even, } M2 \text{ odd} \dots$$

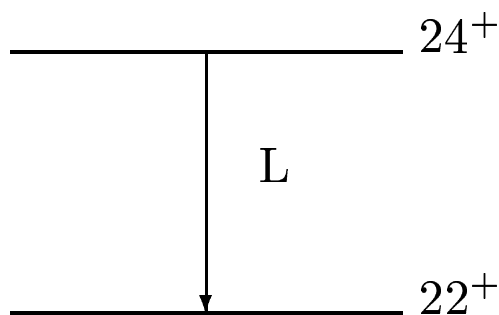
$$\pi(EL) = (-1)^L \quad E1 \text{ odd, } E2 \text{ even} \dots$$

- Example 2



Allowed L from $2 \dots 2$,
with no parity change,
 $\Rightarrow E2$.

- Example 3



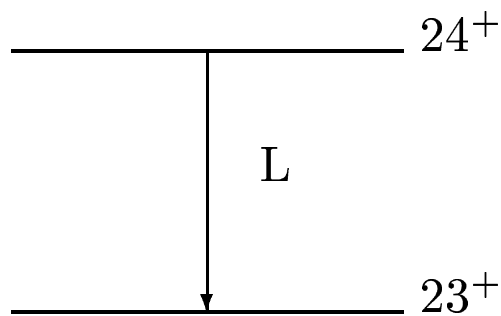
Allowed L from $2 \dots 46$,
with no parity change,
 $\Rightarrow E2, M3, E4 \dots$

However, we do not have to consider all possible multipolarities. Calculations of transition strengths show that:

$$\frac{\lambda(\sigma L)}{\lambda(\sigma L + 1)} \sim 10^4 - 10^9 \text{ and } \frac{\lambda(EL)}{\lambda(ML)} \sim 10^2,$$

Therefore we can ignore all but the lowest multipole of each type. $E2$ and $M1$ transitions could compete (similarly $E3$ and $M2$ etc.) but not $M2$ and $E1$ (or $M3$ and $E2$ etc.) Hence we only need to consider $E2$ in this example.

- Example 4



Allowed L from 1...47,
 with no parity change,
 $\Rightarrow M1, E2, M3 \dots$

In view of the previous example, we only need to consider $M1$ and $E2$ transitions, and we can define a multipole mixing ratio:

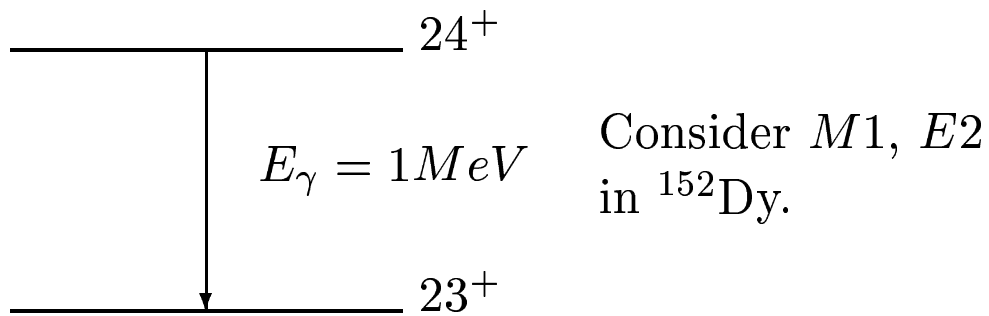
$$\delta_{E2/M1}^2 = \frac{\Gamma(E2)}{\Gamma(M1)}.$$

Neglecting interference terms, the fraction of $E2$ is:

$$\frac{\Gamma(E2)}{\Gamma(M1) + \Gamma(E2)} = \frac{\delta_{E2/M1}^2}{1 + \delta_{E2/M1}^2}.$$

Note that by measuring the angular distribution of the emitted radiation, we can extract not only $\delta_{E2/M1}^2$, but also $\delta_{E2/M1}$ (interference term). $\delta_{E2/M1}$ is related to a matrix element and the sign of $\delta_{E2/M1}$ is a meaningful physical quantity which can be compared to nuclear structure models.

• Example 5



$$\Gamma_{sp}(M1) = 2.1 \times 10^{-2} \text{ eV},$$

$$\Gamma_{sp}(E2) = 4.0 \times 10^{-5} \text{ eV},$$

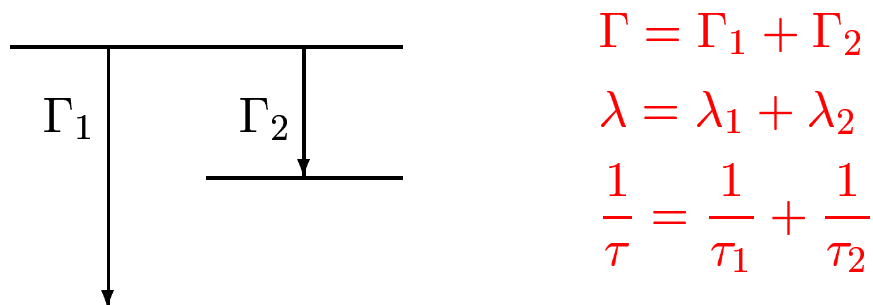
and hence $\delta_{E2/M1}^2 = 2 \times 10^{-3}$ implying the transition is dominated by the $M1$ component.

However, if the nucleus is deformed:

$$B(E2) = \frac{\Gamma_{expt}}{\Gamma_{sp}} \approx 500 \text{ Wu}; \quad B(M1) \sim 1 \text{ Wu},$$

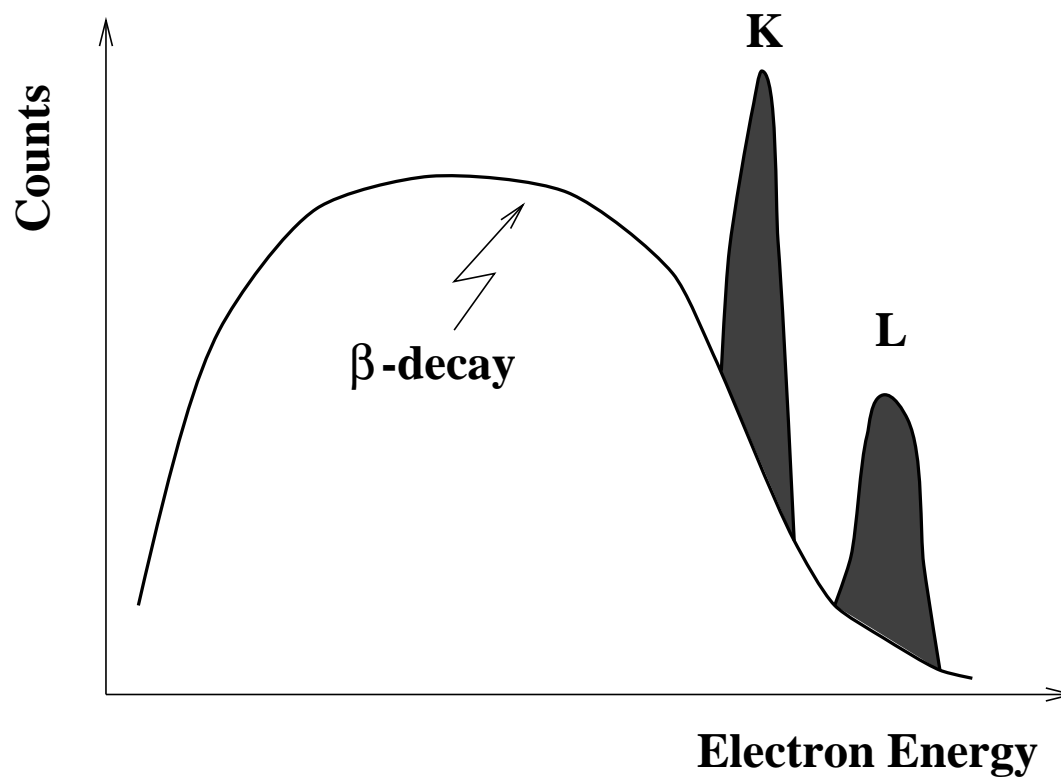
i.e. $\Gamma_{expt}(E2) = 2 \times 10^{-2} \text{ eV}$ and now $\delta_{E2/M1}^2 = 1$ implying equal probability for $M1$ and $E2$.

• Example 6 – Branching



72.7: Internal Conversion

Interaction between the nucleus and the atomic electrons is possible, particularly for the inner (K , L) shells. The electromagnetic multipole field of the nucleus can interact with the electron, transmit energy to it and if this is greater than its binding energy, the electron is then ejected from the atom – Internal Conversion. Internal conversion produces a discrete line spectrum – not continuous like β decay – and both often occur together:



The kinetic energy of the emitted electron is:

$$E(e^-) = E_i - E_f - BE(e^-).$$

Electrons in the $1s_{1/2}$ atomic orbit produce the K line, electrons in the $2s_{1/2}$, $2p_{1/2}$, and $2p_{3/2}$ atomic orbits produce the L lines (L_I , L_{II} , L_{III}). The total decay probability for a nuclear transition ($E_i \rightarrow E_f$) is given by:

$$\lambda = \lambda_\gamma + \lambda_e = \lambda_\gamma \left[1 + \frac{\lambda_e}{\lambda_\gamma} \right] = \lambda_\gamma [1 + \alpha],$$

where α is the internal conversion coefficient:

$$\alpha = \alpha_K + \alpha_L + \alpha_M \dots$$

For a transition of energy E (MeV):

$$\alpha_K(EL) = Z^3 \left[\frac{L}{L+1} \right] \left[\frac{e^2}{4\pi\epsilon_0\hbar c} \right] \left[\frac{2m_e c^2}{E} \right]^{L+5/2}.$$

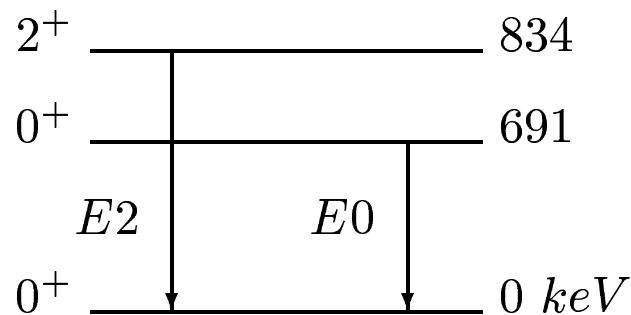
Note:

- $\propto Z^3$ – important for heavy nuclei where inner electron shells are closer to the nucleus.
- $\propto \left[\frac{2m_e c^2}{E} \right]^{L+5/2}$ – important for low energy transitions.
- Larger for magnetic transitions.
- Larger for higher L .

72.8: $0^+ \rightarrow 0^+$ Decay

A $0^+ \rightarrow 0^+$ transition cannot decay by γ decay – no electromagnetic $E0$ because the nuclear monopole moment (charge) cannot radiate to points external to the nucleus. However, $0^+ \rightarrow 0^+$ transitions can proceed via internal conversion, although this is a slow process.

• Example: ^{72}Ge



The lifetime of the 0^+ state at 691 keV in ^{72}Ge , which can only decay by internal conversion, is $\tau \sim 0.42 \mu\text{s}$. This can be compared to the much shorter lifetime of the 2^+ state at 834 keV which is $\tau \sim 3.1 \text{ ps}$. This latter state decays predominantly by γ -ray emission.

73: Nuclear Reactions

There are various types of reaction depending on:

- Energy of the projectile,
- (Z, A) of the target and projectile,
- Proximity of the paths of the target and projectile.

Peripheral Reactions

- Scattering – incident projectile is present afterwards.
 - Elastic scattering – projectile deflected unscathed from unchanged target.
 - Inelastic scattering – target or projectile becomes excited or breaks up.
 - * inelastic nuclear excitation,
 - * direct break up,
 - * Coulomb excitation,
 - * transfer reaction.

Central Reactions

- Collision with fusion of target and projectile – compound nucleus formation.

74: Coulomb Excitation

In Coulomb excitation or Coulex reactions, the kinetic energy of the projectile is transferred into nuclear excitation energy by the long-range Coulomb interaction. The biggest effect is for deformed nuclei with high Z . These deformed nuclei show rotational band structures up to spins in excess of $20\hbar$ in Coulex reactions.

● Example:

^{234}U bombarded by $5.3 \text{ MeV}/A$ ^{208}Pb . Note the beam energy is kept low (less than the Coulomb barrier) so that other reactions (e.g. fusion) do not compete, i.e.

$$\begin{aligned}\text{Beam energy} &= 5.3 \times 208 \text{ MeV}, \\ &= 1100 \text{ MeV} = 1.1 \text{ GeV}.\end{aligned}$$

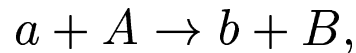
The Coulomb barrier (converting to the lab frame) for this reaction is:

$$\frac{Z_1 Z_2 e^2}{4\pi\epsilon_0(R_1 + R_2)} \times \left(\frac{A_1 + A_2}{A_2} \right) \approx 1300 \text{ MeV}.$$

75: Collision Kinematics

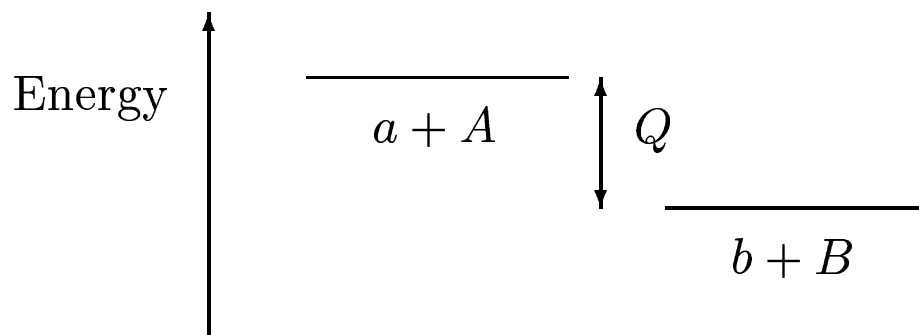
Many quantities must be conserved in nuclear reactions – energy (mass), momentum, angular momentum, parity, charge and at low energies the number of protons and neutrons.

Consider the reaction:



where a is a light projectile bombarding a massive target A (at rest). B is the “target-like” product and b is the “projectile-like” product. The Q -value for the reaction is:

$$Q = [(M_A + M_a) - (M_B + M_b)] c^2.$$



As in chemistry, an exothermic reaction ($Q > 0$) gives off energy (kinetic energy of reaction products); an endothermic reaction ($Q < 0$) requires an input of energy to occur.

Reactions with $Q > 0$ can, in principle, proceed if the collision occurs at zero incident kinetic energy:

$$T_a = \frac{1}{2}M_a V_a^2 = 0.$$

For $Q < 0$, we need to input energy – kinetic energy of incident particle. To take into account the recoil of the products, we consider the kinetic energy available in the centre of mass frame (Williams page 103):

$$T_c = T_a \frac{M_A}{M_a + M_A}.$$

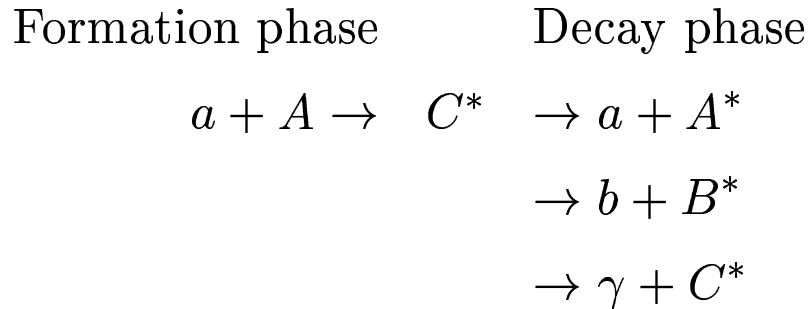
For a negative- Q reaction to occur:

$$T_c + Q > 0; \quad T_c > |Q|; \quad T_a > \frac{M_a + M_A}{M_A} |Q|,$$

and this defines a threshold energy T_a for the reaction to proceed.

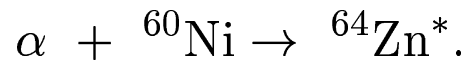
76: Compound Nucleus Model

Introduced by Niels Bohr in 1936:



The model assumes that the incident particle a enters the nucleus A , suffers collisions with the constituent nucleons of A until it has lost its incident energy, and becomes an indistinguishable part of the nuclear constituents C^* .

Consider a beam of alpha particles ($E = 5 \text{ MeV}/A$) on ^{60}Ni :



The energy of the incident particle is:

$$\frac{1}{2}M_\alpha v^2 = 5 \text{ (MeV}/A) \times A,$$

$$\frac{1}{2}Am_N c^2 \left(\frac{v}{c}\right)^2 = 5A,$$

from which $\frac{v}{c} \sim 0.1$ – i.e. nonrelativistic.

It then follows that it takes $\sim 10^{-22}$ s for the incident α particle to travel across the target nucleus. In a compound nucleus, the first emission of a nucleon or a γ -ray takes $> 10^{-20}$ s, and often $\gg 10^{-20}$ s – the α particle could traverse the nucleus more than a hundred times! Hence, within this timescale, the compound nucleus equilibrates all its degrees of freedom – it shares out energy between all the nucleons. The projectile is absorbed and the system loses its memory of how it was formed.

Bohr's hypothesis of independence states that the formation and decay of a compound nucleus are independent. It does not matter how we form the compound nucleus – the decay modes will be the same. Note, however, that the excitation energy and angular momentum are remembered!

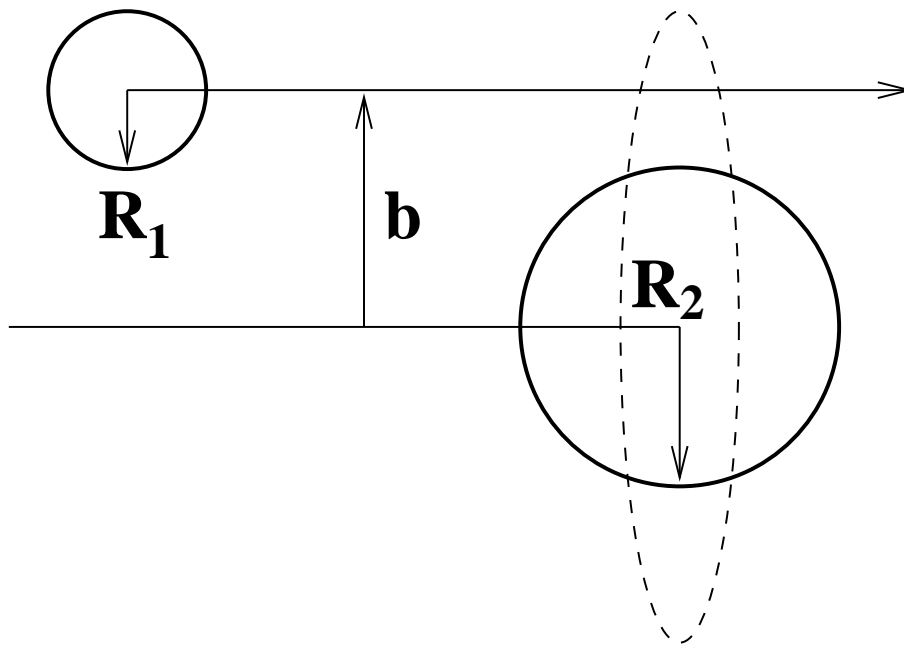
We could make ${}^{64}\text{Zn}$ by $\alpha + {}^{60}\text{Ni}$ or $p + {}^{63}\text{Cu}$ reactions. If the excitation energy (and spin) brought into the compound system were the same for each reaction, then the probability of each decay channel would be the same.

77: Geometric Cross-Section

The concept of a cross-section is statistical.

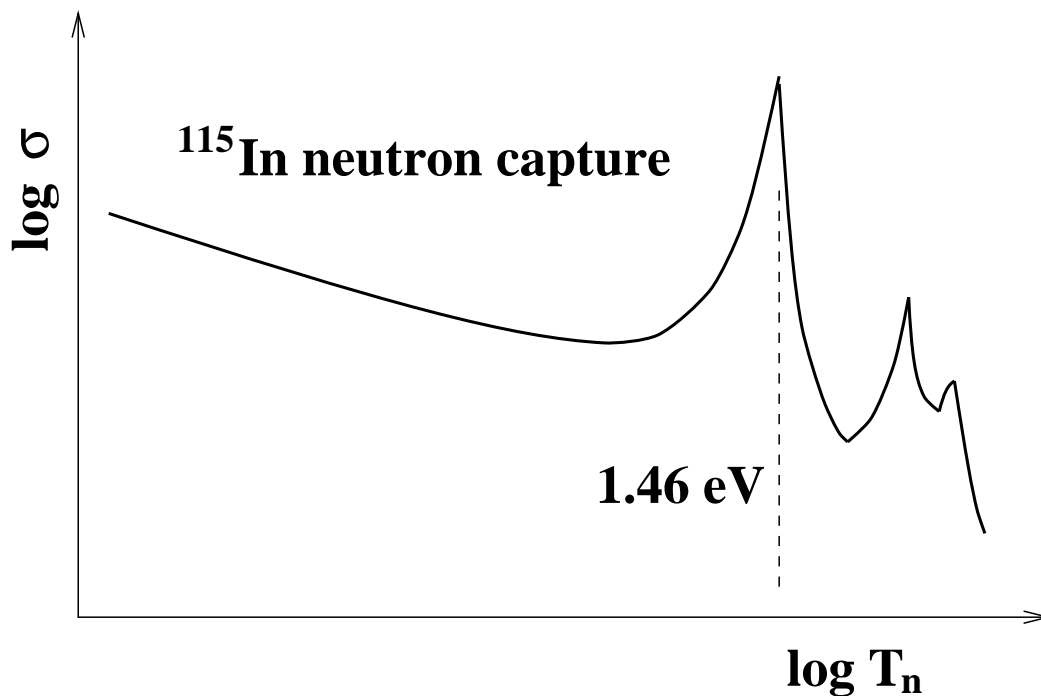
• Definition: The cross-section is the number of processes per second when one scattering centre is exposed to unit flux of incident particles.

In the classical picture shown below, the projectile and target nuclei will interact (fuse) if the impact parameter b is less than the sum of their radii. A disk of area $\pi(R_1 + R_2)^2$ is swept out which defines a geometric cross-section. Remember – the units of cross-section are area ($1 \text{ b} = 100 \text{ fm}^2$)!

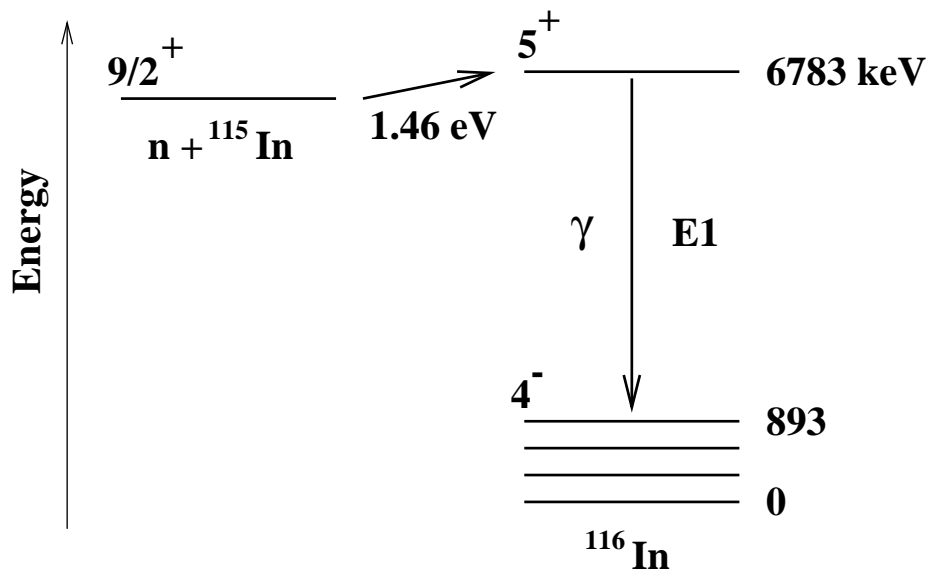


78: Neutron Capture

Low energy neutron-capture cross-sections exhibit peaks manifesting a compound system and these peaks are often called resonances. An example is the neutron capture of ^{115}In to form ^{116}In .



The neutron needs only 1.46 eV to form an excited compound state in $^{116}\text{In}^*$. But note that the excitation energy in ^{116}In is much greater than 1.46 eV – it is in fact 6.8 MeV ! So even though we only put in 1.46 eV , the compound system is highly excited due to the binding energy of the neutron.



● Cross-section:

At 1.46 eV, the total cross-section for neutron capture is $\sigma \sim 2.8 \times 10^4$ barns. This is much larger than the geometric cross-section ($\pi R^2 \sim 1.1$ b, with $R \sim 6$ fm). This is a quantum effect and we need to consider the de Broglie wavelength ($\lambda/2\pi$) instead of the nuclear radius – slow neutrons have a large wavelength and hence a long range influence. The cross-section becomes:

$$\pi R^2 \Rightarrow \pi \left(\frac{\lambda}{2\pi} \right)^2.$$

The momentum of the neutron is:

$$\begin{aligned} p_n &= \sqrt{2m_n E} = \sqrt{2 \times 939 \times 1.46 \times 10^{-6}}, \\ &= 0.052 \text{ MeV}/c. \end{aligned}$$

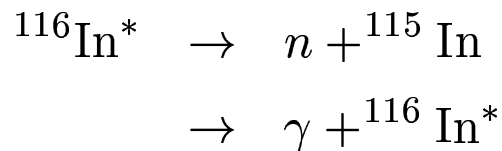
The de Broglie wavelength is then:

$$\begin{aligned} \left(\frac{\lambda}{2\pi} \right) &= \frac{\hbar c}{p_n c} = \frac{197}{0.052}, \\ &= 3.7 \times 10^3 \text{ fm}, \end{aligned}$$

and hence the cross-section becomes $4.3 \times 10^5 \text{ b}$.

The measured value is only 6% of this latter estimate – we must also consider other effects such as the spins of the neutron, target and compound nucleus.

• Decay of the compound state:



For compound nucleus decay, neutron decay with energies $> 1 \text{ MeV}$ are more likely than γ -decay. However, for the example of ${}^{116}\text{In}^*$ the neutron could only be emitted with the same low 1.46 eV . Consequently, γ -decay (e.g. the 5.89 MeV ($E1$) $5^+ \rightarrow 4^-$ transition) dominates, and we find that:

$$\frac{\Gamma_n}{\Gamma_\gamma} = 0.04,$$

i.e. there is a 96% probability for γ -decay and only a 4% probability for neutron emission.

At this energy, there are no other decay modes open and so

$$\frac{\Gamma_n}{\Gamma} \approx 0.04,$$

where Γ is the total decay width or decay probability ($\Gamma = \Gamma_n + \Gamma_\gamma$).

We can also link this decay fraction to the formation cross-section:

$$\pi \left(\frac{\lambda}{2\pi} \right)^2 \times \frac{\Gamma_n}{\Gamma}.$$

Recall that the measured formation cross-section was only 6% of the estimate using the de Broglie wavelength – this factor is similar to the partial neutron decay width!

• Wavefunction picture of a resonance:

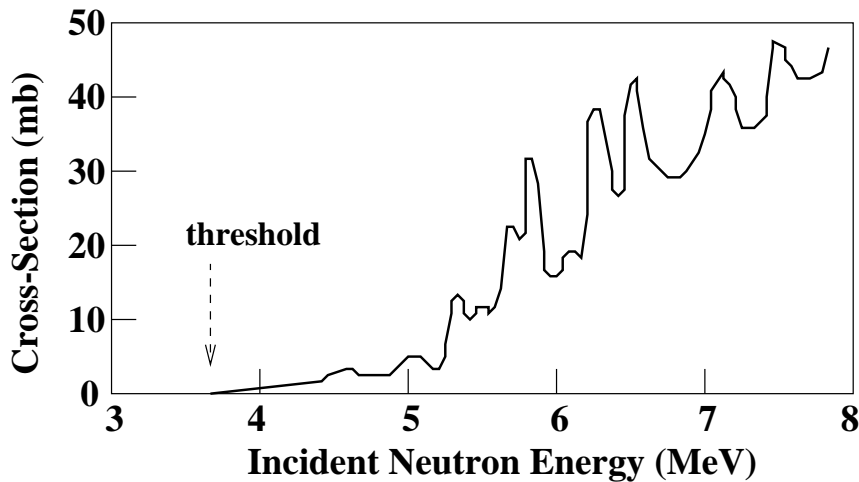
There is a matching of the phase of the wavefunctions of the target and projectile at the surface of the target if the derivative at the surface is zero. Once there is a match to penetrate the target, it does not match to get out. There are many reflections and equilibration of the energy.

79: Proton Capture

In the case of charged-particle capture (and decay), we have to consider the Coulomb barrier which inhibits the formation (or decay). We need sufficient energy to overcome this barrier (several MeV) and so the wavelengths are much smaller than for neutrons. Consequently, the cross-sections for proton capture are $\sim 1 b$ at maximum.

For heavier ions (e.g. α , ^{12}C , ^{32}S), the Coulomb barrier is larger still and the particle enters a continuum of very high level densities and overlapping resonances. The excitation energy of the compound nucleus is much higher (10–80 MeV) and since the neutron binding energy is only $\sim 8 MeV$, several neutrons are emitted before γ -ray emission becomes dominant. These fusion evaporation reactions also bring large amounts of angular momentum into the compound system.

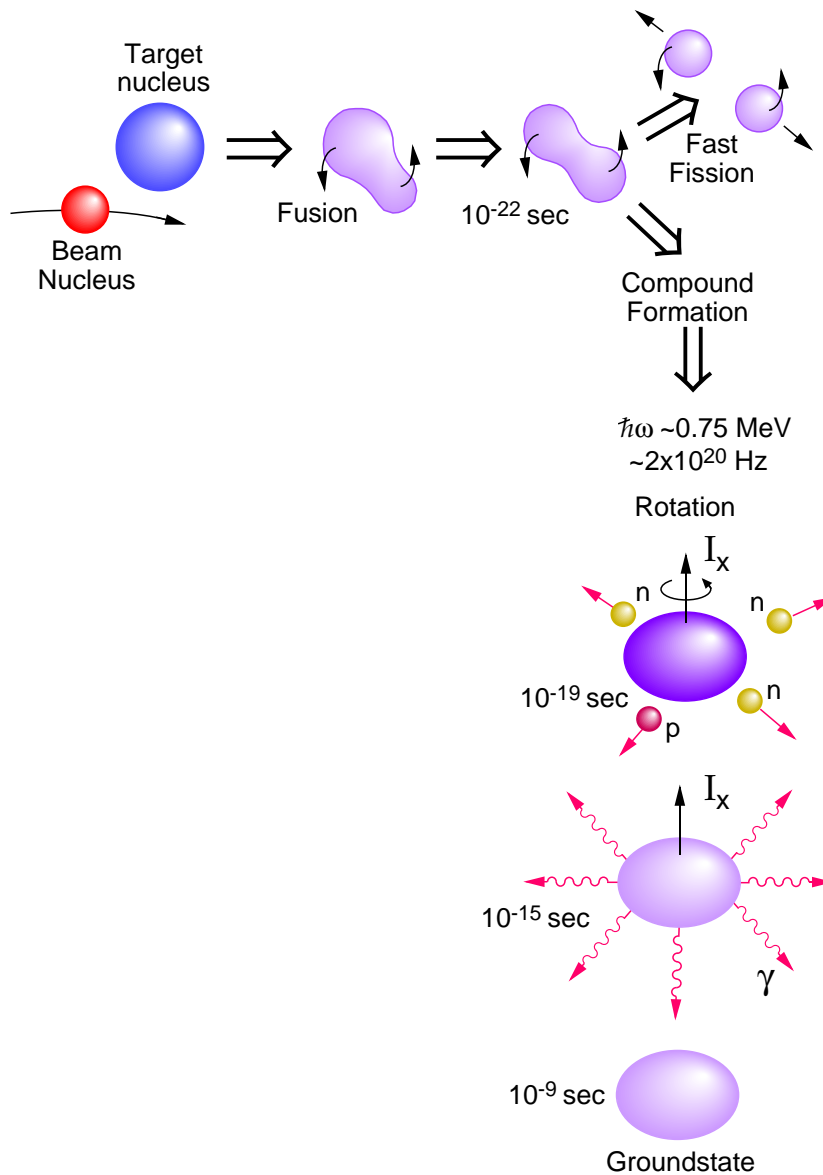
80: Charged Particle Decay



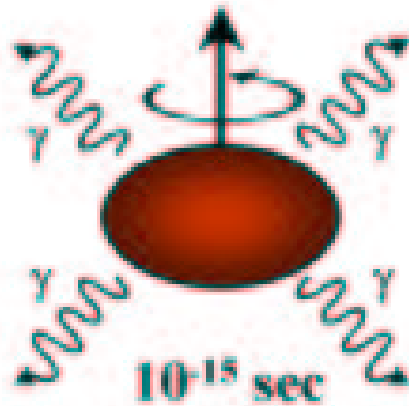
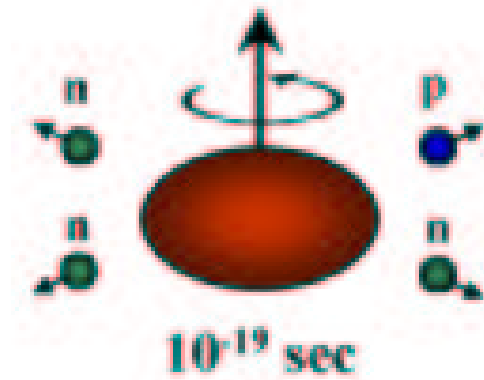
Consider the ${}^{23}_{11}\text{Na}(n,p){}^{23}_{10}\text{Ne}$ reaction (Williams page 119) – a neutron is captured by ${}^{23}\text{Na}$ to form a ${}^{24}\text{Na}^*$ compound system which then decays by emitting a proton. The Q -value for this reaction is -3.59 MeV (i.e. energy to change n into p) and the threshold (neutron) energy is 3.75 MeV (taking into account the recoil energy of the ${}^{23}\text{Ne}$ nucleus). The Coulomb barrier for the outgoing proton has a height of $\sim 4 \text{ MeV}$. Just above threshold, the proton channel is not present as the Coulomb barrier must be overcome. Above 5 MeV , the barrier becomes increasingly “transparent” to the outgoing proton and resonances occur – although the cross-sections are only mb !

81: Fusion-Evaporation Reactions

Heavy Ion (HI, xn) fusion-evaporation reactions are useful in nuclear structure studies. These reactions can bring in large amounts of angular momentum and excitation energy.



Some typical numbers of a rapidly rotating nucleus...

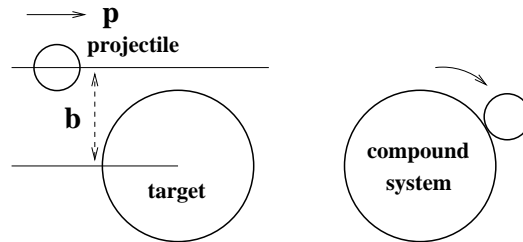


$$\hbar\omega \sim 0.8 \text{ MeV}$$

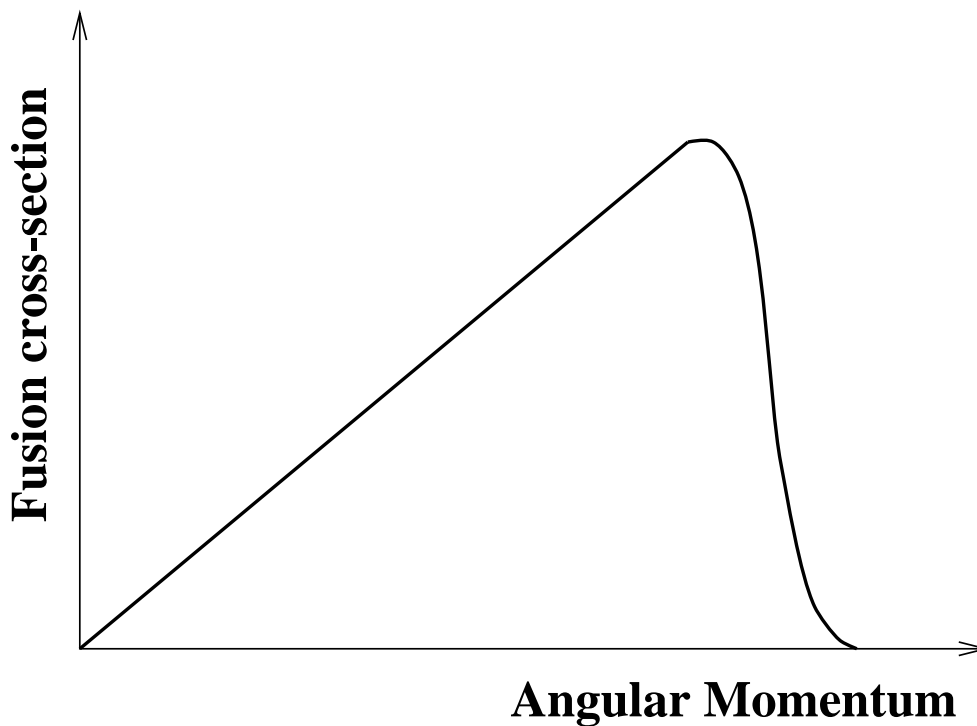
$$\nu \sim 2 \times 10^{20} \text{ Hz}$$

$$V(\text{surf}) \sim 0.04c$$

The angular momentum brought into the compound system is dependent on the impact position of the projectile on the target:



The angular momentum is: $\vec{l} = \vec{b} \wedge \vec{p}$,
 where b is the impact parameter and p the momentum of the projectile. The partial fusion cross-section is proportional to the angular momentum: $d\sigma_{fus}(l) \propto l$.



The nucleus ^{132}Ce can be formed by bombarding a stationary ^{100}Mo target with a beam of ^{36}S at an energy of 155 MeV (4.31 MeV/nucleon). At this chosen energy, the residual nucleus with the largest cross-section is ^{132}Ce which is produced by boiling off four neutrons.

- Compound nucleus formation:

10^{-20} s after impact, the target has thoroughly absorbed the projectile to produce the excited compound nucleus $^{136}\text{Ce}^*$.

- Neutron emission:

After 10^{-19} s , four neutrons are boiled off which each carry away large amounts of energy (at least equal to the binding energy of $\sim 8\text{ MeV}$), but little angular momentum.

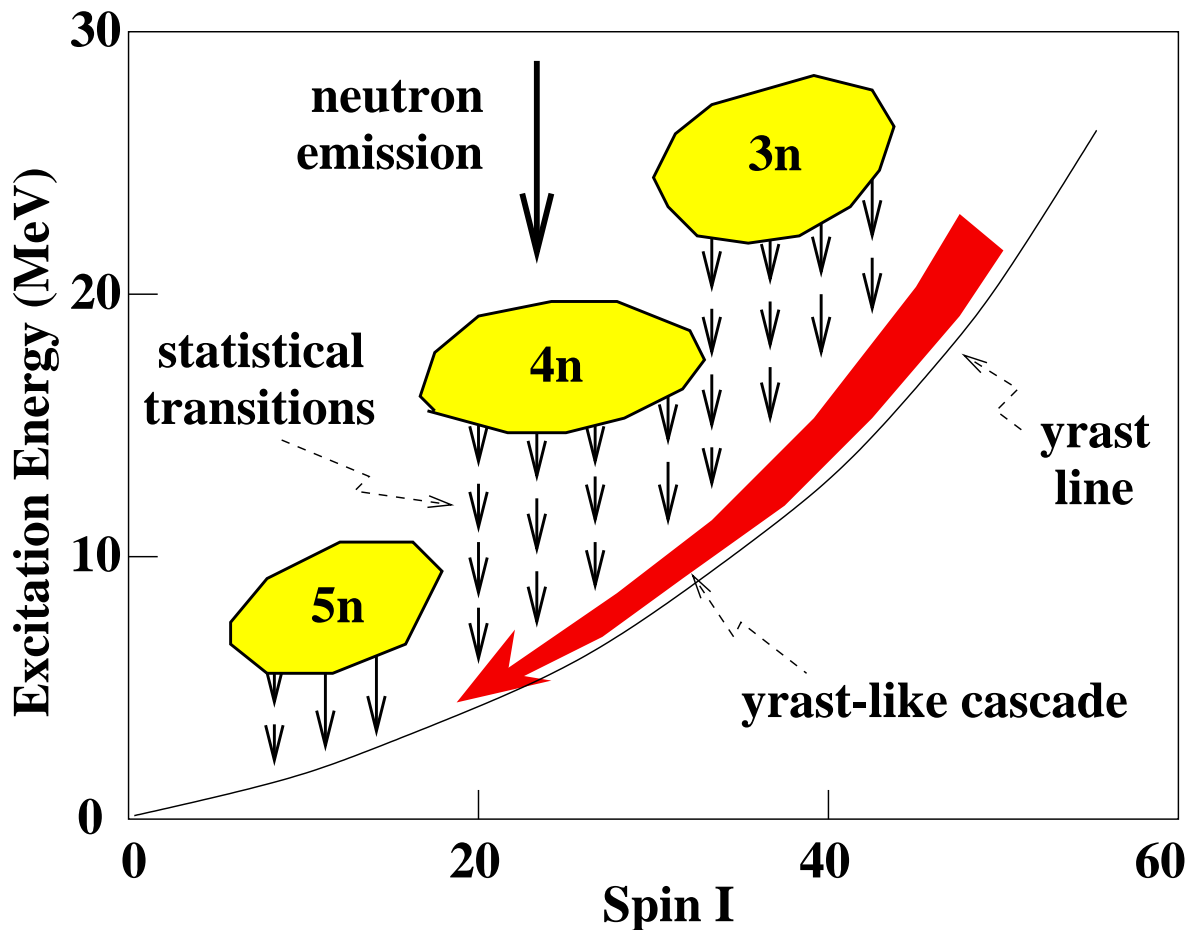
- Statistical (cooling) γ -ray emission:

After 10^{-15} s , high energy ($E1$) γ -ray transitions remove excitation energy but little angular momentum. The nucleus “cools” towards the yrast line where all the excitation energy is involved in the rotation – $E \propto I(I + 1)$.

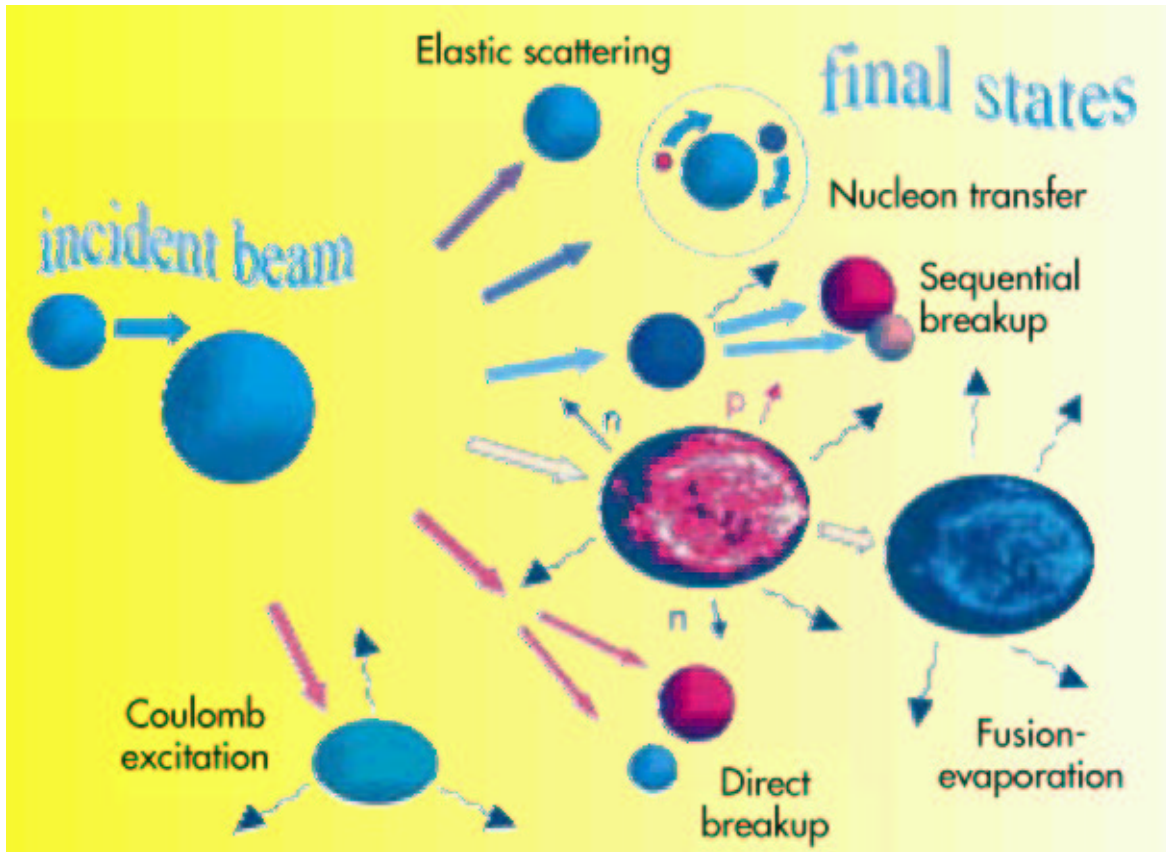
- Quadrupole (slowing down) γ -ray emission:

After 10^{-12} s, quadrupole ($E2$) γ -ray emission takes over, dissipating the angular momentum – slowing down the nuclear rotation.

After about 10^{-9} s, the nucleus reaches its ground state after about 10^{11} rotations. This is similar to the number of revolutions of the earth since its creation!



82: Other Reactions



83: Transfer Reactions

Transfer reactions occur within a timescale comparable with the transit time of the projectile across the nucleus. The cross-sections are comparable to a fraction of the nuclear area and they vary smoothly and slowly with the projectile energy. The de Broglie wavelength of a 20 MeV incident nucleon is 1 fm and therefore it “sees” or interacts with individual nucleons. These will be the valence nucleons at the nuclear surface and they are transferred to/from the target nucleus.

For example, a (d,p) reaction strips a neutron off the projectile (deuteron) leaving a proton, and adds it to the target. Conversely, in a (p,d) reaction, the projectile (proton) picks up a neutron from the target to form a deuteron.

The angular distribution (variation of intensity with angle) of the outgoing modified particle (p or d) contains information on the orbit (state) of the captured (lost) neutron. For instance, it contains data on l the transferred angular momentum.

84: Interaction with Matter: α -particles

Charged particles interact via the Coulomb force between their positive charges and the negatively charged orbital electrons of absorber atoms. The electrons of the absorber atoms are either excited or completely removed (ionisation). The α particle loses energy on each interaction, but its large mass (relative to the electron) means it is not deflected much. In any one collision, the maximum energy transfer is:

$$\frac{\Delta T_{max}}{T} \approx 4 \frac{m_e}{M_\alpha},$$

which is about 1/2000 for α particles, and hence the incident particle loses its energy through many such interactions during its passage through the absorber material. More rarely, the α particle can interact directly with the nuclei of the absorber atoms.

The linear stopping power S is defined as the energy loss per unit path length in a material:

$$S = -\frac{dT}{dx}.$$

85: Interaction with Matter: β -particles

As opposed to α particles, the low mass of the incident β -particles (electrons or positrons) means that relatively larger amounts of energy are transferred per collision (again via the long-range Coulomb interaction), and the beta particles are deflected significantly at each collision.

The β particles can also lose energy by radiation – bremsstrahlung – “braking radiation” in German. The total linear stopping power is then given by the sum of collisional and radiative losses:

$$S = -\frac{dT}{dx} = -\left[\left(\frac{dT}{dx}\right)_{coll} + \left(\frac{dT}{dx}\right)_{rad}\right].$$

For energies below a few MeV , radiative losses are small and only collisional losses are significant.

The quantity dT/dx is called the specific energy loss or rate of energy loss of the charged particle.

86: Bethe-Bloch Formula

A classical expression that describes energy loss of a charged particle in an absorber material:

$$-\frac{dT}{dx} = \frac{4\pi z^2 \alpha^2 (\hbar c)^2}{m_e v^2} N_a B,$$

$$B = Z_a \left[\ln \left(\frac{2m_e v^2}{I(1 - v^2/c^2)} \right) - \frac{v^2}{c^2} \right],$$

where (v, z) are the velocity and charge state of the incident particle, (N_a, Z_a) are the number density and atomic number of the absorber, m_e is the electron rest mass, α is the fine structure constant, and I is the average ionisation and excitation energy of the absorber (determined experimentally).

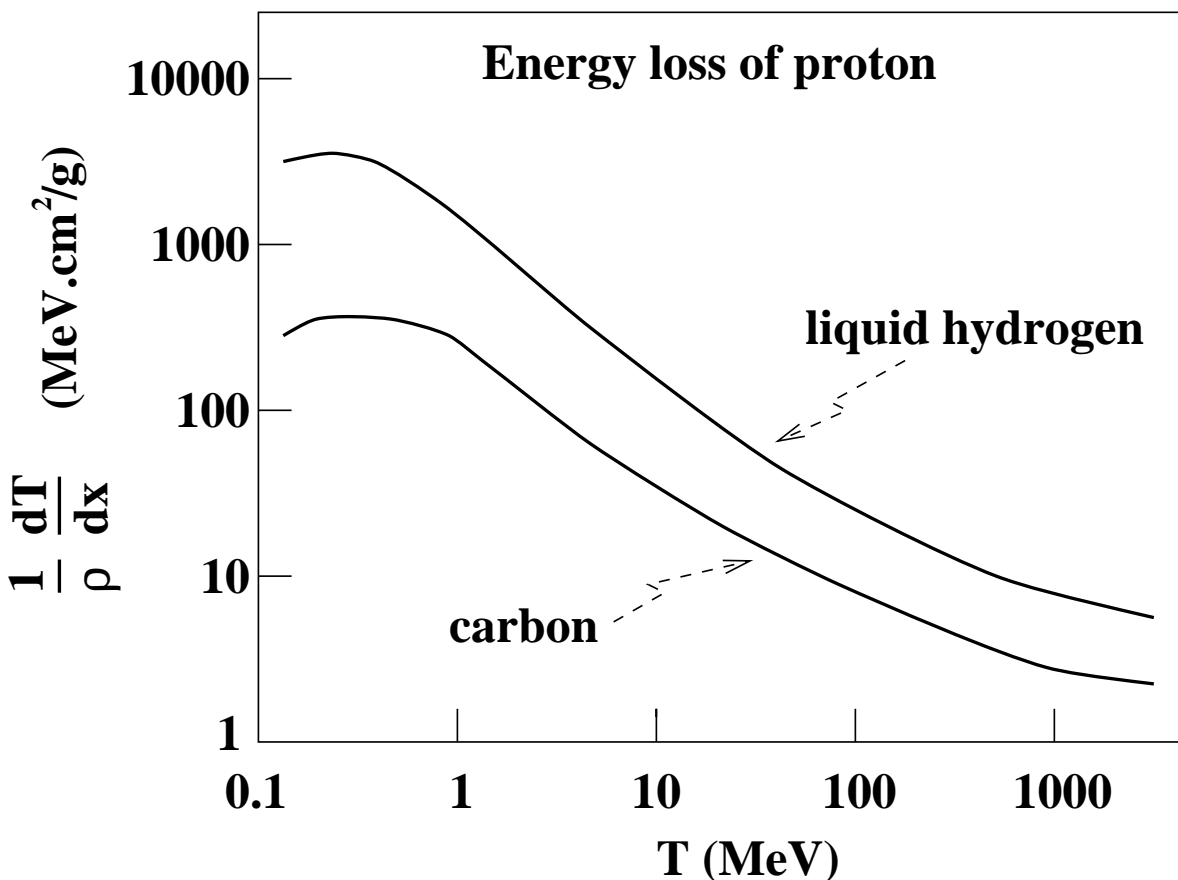
Notes:

- Higher density materials (larger N_a) have greater stopping power. Similarly for large Z_a .
- B varies slowly with particle energy.
- $\frac{dT}{dx} \propto \frac{1}{v^2} \propto \frac{1}{\text{energy}}$.
- $\frac{dT}{dx} \propto z^2 - \alpha$ particles lose energy faster than protons, but more slowly than heavier charged particles.

The energy lost in traversing normally (i.e. perpendicularly) a layer of absorber material of unit mass per unit area is defined as:

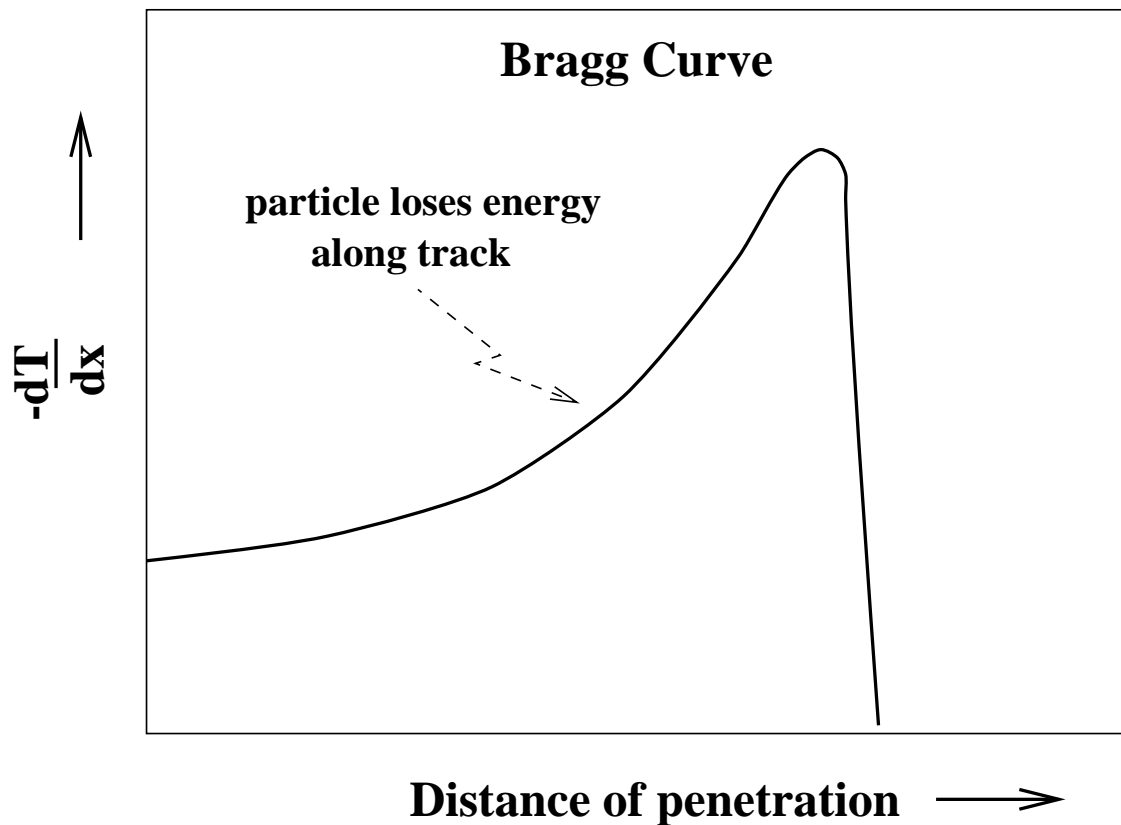
$$-\frac{1}{\rho} \frac{dT}{dx} = \frac{4\pi z^2 \alpha^2 (\hbar c)^2}{m_0 v^2} \frac{N_a}{A} B.$$

An example is shown below, for the energy loss of a proton, as a function of energy, in liquid hydrogen and carbon absorbers.



87: The Bragg Curve

A plot of the specific energy lost along the track of a charged particle is known as the Bragg curve. An example for an α particle is shown below. For most of the curve, the charge on the α is $+2$ and the energy loss increases roughly as $1/T$. However, near the end of the track, the charge on the α changes through electron pickup and the curve rapidly falls off.



88: Range

The range of a particle is defined as the distance R traversed by a particle of initial kinetic energy T_0 before it comes to rest in the stopping material:

$$R = \int_{T_0}^0 \frac{dT}{dT/dx}.$$

For nonrelativistic particles (mass M , charge z):

$$-\frac{dT}{dx} \approx a \frac{z^2}{v^2},$$

where a is a constant. Hence, with $T_0 = \frac{1}{2}Mv_0^2$:

$$R = \frac{aT_0^2}{z^2M} = \frac{aMv_0^4}{4z^2},$$

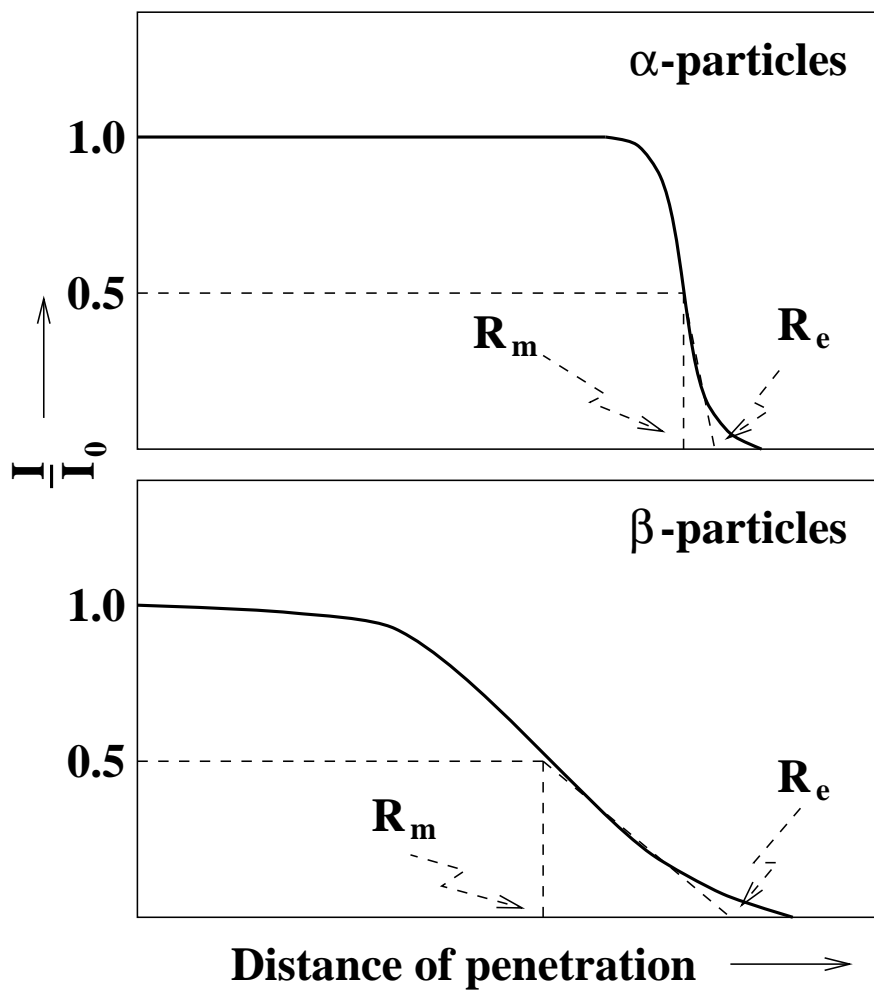
i.e. the range is proportional to M/z^2 if the initial velocity is the same.

The loss of energy is not smooth and the actual energy loss can fluctuate from the expected value – straggling. The energy is dissipated in the stopping material mainly by ionisation of the atomic electrons.

89: Range - Definitions

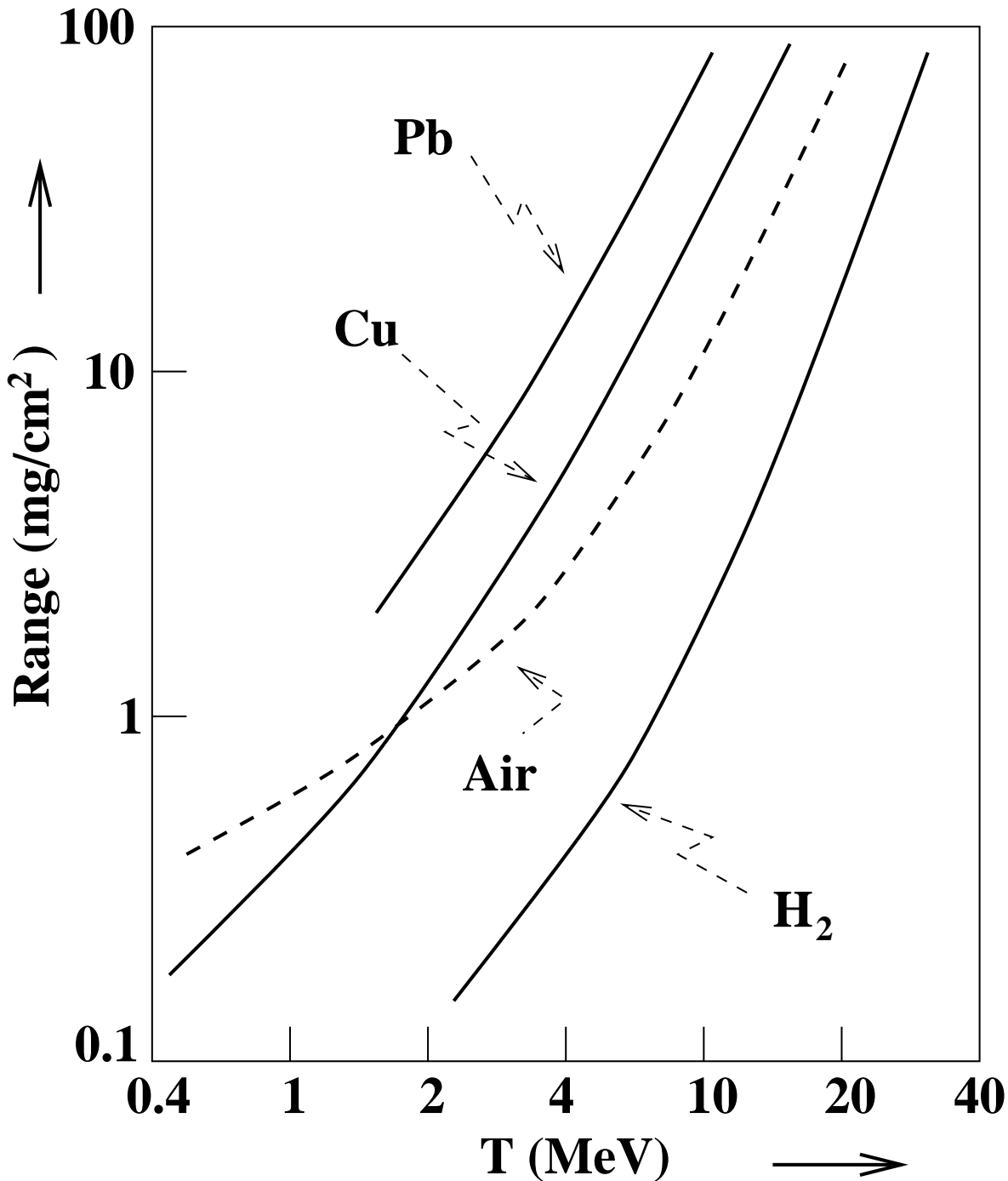
The mean range R_m is the absorber thickness that reduces the incident intensity to half its initial value. The extrapolated range R_e is obtained by extrapolating the linear portion of the end of the transmission curve to zero.

Examples are shown below for α and β particles:



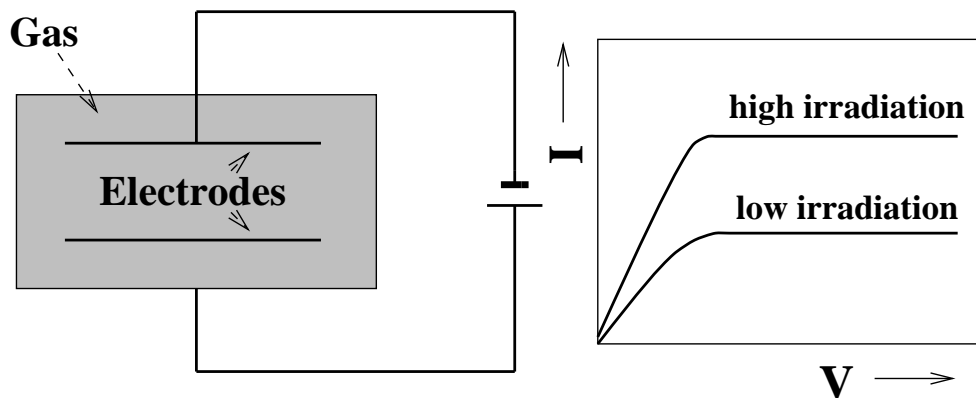
90: Range of α -Particles

Target “thickness” d may be measured as an areal density (mg/cm^2), i.e. density \times thickness ($\rho \times x$).

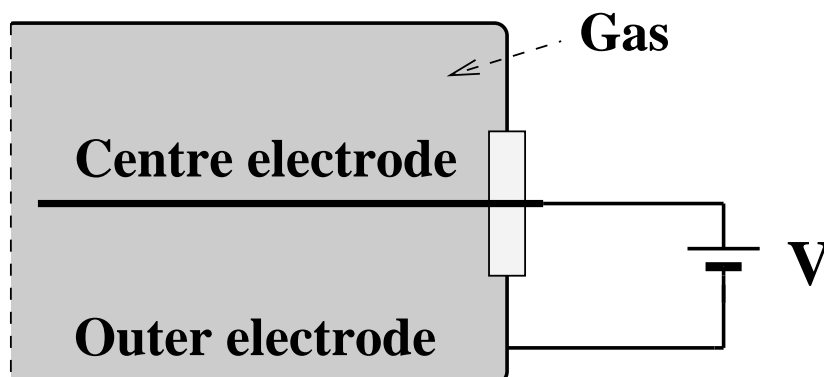


91: Gas-filled Detector

A gas ionisation chamber can be regarded as a parallel plate capacitor with the region between the plates filled by gas.



Another geometry is a cylinder with a thin central electrode (wire). Large electric fields occur near the wire.



Virtually any gas can be used for the chamber, air being the most common. Denser gases may be used to increase the ionisation density. Charged particles ionise the gas into electrons and positively charged molecules. An electric field prevents electrons and ions of the absorber recombining and they drift in opposite directions producing an ion current, which is measured.

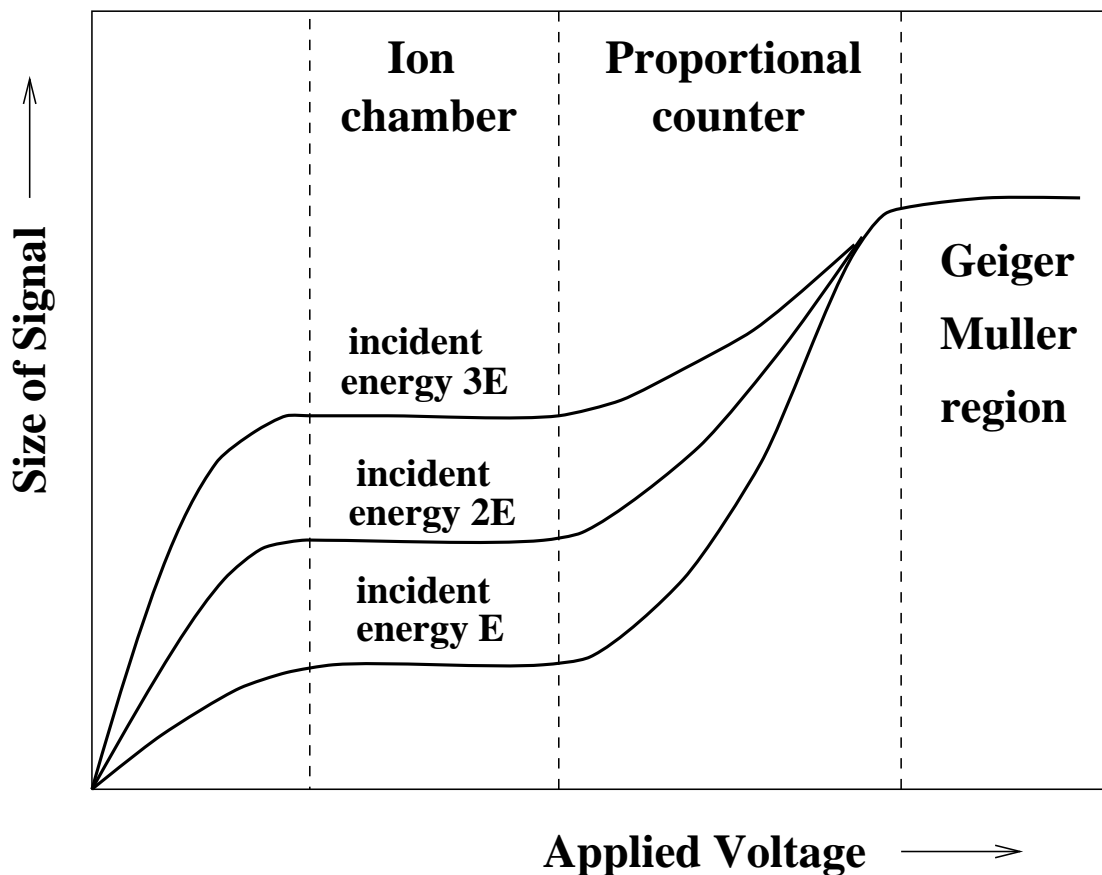
In air the average energy to produce an ion is 34 eV , and so the maximum number of electrons and ions is 3×10^4 per MeV . For example, if the chamber is 10×10 cm with a plate separation of 1 cm , then the capacitance is $\sim 9 \times 10^{-12}$ F and the voltage pulse is

$$\frac{3 \times 10^4 \times 1.6 \times 10^{-19}}{9 \times 10^{-12}} \approx 0.5 \text{ mV},$$

i.e. we need amplification of the signal. Instead of an external amplifier we can use the internal multiplication of the charge in the gas – avalanche effect.

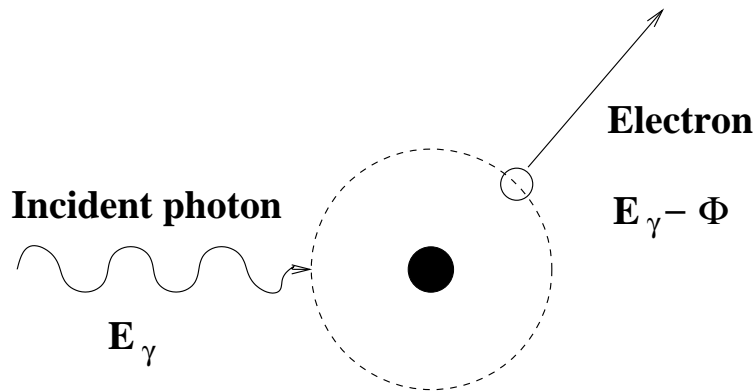
For large electric fields, the electrons produced by the incident particle are accelerated and create more ionised atoms in collisions. Such an avalanche produces $10^3 - 10^5$ secondary ions and electrons. If the number of secondary events is proportional to the number of primary events, the detector operates as a proportional counter. At sufficiently large fields, the whole gas region is involved in many avalanches created by electrons and photons emitted in the first avalanche – Geiger-Müller region.

Properties of a gas filled detector



92: Interaction with Matter: photons

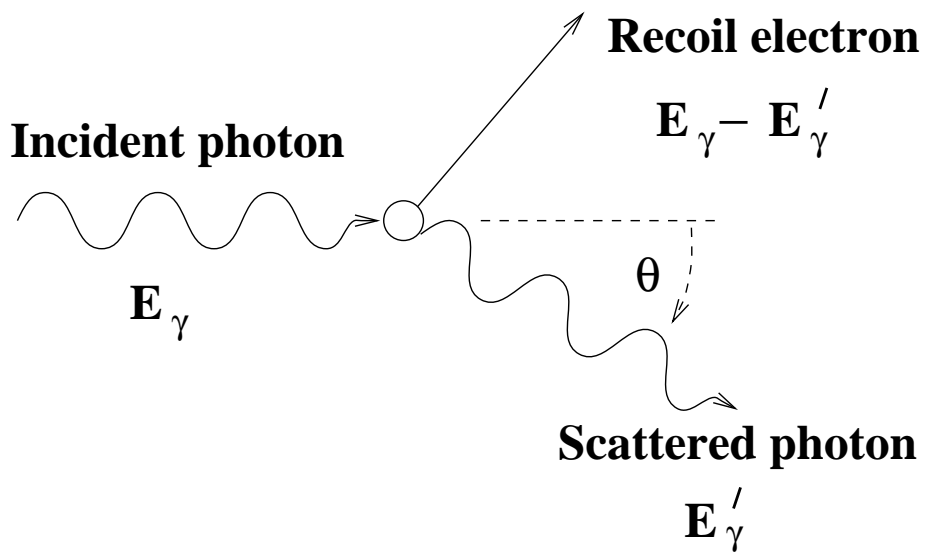
• Photoelectric Effect



A single electron is ejected from an atom on absorption of a photon. There is a complete transfer of energy to a bound atomic electron. The energy of the photoelectron is equal to the energy of the incident photon (γ -ray) minus the binding energy of the electron. Ejection from the K electron shell dominates. The cross-section decreases with increasing γ -ray energy, but increases with the Z of the material ($\sim Z^4$). The photoelectric effect is important for γ -rays of energy up to 100 – 500 keV .

The vacancy in the atomic shell can be filled by another electron from a higher shell – cascade x -rays are produced.

- Compton Scattering



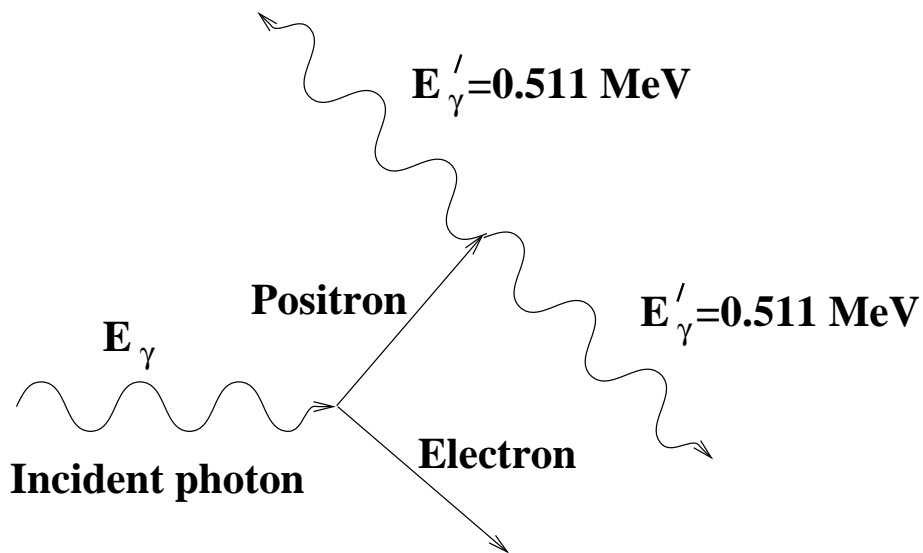
The incident photon (E_γ) is scattered from a “free” atomic electron (outer shell) transferring some of its energy to the electron, and thus emerges with a lower energy (E'_γ). The Compton scattering formula is:

$$\frac{1}{E'_\gamma} - \frac{1}{E_\gamma} = \frac{1}{m_e c^2} (1 - \cos \theta),$$

where $m_e c^2 = 511 \text{ keV}$. Note that $E'_\gamma \rightarrow E_\gamma$ as $\theta \rightarrow 0^\circ$ and $E'_\gamma \rightarrow \sim 200 \text{ keV}$ as $\theta \rightarrow 180^\circ$ if the incident γ -ray energy $E_\gamma > 1 \text{ MeV}$.

The Compton effect dominates from a few hundred keV up to $5 - 7 \text{ MeV}$.

• Pair Production



If the incident photon has sufficient energy ($E_\gamma > 2m_e c^2 > 1.022 \text{ MeV}$), it can produce an electron-positron pair. This can only happen in the presence of a large atom which is required to conserve momentum. The kinetic energy which is shared between the electron and positron is:

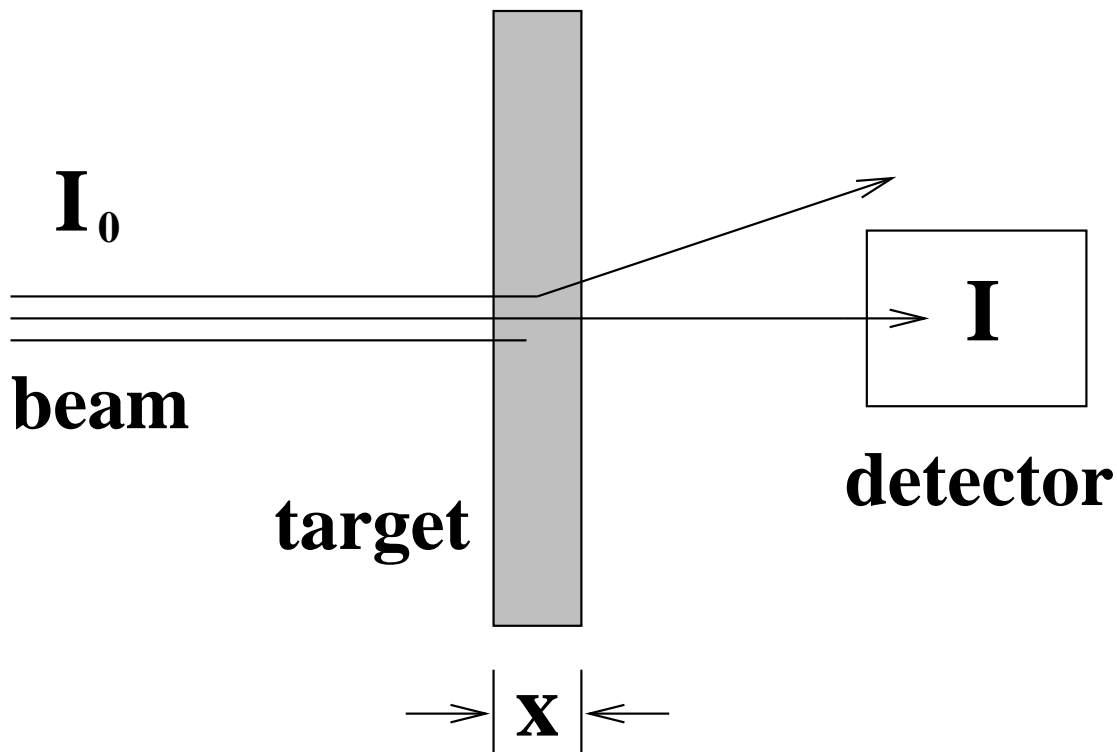
$$T_{e^-} + T_{e^+} = E_\gamma - 2m_e c^2.$$

The positron has a short range and it is rapidly annihilated when it meets another electron creating two 0.511 MeV γ -rays, emitted back to back in the centre of mass frame.

93: Linear Attenuation Coefficients

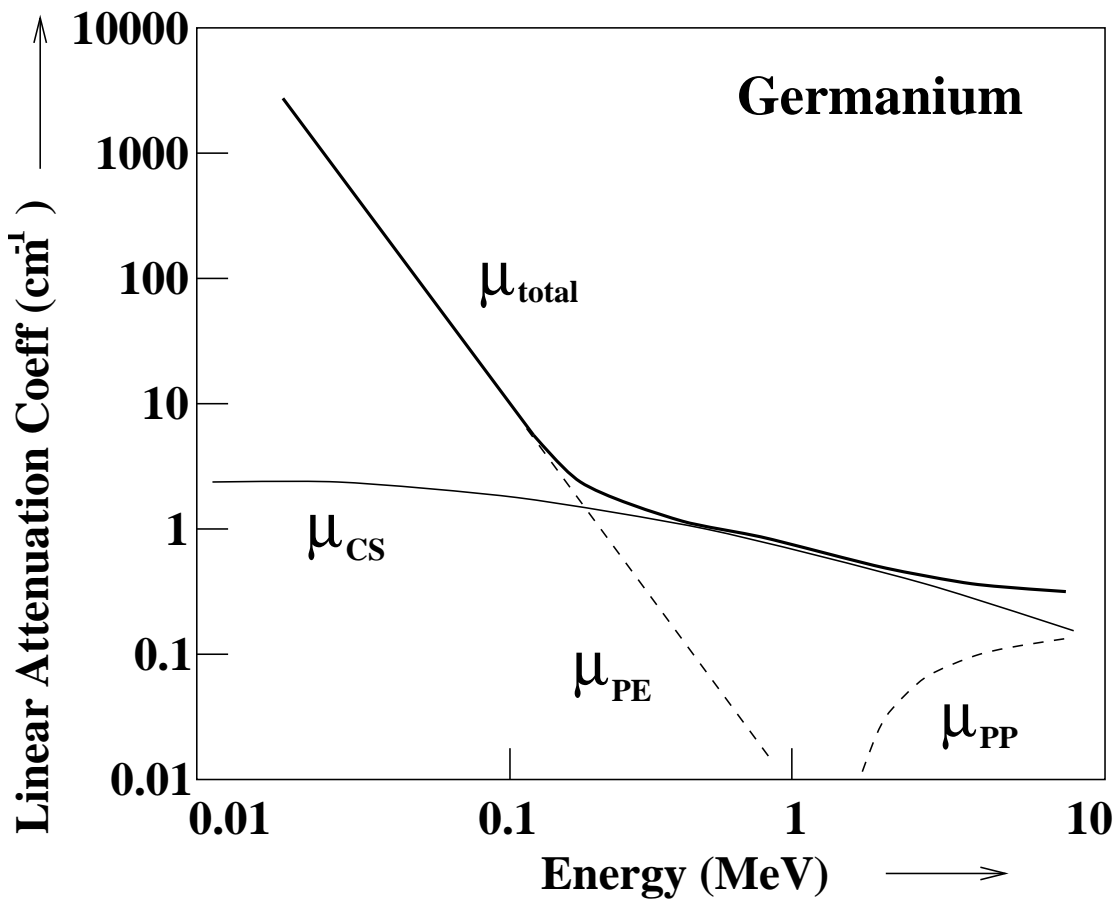
The linear attenuation coefficient μ is the probability per *cm* of absorber that a γ -ray has an interaction. Suppose we have a beam of particles of initial intensity I_0 which passes through a target of thickness x and we subsequently measure the intensity as I . The measured intensity I is related to the initial intensity by:

$$I = I_0 \exp(-\mu x).$$



The total attenuation coefficient μ may be expressed in terms of the three main interactions (photoelectric, Compton and pair production):

$$\mu = \mu_{PE} + \mu_{CS} + \mu_{PP}.$$



The mass attenuation coefficient μ_{mass} is given by μ/ρ and hence:

$$I = I_0 \exp(-\mu_{mass}\rho x) = I_0 \exp(-\mu_{mass}d),$$

where $d = \rho x$ is the “thickness” measured in g/cm^2 .

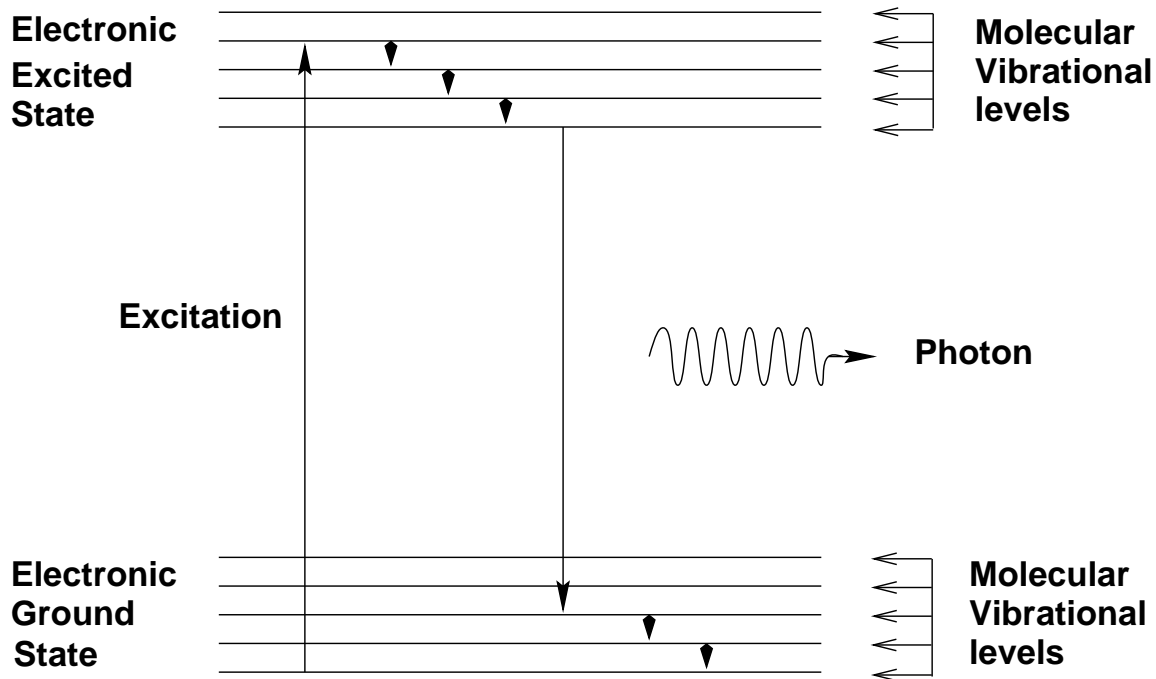
94: Scintillation Detectors

All scintillators work on the same basic principle – the incident radiation raises electrons of the scintillator material from their ground state to higher lying excited states. The excited electrons rapidly arrange themselves through radiationless transitions to lower, but still excited, states. Electrons then deexcite from these latter states to the ground state with the emission of optical photons – fluorescence.

- Organic Scintillators:

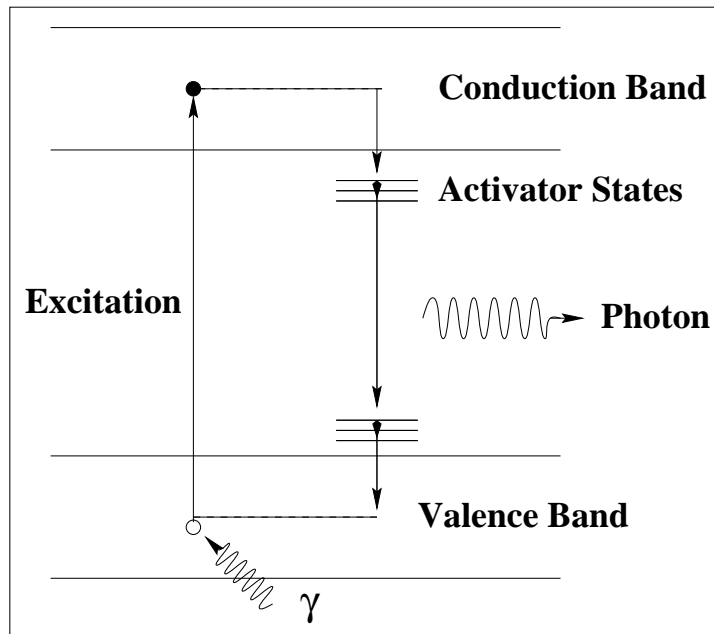
For organic scintillators the transitions arise from molecular energy levels. Therefore the state of the scintillator is not important. For example anthracene can fluoresce as a solid, a gas, or part of a liquid solution.

Pure organic scintillators are usually fragile materials. They may be dissolved in a solvent – liquid scintillator, or in a polymerised solvent – plastic scintillator.



The characteristic decay time of organic scintillators is 10^{-9} s. Longer lived excited states with lifetimes of 10^{-3} s can also be populated. The decay from such excited states, lower energy photons, produces phosphorescence – source of background in detectors. Since the fluorescence produces photons of lower energy than needed to populate the initial highly excited states, the scintillator is transparent to its own emission – useful property! Densities are typically 1 g/cm^3 , refractive indices ~ 1.5 , and wavelengths $\sim 400 \text{ nm}$.

- Inorganic Scintillators:



The operation of inorganic scintillators relies on the band structure of crystals (i.e. valence and conduction bands) and the presence of activator sites in the normally forbidden band gap. Electrons are promoted from the valence to the conduction bands leaving behind a positively charged hole in the valence band. The electrons and holes rapidly drift into the activator sites where they recombine with the emission of an optical photon with a half life of 10^{-7} s. Since the energy difference between the activator sites is less than the band gap, the scintillator is transparent to its own emissions.

95: Common Inorganic Scintillators

- Sodium Iodide:

Thallium activated sodium iodide – NaI(Tl) – is one of the best scintillators. Its density is 3.6 g/cm^3 and contains high- Z iodine ($Z = 53$). The index of refraction is 1.8, and the maximum wavelength of the emitted light is 415 nm . It is possible to grow and fabricate very large crystals. The drawback is that it is hygroscopic and so the crystals must be canned in an air-tight container.

It takes on average three times the band-gap energy to produce an electron-hole pair – 1 MeV of incident energy produces about 5×10^4 electron hole pairs in NaI(Tl). The intrinsic scintillation efficiency has been measured as 13%. Therefore, absorption of 1 MeV of energy yields about $1.3 \times 10^5 \text{ eV}$ in total light energy or about 4.3×10^4 photons with an average energy of 3 eV . The yield is very nearly one photon per electron-hole pair originally formed.

- Bismuth Germanate (BGO):

Bismuth germanate – $\text{Bi}_4\text{Ge}_3\text{O}_{12}$ – has a high cross-section for γ -ray interactions because of its high Z (Bi: $Z = 83$). Its density is 7.1 g/cm^3 , its refractive index is 2.1, and it emits photons with a wavelength of 480 nm .

One cm of BGO is equivalent to 2.5 cm of NaI(Tl) , and hence an equivalent volume of $(1/2.5)^3 \approx 1/15$. It is used widely in multidetector γ -ray spectrometers as a “Compton suppressor” of photons escaping from the primary detector. BGO has good mechanical and chemical properties, but its light output is low – 8% of NaI(Tl) .

- Barium Fluoride:

Barium fluoride – BaF_2 – decays by two low intensity components: The short component has a half-life of 0.8 ns and the long component a half-life of 620 ns . It can be used for good timing on a strong signal.

96: Light Collection

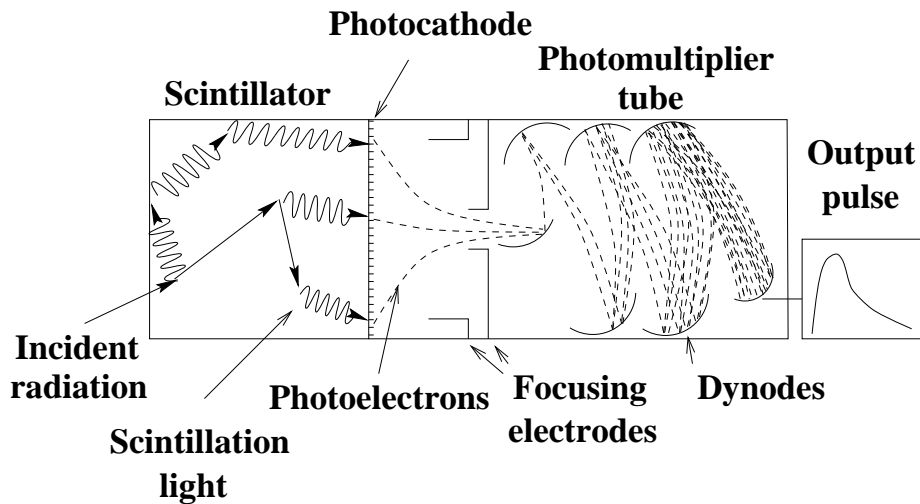
In any scintillator it is desirable to collect as much of the light produced as possible. Two effects lead to less than perfect light collection – self-absorption and losses at the scintillation surfaces.

Except for very large scintillators, self-absorption can be ignored. Poor light collection means that fewer photons are counted and the response of the detector will worsen due to the poor statistics.

Uniformity of the light collection is also important – it should not matter where the interaction took place.

The scintillation light is collected by a photomultiplier tube optically coupled to one surface of the scintillator crystal. The scintillation light is emitted in all directions and only a small fraction will directly impinge on the photomultiplier tube. Hence the scintillator is coated with a reflective surface.

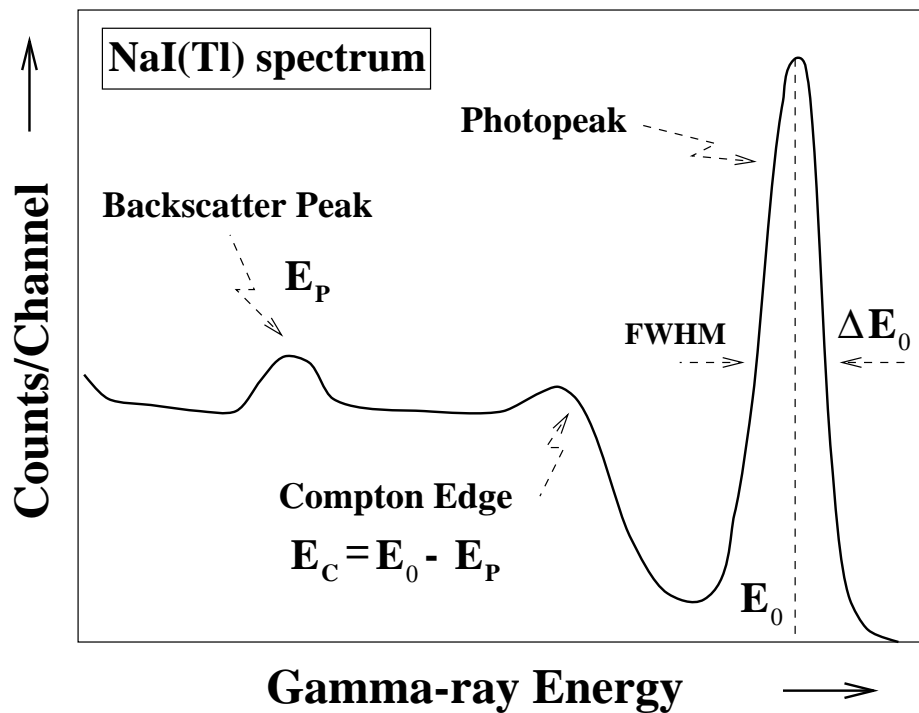
97: Photomultiplier Tube



The light output from a scintillator needs to be converted to an electrical signal, and that signal needs to be amplified. The photomultiplier consists of two main components: The photocathode is a photosensitive layer which converts the photons into low energy electrons. Typically only a few hundred photoelectrons are involved at this point. The electron multiplier serves as a near ideal amplifier which greatly increases the number of electrons. After amplification there are $10^7 - 10^{10}$ electrons which are easily detected as a charge pulse. The amplification is very linear – the size of the output pulse is proportional to the initial energy of the incident ionising radiation.

98: Gamma-Ray Spectrum

A spectrum from an NaI(Tl) crystal with a photomultiplier, detecting γ -ray from a ^{137}Cs radioactive source, is shown below. The source emits monoenergetic γ -rays of energy $E_0 = 662 \text{ keV}$. The Compton edge occurs at $E_C = 478 \text{ keV}$ and a backscatter peak at $E_P = 184 \text{ keV}$ (Note: $E_C + E_P = E_0$). The FWHM (full width half maximum) of the photopeak is 76 keV and the energy resolution of NaI(Tl) at 662 keV is thus $\Delta E/E = 11.5\%$.



99: Semiconductor Detectors

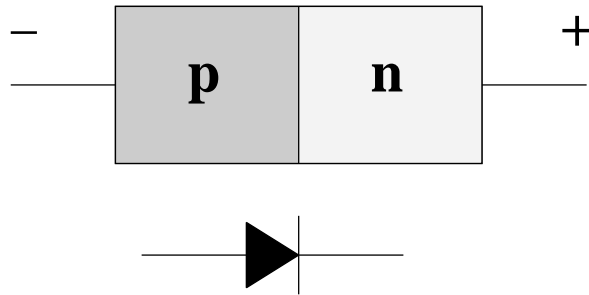
Semiconductor detectors essentially work as solid state ionisation detectors. They are much more dense than gas ionisation detectors! A charged particle (or for γ -rays a photoelectron) creates electron hole pairs as it travels through the crystal. The crystal is situated in an electric field between two electrodes from which charge can be collected.

Pure semiconductors have a valence band full of electrons and an empty conduction band, separated by a band gap. Electrons can be excited across the band gap into the conduction band, leaving behind a hole in the valence band. The number of electrons and holes are equal in an intrinsic semiconductor.

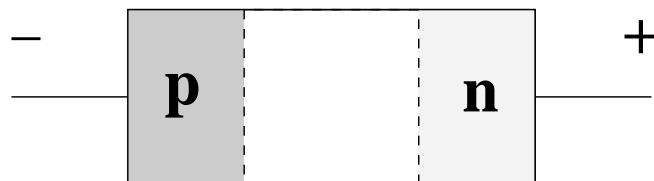
The formation of an electron-hole pair requires only 3.6 eV in silicon (Si) and 2.9 eV in germanium (Ge), which is much smaller than the energy required in a gas (30 eV) or a scintillator (300 eV). The intrinsic resolution is thus better since many more electron-hole pairs are produced which increase the counting statistics.

100: Semiconductor Junction

A semiconductor detector is a large silicon or germanium diode of the p-n type operated in reverse diode mode:



When p- and n-type materials are brought into contact, charge migrates and creates a region free from charge carriers around the interface. This depletion layer forms the active volume of a semiconductor radiation detector. The depletion layer has a charge carrier density of 10^2 cm^{-3} compared with 10^{10} cm^{-3} outside the layer.



Ionising radiation produces electron-hole pairs in the active volume which are swept out by the reverse bias ($\sim 3500 \text{ V}$) across the junction.

101: Silicon and Germanium Detectors

Germanium semiconductor detectors are mainly used for γ -ray detection. They are preferred to silicon as the material has a higher atomic number ($Z = 32$ for Ge, but $Z = 14$ for Si). The result is that there is a much higher probability for interaction between Ge and a γ -ray than for Si and a γ -ray.

Semiconductor detectors which are to be used for highly penetrating radiation must have wide depletion regions. In Ge and Si of normal semiconductor purity, the maximum thickness that can be achieved is 2–3 *mm*, even with voltages near breakdown. A much thicker depletion layer is required. The thickness of the depletion layer is given by:

$$d = \sqrt{\frac{2\varepsilon V}{eN}},$$

where V is the bias voltage and N is the net impurity concentration. At a given value of V , the only way to increase d is to decrease N .

There are two main ways of decreasing N :

- Lithium Drifting:

The most difficult impurity to remove from Si is boron, so the highest purity crystals are p-type. The boron is fully ionised at room temperature. The impurity concentration may be compensated by doping. The best method of producing accurately compensated Si and Ge is the lithium ion drift process. The doping has to be done after the crystal has been grown. Note that a Ge(Li) detector must be kept cool (liquid nitrogen temperatures) otherwise the lithium will drift out of place!

- High Purity Crystals:

The impurity concentration needs to be $< 10^{10}$ atoms/cm³ to achieve the correct depletion thickness. High-purity Ge (HPGe) crystals can be grown with $< 10^9$ impurity atoms per cm³. If the remaining low level impurity is a donor, HPGe n-type results; if it is an acceptor, the crystal will be HPGe p-type.

- Leakage Current:

When a reverse bias is applied across the junction a small current will be generated – leakage current.

This arises since the resistance of the material is not infinite. Leakage current can arise due to thermal generation of electron-hole pairs. The probability of formation of electron-hole pairs at temperature T is:

$$P(T) = CT^{3/2} \exp \left[\frac{-E_g}{2kT} \right],$$

where E_g is the band gap. Semiconductor detectors are usually cooled (liquid nitrogen) to reduce this effect.

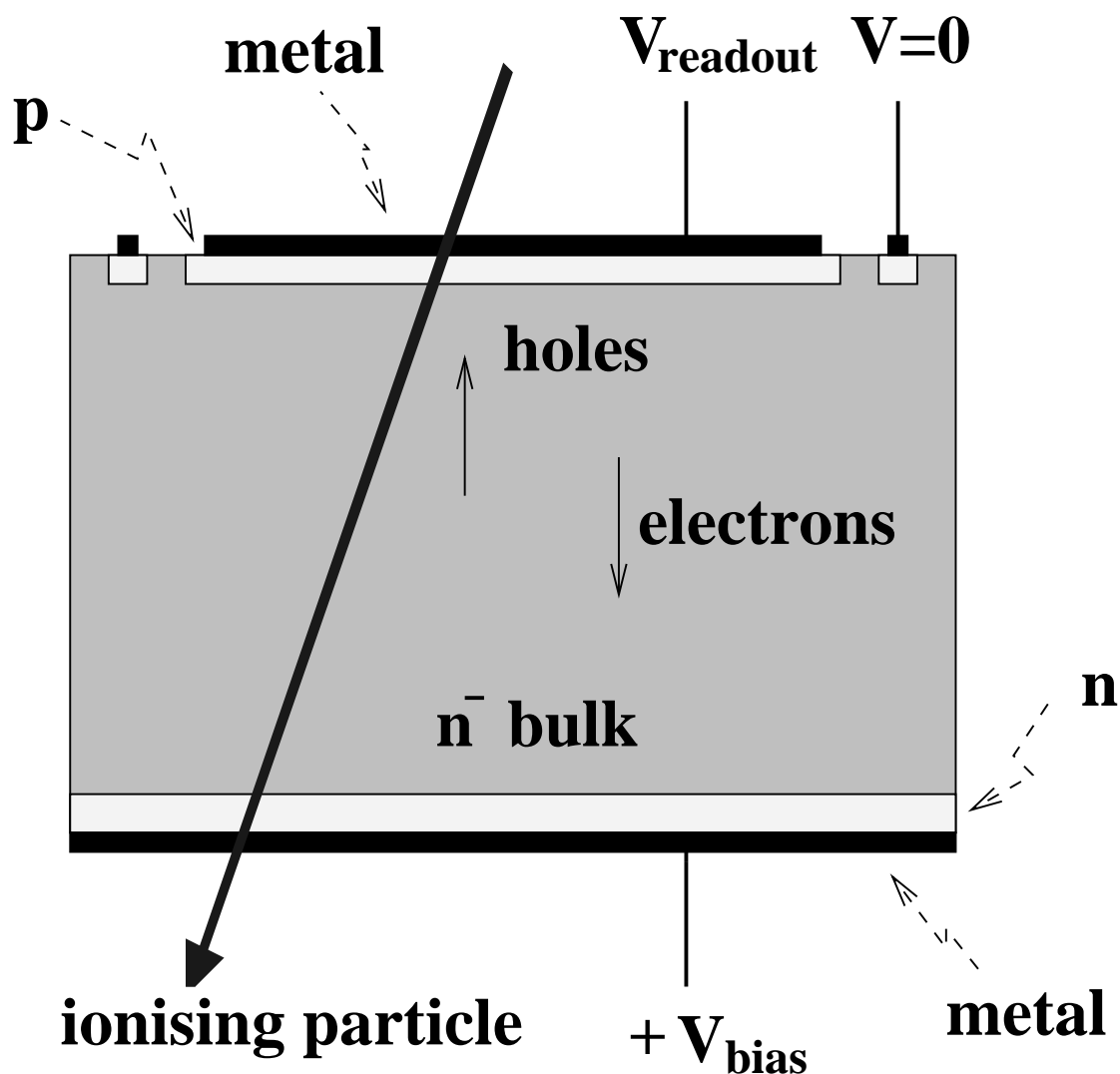
Surface leakage currents can also be generated at the edges of junctions where there are large voltage gradients. A large leakage current leads to a noisy detector and poor performance.

- Charge Collection Time:

This depends on the mobility of the electrons and holes. The maximum drift velocity is $\sim 10^7$ cm/s.

102: Silicon Detectors

Silicon detectors are primarily used to detect charged particles. They also have a wide range of uses as X-ray detectors. They are commercially available in thicknesses between 10 and 5000 μm . The detector is totally depleted if the thickness of the depletion layer is thicker than the detector.



103: Particle Identification

In thin detectors, charged particles will only lose part ΔT of their energy. The important parameter is the specific energy loss dT/dx for the radiation. For nonrelativistic particles of mass m and charge z , the Bethe-Bloch formula gives:

$$\frac{dT}{dx} = C_1 \frac{mz^2}{T} \ln \left[C_2 \frac{T}{m} \right],$$

where C_1 and C_2 are constants. The quantity

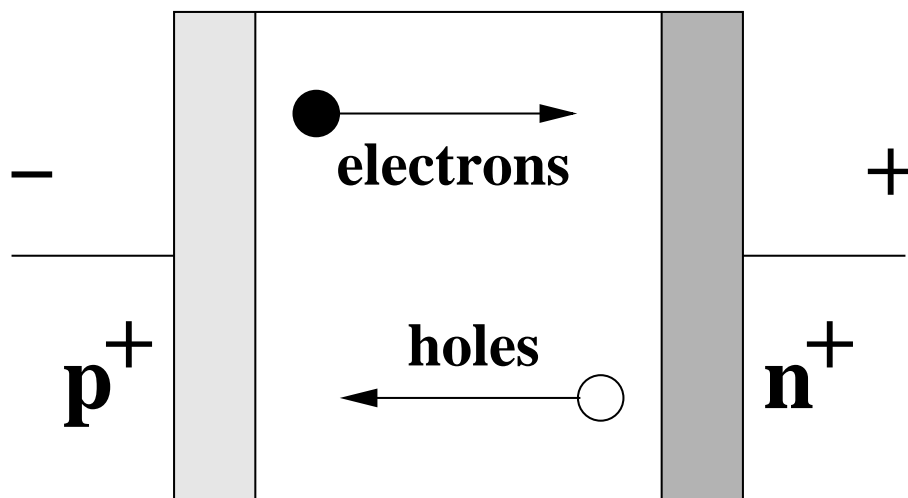
$$T \times \frac{dT}{dx}$$

has a small energy dependence but is sensitive to mz^2 which characterises the particle. Hence by using a combination of a thin ΔT and a thick T detector gives particle identification. This combination of detectors is called a telescope.

104: Germanium Detector

Most Ge detectors used in γ -ray spectroscopy are n-type. The outer p^+ contact is a very thin ($0.3 \mu m$) ion implanted layer and does not attenuate incoming γ -rays. The inner n^+ contact is thicker ($600 - 1000 \mu m$). The p^+ contact serves as a rectifying contact (injects holes) and the depletion region extends from this contact as the voltage is raised. The n^+ contact is a blocking (noninjecting) contact in which there are very few holes.

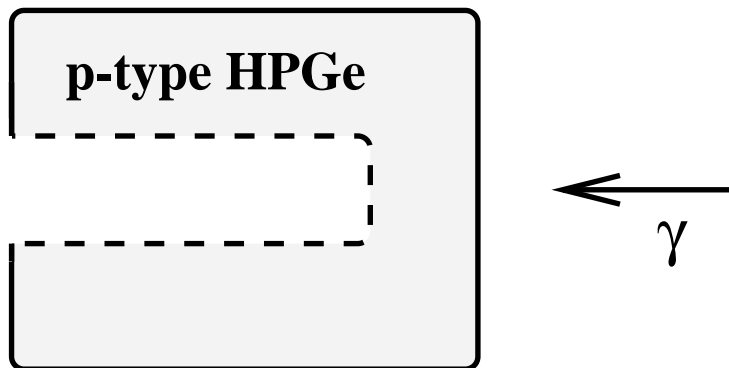
Ge detectors should be fully depleted and slightly overbiased so that the charge carriers reach saturation drift velocity, and charge collection time is minimised. This requires a field of $10^5 V/m$.



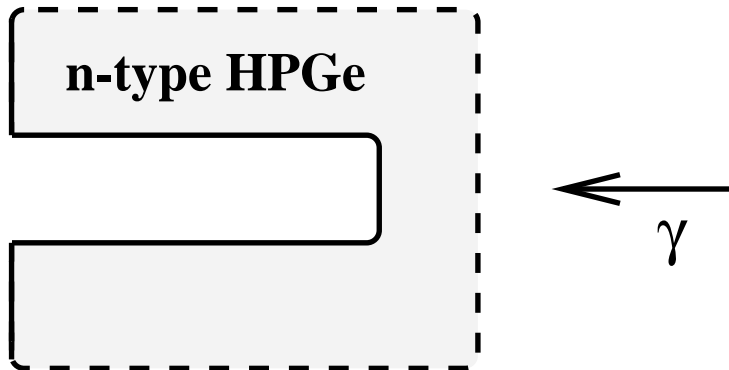
105: Types of Ge Detector

Both planar and coaxial detectors are used. Coaxial detectors are more common, and an example is shown below:

Conventional HPGe



Reverse Electrode HPGe

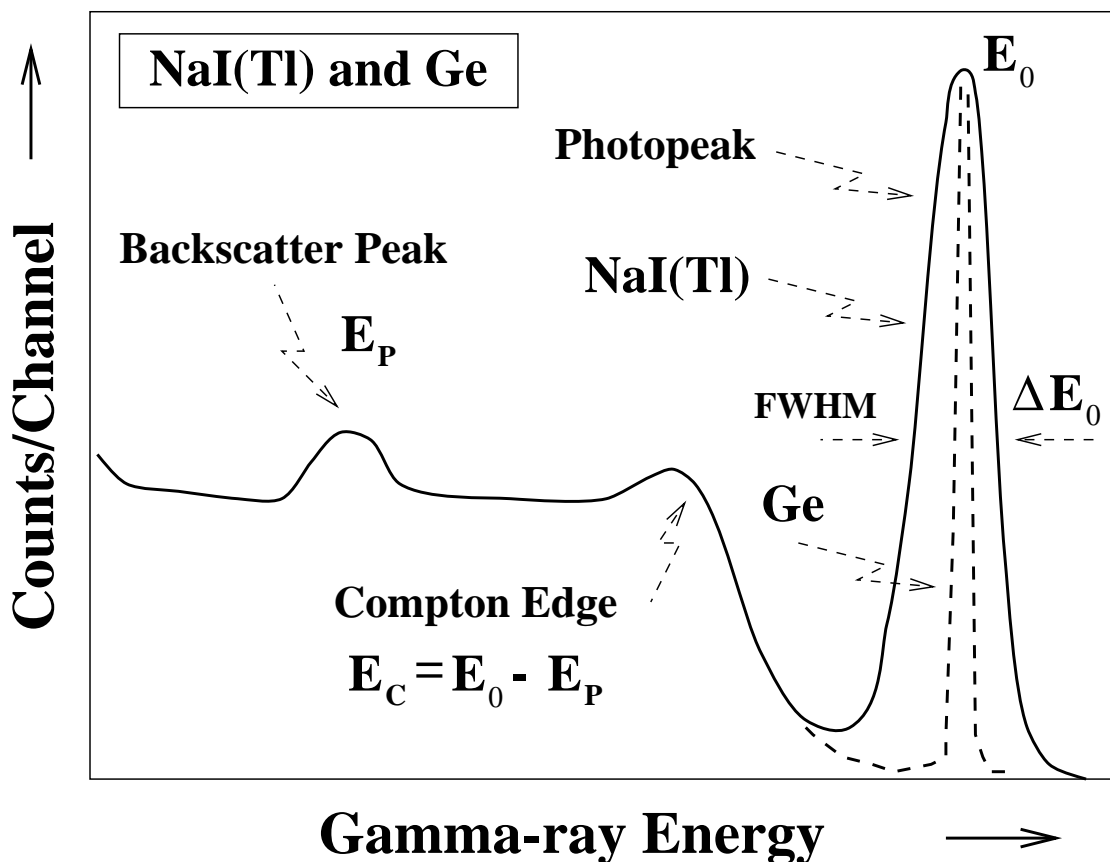


———— very thick contact

- - - - very thin contact

- Energy Resolution of a Ge Detector:

The energy resolution of a Ge detector is usually defined as the full width at half maximum (FWHM) of the 1.33 MeV γ -ray from a ^{60}Co source. It is typically 2.0 keV ($\Delta E/E \sim 1.5\%$), which is much better than a sodium iodide detector ($\Delta E/E \sim 11.5\%$). The energy resolution is also dependent on the γ -ray energy – the resolution at 122 keV is typically 850 eV.



The energy resolution is made up from two main components. There is a component $\propto (E_\gamma)^{1/2}$ which arises from the statistical fluctuations in the number of electron-hole pairs created. The second component arises from the electronic components of the circuit and the capacitance of the detector – this is fixed for a particular system. For very large detectors a third component can arise from incomplete charge collection. The energy resolution is also temperature dependent – Ge detectors are operated at liquid nitrogen temperatures.

● Efficiency of a Ge Detector:

The relative efficiency of a Ge detector is defined in relation to a 3 inch (diameter) by 3 inch (length) sodium iodide detector. For a standard measurement a ^{60}Co source is placed 25 *cm* from the face of the crystal and the counting rate per (*Bq*) into the 1.33 *MeV* photopeak measured. The absolute efficiency of the sodium iodide crystal is defined as 1.2×10^{-3} . An approximate formula for the relative efficiency of a Ge detector is:

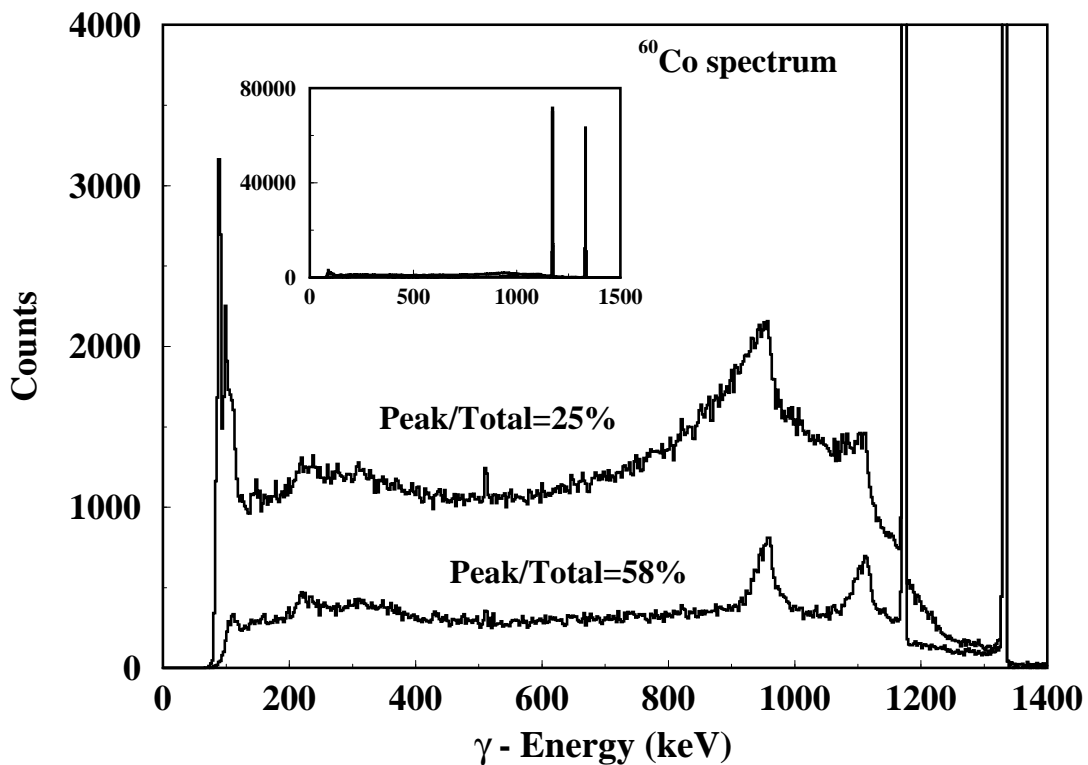
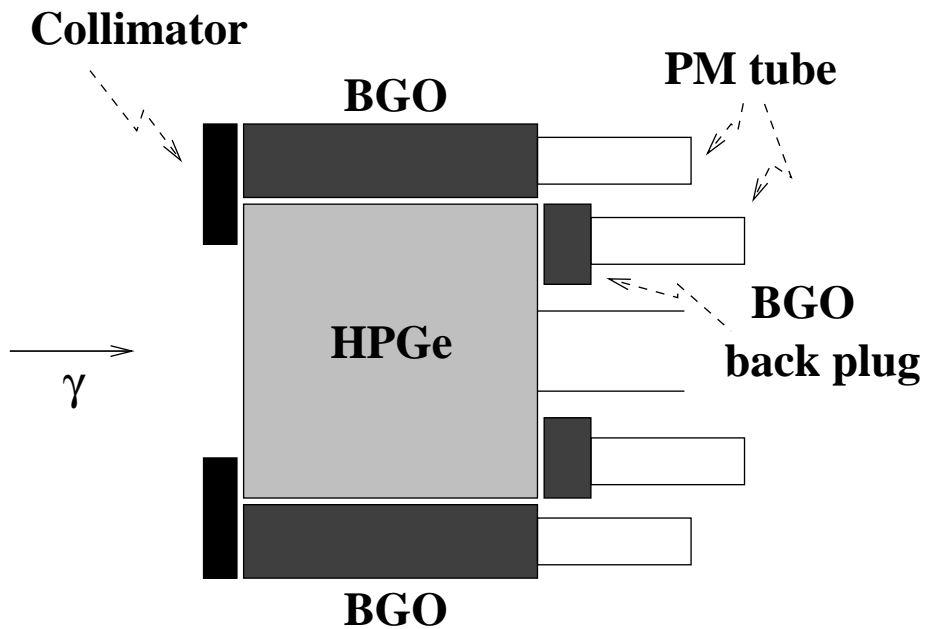
$$\text{Relative Efficiency (\%)} = \text{Volume (cm}^3\text{)}/4.3.$$

106: Compton Suppression

High purity Ge detectors are currently the best for detecting γ -rays. However, for the γ -ray energy range appropriate to nuclear structure studies ($E_\gamma = 400 - 1500 \text{ keV}$) Compton scattering is the most important interaction between the incident γ -ray and the detector. The incoming γ -ray Compton scatters within the detector and is very likely to escape. This leads to an incomplete energy deposition in the detector and contributes to a Compton background.

A way to decrease this unwanted background is to surround the primary Ge detector by an antiCompton shield. If an event occurs at the same “time” in the primary detector and the shield, then a Compton scatter must have taken place – we can reject or veto this event. A bismuth germanate (BGO) scintillation detector is an ideal candidate for a suppression shield due to its high density.

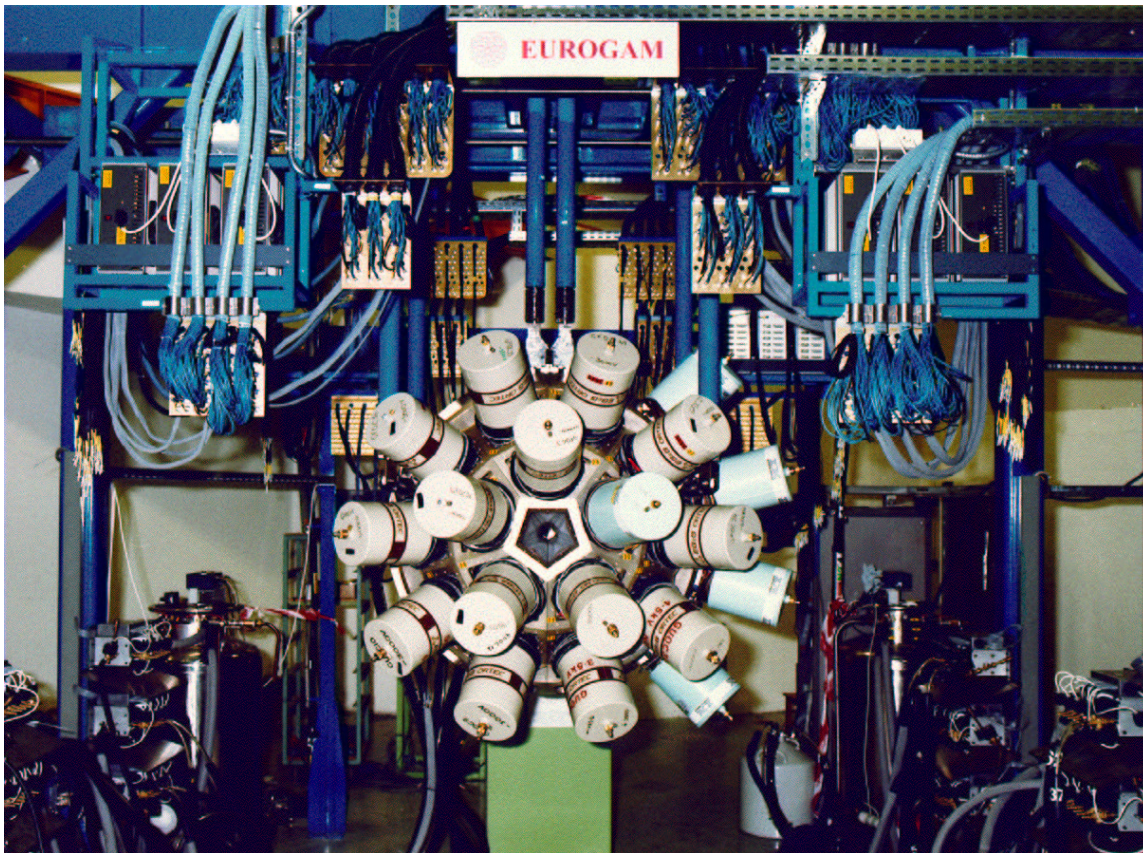
107: Escape-Suppressed Spectrometer



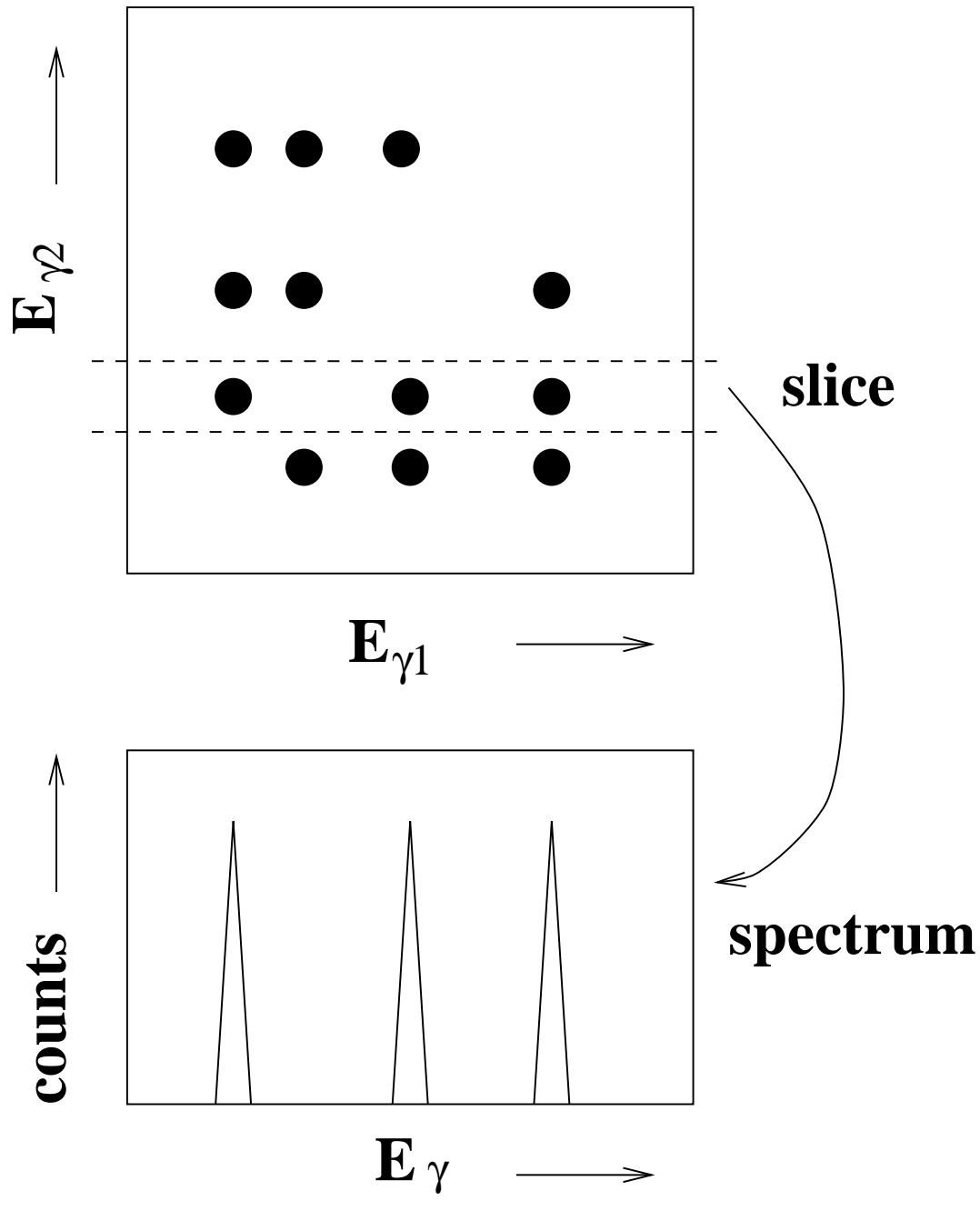
108: Multidetector Arrays

The escape-suppressed spectrometer is a basic unit in γ -ray spectrometry and several detectors may be built into a multidetector array. An example of such a state of the art spectrometer is shown below for the **Eurogam** spectrometer. More information can be found starting at the URL:

<http://ns.ph.liv.ac.uk/>



109: Gamma-Ray Coincidences



110: High-Fold Coincidences

An excited (spinning) nucleus emits about 30 γ -rays at the same time, which we can measure in coincidence in order to build a level scheme.

